Dispersion in crystal structures of 1-chloro-3-aryl-5-trihalomethyl-1λ⁴,2,4,6-thiatriazines: towards an understanding of the supramolecular organization of covalent thiazyl chlorides

Savini Suduweli Kondage,[1] Tracey L. Roemmele[1] and René T. Boeré*[1,2]

[1] Department of Chemistry and Biochemistry, University of Lethbridge, 4401 University Dr. W, Lethbridge, AB, Canada T1K 3M4

[2] The Canadian Centre for Research in Advanced Fluorine Technologies (C-CRAFT), University of Lethbridge, 4401 University Dr. W, Lethbridge, AB, Canada T1K 3M4

Corresp. author: Prof. René T. Boeré (email: boere@uleth.ca) https://orcid.org/0000-0003-1855-360X

Journal: Synlett – Cluster on Dispersion in Synthesis

Manuscript ID: ST-2023-02-0082-C

Abstract

The syntheses of five new 1-chloro-3-aryl-5-trichloromethyl-1λ⁴,2,4,6-thiatriazines, aryl = 4-R-C_6H_4- (R = CH_3O, CH_3, H, Cl and CF_3), are reported with full characterization. Single-crystal X-ray diffraction structure determinations on all, as well as the 5-CF_3 analogue which also has R = CF_3, with models produced by Hirshfeld atom refinement, produced high-accuracy structures. All six exemplars form lateral dimers with short contacts that define a centrosymmetric $\{^{\delta+}S\cdots N^{\delta-}\}_2$ motif, with interaction distances from 3.0473(9) to 3.422(3) Å, which do not vary in an expected manner with R. Normal population analysis charges computed by B3LYP-D3/6-311++D(d,p) DFT methods show small variations, and entirely as expected from the inductive effects of R. Gas-phase minimization of the dimers with M06-2X/aug-cc-pVDZ or B3LYP-D3/6-311++D(d,p) methods, with full counterpoise correction, replicate the experimental geometries for the 5-CF_3, the 5-CCl_3/$CH_3OC_6H_4$ and the 5-CCl_3/$CH_3C_6H_4$ experimental structures, but diverge for other CCl_3 exemplars. Interaction energies are more than double those computed for $[(HC)_2N_2S]_2$. Using a geometry optimized model with H in place of CX_3, the interaction energy reduces to a very realistic −22 to −24 kJ/mol for just the $\{^{\delta+}S\cdots N^{\delta-}\}_2$ motif, suggesting that CX_3 interactions contribute 21% (CF_3) to 37% (CCl_3) of the total.

Keywords

Chlorothiatriazine, thiazyl, supramolecular interaction, dispersion correction, counterpoise correction, density functional theory, X-ray crystallography, molecular squares

There is a strong current interest in supramolecular interactions between heterocyclic thiazyls (i.e. compounds containing unsaturated S–N bonds) and their heavier chalcogen (Se,Te) analogues.[1-12] A very common motif in all thiazyl intermolecular contacts is an approximately parallelepiped 'double S···N' interaction (Figure 1, **A**-**C**).[13] This motif, which will be designated here as $\{^{\delta+}S\cdots N^{\delta-}\}_2$, has received special attention in thiazyl radicals and triplet diradicals, many of which also form 'pancake bonded' dimers, as commonly but not exclusively observed for 1,2,3,5-dithiadiazolyls, **A**,[3-11] and for all known exemplars of 1,3,2,4,6-dithiatriazines, **B**.[14] For these, the $\{^{\delta+}S\cdots N^{\delta-}\}_2$ motifs usually further link dimers in an out-of-register

fashion, as shown in Fig. 1. The motif is also extremely common for simple diamagnetic thiazyls such as the 1,2,5-thiadiazoles, **C**.[2] For this case, the interactions have been accorded definitive supramolecular synthon status and have received intense interest in connection with σ-hole type chalcogen bonding, especially for the heavier Se and Te congeners.[1,2,15] A number of different approaches have been used to rationalize the observed $\{^{\delta+}S\cdots N^{\delta-}\}_2$ interactions, ranging from simple geometric parameters (distances, angles, interplanar separations),[7,11,16] electrostatic interactions using molecular electrostatic potentials (MEP),[9,10] and formal computation of σ-holes.[2,3,4,5,7,8]

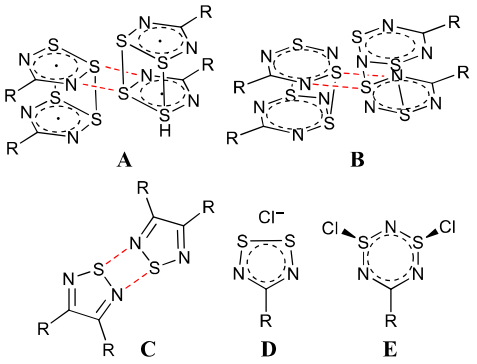

Figure 1. Intermolecular interactions in thiazyls, with $\{^{\delta+}S\cdots N^{\delta-}\}_2$ indicated by red dashed lines (**A** – **C**), and ionic vs covalent thiazyl chlorides (**D**, **E**).

By contrast, very little interest has been shown in the supramolecular structures of thiazyl halides, even though especially the chlorides are by far the most common precursors to many of the above-mentioned neutral thiazyls.[17] This may, in part, be a consequence of the very finely tuned balance between charge-separated $(thiazyl)^+Cl^-$, such as **D** and the covalent thiazyl chlorides such as **E**.[17] The origins of the choice between these rather drastic structure alternatives is poorly understood. Additionally, there is far less structural data available for the chlorides, which is likely a consequence of their class-typical extreme sensitivity to hydrolysis. Nevertheless, within the known solid-state structures, the $\{^{\delta+}S\cdots N^{\delta-}\}_2$ motif is frequently observed.[18] Herein we report on such interactions as they occur in the title compounds.

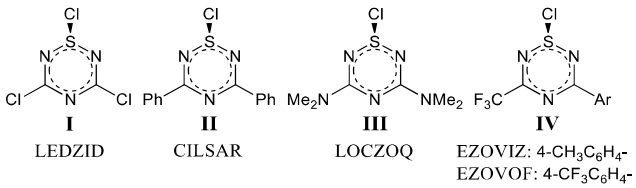

Figure 2. Reported 1-chloro-1λ⁴,2,4,6-thiatriazine structures with their CSD Refcodes (the Cambridge Structural Database, release 2022.2.0).[19]

Previously reported single-crystal X-ray diffraction (SC-XRD) structures of 1-chloro-1λ⁴,2,4,6-thiatriazines are shown in Fig. 2.[20-23] 3D coordinates are unfortunately not available for LEDZID;[20] however, for the other four structures the $\{^{\delta+}S\cdots N^{\delta-}\}_2$ motif is definitely present in CILSAR,[21] LOCZOQ [22] and EZOVOF,[23] whereas EZOVIZ does not show it and instead has a lattice structure that is dominated by π-stacking of the C_2N_3S rings. Through the synthetic work reported here that produced a systematic series of five new 1-chloro-3-aryl-5-

trichloromethyl-1λ^4,2,4,6-thiatriazines, all of which were isolable as single crystals and subjected to SC-XRD, there is an unprecedented opportunity to investigate the scope of $\{^{\delta+}S\cdots N^{\delta-}\}_2$ interactions in this class of thiazyl chlorides. Crystal quality was overall very high and by using Hirshfeld atom refinement (HAR) methods,[24-28] full refinement of the H-atom positions and anisotropic displacements was possible for these six species (including a new HAR on EZOVOV, identified henceforth as **3e**), the molecular and supramolecular structures of which are the subject of this report.

The preparation of the compounds is outlined in Scheme 1. Full synthetic and characterization details for the starting aryl/trichloromethyl imidoylamidines, **1**, are provided in the Supplementary Information (Sections S1 and S2; Tables S1-S3; Fig. S1), and the SC-XRD of these key starting materials have previously been published.[29,30] These versatile nitrogen-rich reagents were first passivated by protonation with anhydrous hydrogen chloride in ether, and then the dried powders of **2** were immediately suspended in highly purified and rigorously dry acetonitrile, reacted with an excess of freshly distilled sulfur dichloride, and then heated to reflux until HCl evolution ceased. Concentration and cooling of the solutions enabled the direct growth of pure crystals suitable for SC-XRD (see below), whilst bulk product was obtained by removal of all volatiles and recrystallization from hot, dry, *n*-heptane. Yields were reasonable (>65%) relative to the high sensitivity to hydrolysis. ^{1}H NMR spectra confirmed the condensation reactions by the complete absence of the prominent NH peaks of **1** or **2**. Electron impact mass spectrometry confirmed the parent ions, which is rare for thiazyl halides since the chlorine attached to S is usually lost on ionization, but combustion analysis could not be obtained due to hydrolytic instability. Fortunately, all exemplars **4a**-**e** are fully characterized via SC-XRD (Fig. 3).[31] For crystal and refinement data see Tables S4,S5 in the Supplementary Information and for selected interatomic and interplanar distances and angles, Table S6. The trifluoromethyl analogue **3e** was prepared in a completely analogous fashion, as previously reported. [23]

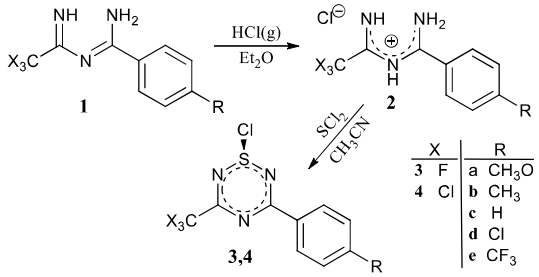

Scheme 1. Synthetic route for the preparation of **3** and **4**.

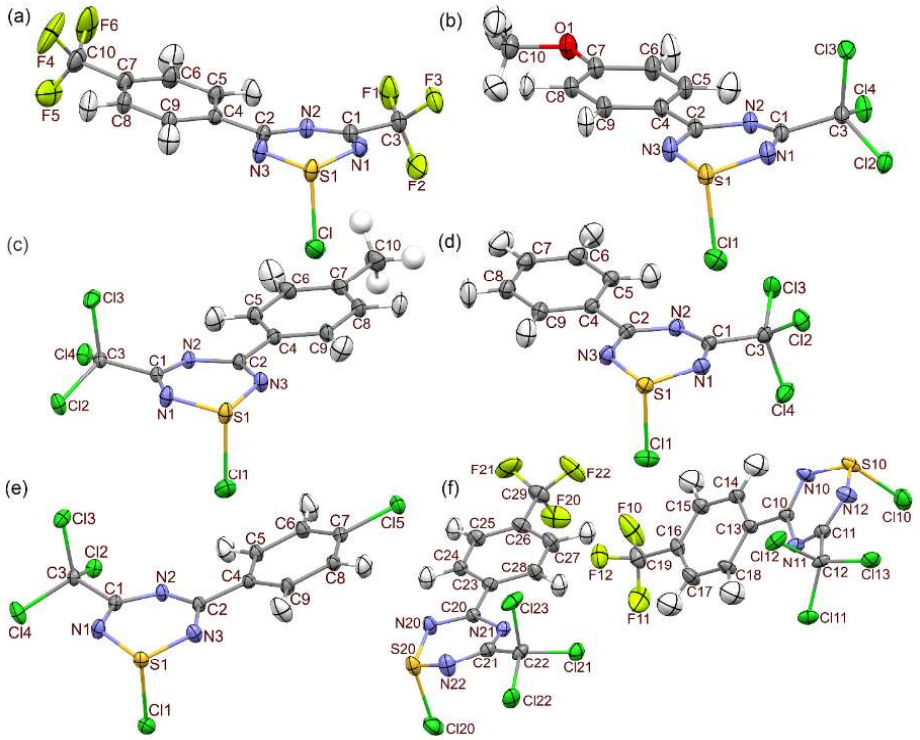

Figure 3. Displacement ellipsoids plots (40% probability) of the molecular structures of (a) **3e**, (b) **4a**, (c) **4b**, (d) **4c**, (e) **4d** and (f) **4e** as found in their respective crystal lattices at 173 K. H-atom positional and anisotropic displacement parameters were refined using NoSpherA2; the methyl group in **4b** was modelled as a two-part disorder model. Full details in the Supplementary Information.[31]

The crystal structures of **3e** and **4a–d** each have one independent molecule in the asymmetric unit, while **4e** has two. The six-membered C_2N_3S ring is effectively planar over the C_2N_3 moiety, with a small 'envelope' tilt angle averaging to 20(2)° for the NSN component (Table S6). In all cases the S-Cl bond is oriented almost perpendicular to these ring planes, which is consistent with other reports of thiazyl rings bearing covalent chlorides.[19,20,32-35] The S–Cl bond distances, averaging to 2.171(15) Å, may be compared to the CSD average of 2.21(1) Å for S–Cl bond lengths in 58 ring compounds, excluding those containing S=O bonds.[19] The most common S–Cl bonds are in S(VI) compounds of type X–S(=O)$_2$–Cl, for which the average length over 97 exemplars is significantly shorter at 2.02(4) Å.[22]

As is evident from the data in Table S6, the molecular structures of 1-chloro-3-aryl-5-trichloromethyl-1λ^4,2,4,6-thiatriazines are extremely well determined from our results and show significant uniformity. Now we turn to consider their lattice structures. Significantly, all five 5-CCl_3 species, the only known cases, share similar lateral dimeric structures and posses the $\{^{\delta+}S\cdots N^{\delta-}\}_2$ motif, as illustrated for the representative example **4a** in Fig. 4 (for additional pictures, see Figs. S2-S7). As shown, in addition to the expected dual S···N contacts, there are also contacts from the CCl_3 atom Cl2 to S1, and a selected listing of relevant contacts in all six structures is presented in Table 1. (For a comprehensive listing of intermolecular contacts less than $\sum r_{vdW}$ in these structures, see Table S7 in the Supplementary Information).

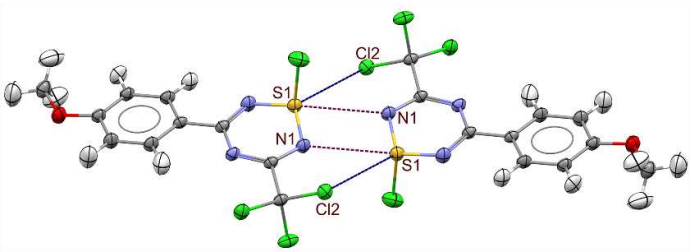

Figure 4. Representative intermolecular S···N and S···Cl short contacts, shown for **4a**, drawn as a displacement ellipsoids plot (40%).

What is quite striking from a comparison of the interaction plots (Fig. 4, S2-S7) and the data in Table 1, is how large the variation in specific geometric parameters is, despite the general uniformity in packing arrangements. Thus, while all six cases show the $\{^{\delta+}S\cdots N^{\delta-}\}_2$ motif, along with the close approach of CX_3 groups to the opposing ring edges, the *d*(S···N) values, as well as the planar offsets (measured from the C_2N_3 planar components of the thiatriazine rings, see also Fig. S8) vary greatly; by up to 0.38 Å in distance and 0.64 Å in offset. In addition, there are numerous *d*(S···Cl) contacts (Table 1), which also vary significantly in length. These surprising variations are addressed in this Letter.

Table 1. Short lateral S···N and S···Cl donor:acceptor contacts with ring offset distances.

Comp.	A	D1 [a]	Dist., Å	$\sum r_{vdW}$, Å	Sym code	D2 [b]	Dist., Å	$\sum r_{vdW}$, Å	Sym code	Offset, Å [c]
3e	S1′	N1	3.0473(9)	−0.303	2-x,1-y,-z	Cl1	3.4653(5)	−0.085	x,3/2-y,-1/2+z	0.44
4a	S1′	N1	3.1314(12)	−0.219	1-x,1-y,2-z	Cl2	3.5742(5)	+0.024	1-x,1-y,2-z	0.23
4b	S1′	N1	3.1653(9)	−0.185	1-x,1-y,1-z	Cl2	3.5747(4)	+0.025	1-x,1-y,1-z	0.26
4c	S1′	N1	3.3069(12)	−0.043	-x,-y,1-z	Cl2	3.7234(8)	+0.173	-x,-y,1-z	0.55
4d	S1′	N1	3.422(3)	+0.072	1-x,2-y,-z	Cl1	3.585(4)	+0.199	2-x,2-y,-z	0.87
						Cl1	3.749(3)	+0.363	1-x,2-y,-z	
4e (1)	S10′	N11	3.203(15)	−0.147	-x,1-y,1-z	Cl4	3.65(2)	+0.100	-x,1-y,1-z	0.35
4e (2)	S20′	N21	3.219(15)	−0.131	1-x,2-y,-z	Cl5	3.66(2)	+0.106	1-x,2-y,-z	0.38
Range			0.375	0.375			0.258			0.64

[a] All the interactions are centrosymmetric so that *d*(N1···S1') = *d*(S1···N1'). [b] d(S···Cl) contacts are as shown in Fig. 4 except the shorter contact in **4d**. [c] Separation between crystallographically parallel planes defined on C1,C2,N1,N2,N3 and C1',C2',N1',N2′,N3', calculated in Mercury 2.4.[36]

As a first step in attempting to rationalize the observed ranges in short contact distances, the molecular electrostatic potentials (MEP) were computed as has been successfully reported by Haynes *et al*. for 'side-ways' S···N interactions between 1,2,3,5-dithiadiazolyl radicals (Type **A** in Fig. 1).[10] Thus, the six exemplars **3e**, **4a**-**4e** were fully geometry optimized as monomers (and checked by frequency calculations to be local minima) at the B3LYP-D3/6-311++D(d,p) level of theory, a validated method for neutral thiazyl compounds, which are inherently very electron rich compared to typical hydrocarbons. Charges were computed from the natural population analysis (NPA) method using natural bonding orbitals as implemented in Gaussian W16, and the MEP surfaces computed from the SCF potentials. The NPA charges are listed in Table 2, while a representative MEP surface is shown in Fig. 5. The NPA charge variation at both N1 and N3 for **4a** – **4e** is entirely consistent with the expected inductive effects of the 4-aryl substituents, decreasing with increased

electron withdrawing abilities of the aryl substituents. Fascinatingly, the charges on S are almost invariant, but those on the attached Cl1 follow the trends on N but with a three-fold larger variation. The values for **3e** differ significantly, reflecting the direct inductive effect of the 5-CF_3 versus 5-CCl_3 groups. Most interestingly, the N3 charges are always substantially larger than N1. This last effect suggests that if charges dominated the observed supramolecular synthons, the alternative pairing geometry, i.e. $^{\delta+}$S···N3$^{\delta-}$ rather than $^{\delta+}$S···N1$^{\delta-}$, should occur (Fig. S9), but this has never been observed in 5-CX_3-substiuted chlorothiatriazines. Importantly, neither the variation in MEP surfaces nor in NPA values correlates in any meaningful way with the *d*(S···N) observed experimentally for **3e** – **4e** (Table 2).

Table 2. Computed NPA charges, on monomers and dimers, with experimental and computed *d*(S···N).[a]

Comp.	C1	N1	S1	N3	C2	N2	Cl1	CX_3 (av)	*d*(S···N), Å
3c	0.394	−0.674	1.225	−0.725	0.488	−0.529	−0.332	−0.339	n/a [b]
	0.399	*−0.700*	*1.257*	*−0.727*	*0.500*	*−0.538*	*−0.333*	*−0.340*	*3.1002* [c]
3e	0.397	−0.699	1.225	−0.723	0.496	−0.533	−0.316	−0.337	3.0473(9) [d]
	0.401	*−0.698*	*1.256*	*−0.723*	*0.497*	*−0.534*	*−0.317*	*−0.339*	*3.0985* [c]
4a	0.432	−0.688	1.231	−0.737	0.496	−0.549	−0.353	+0.067	3.1314(12) [d]
	0.441	*−0.743*	*1.270*	*−0.720*	*0.434*	*−0.541*	*−0.364*	*+0.066*	*3.1344* [c]
4b	0.432	−0.685	1.230	−0.731	0.498	−0.545	−0.345	+0.068	3.1653(9) [d]
	0.442	*−0.743*	*1.269*	*−0.712*	*0.487*	*−0.487*	*−0.356*	*+0.067*	*3.1298* [c]
4c	0.435	−0.683	1.231	−0.727	0.490	−0.544	−0.339	+0.069	3.3069(12) [d]
	0.444	*−0.741*	*1.268*	*−0.709*	*0.487*	*−0.540*	*−0.349*	*+0.068*	*3.1298* [c]
4d	0.434	−0.682	1.230	−0.729	0.487	−0.544	−0.334	+0.070	3.422(3) [d]
	0.485	*−0.742*	*1.218*	*−0.710*	*0.485*	*−0.542*	*−0.644*	*+0.069*	*3.1286* [c]
4e	0.435	−0.678	1.230	−0.727	0.496	−0.543	−0.324	+0.071	3.203(15); 3.219(15) [d]
	0.447	*−0.741*	*1.266*	*−0.704*	*0.485*	*−0.541*	*−0.332*	*+0.070*	*3.1260* [c]
5c	0.336	−0.697	1.217	−0.727	0.480	−0.541	−0.364	+0.191	n/a [b]
	0.343	*−0.716*	*1.246*	*−0.729*	*0.480*	*−0.540*	*−0.376*	*+0.190c*	*3.0877* [c]
Δ [e]	0.003	0.010	0.001	0.010	0.000	0.006	0.047	0.004	0.296

[a] NPA values from NBO calculations in B3LYP-D3/6-311++D(d,p). Second rows of entries (in Italics) are average values from components of the optimized dimers, see text. [b] No experimental value, as **3c** and **5c** are model systems. [c] Computed distance, average of two very similar values. [d] Experimental X-ray distance is centrosymmetric, *d*(N1···S1') = *d*(S1···N1'). [e] Ranges are calculated over **4a**–**4e**; the pattern in **3e** is expected to be different, see text.

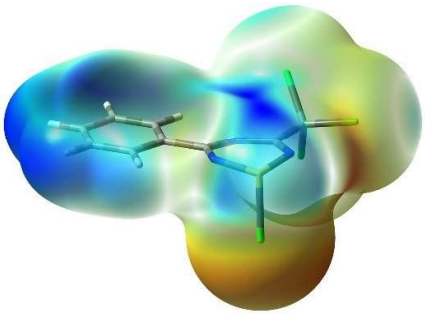

Figure 5. MEP surface computed from the B3LYP-D3/6-311++D(d,p) structure of **4c**, showing the regions of relatively negative (red: −0.031) through to relatively positive (blue: +0.031) charges (plot isovalue 0.004 *e*/Å^3).

Next, we consider the approach used by Scheiner for 3,5-dihydro-1,2,5-thiadiazole {$^{\delta+}$S···N$^{\delta-}$}$_2$ interactions (Type **C** in Fig. 1),[2] who reported interaction energies, with and without counterpoise correction (CC), at the

M06-2X/aug-cc-pVDZ level of theory (double ζ basis set, using the built-in dispersion correction of the M06-2x functional).[37] The CC-corrected interaction energy computed for the parent $(HC)_2N_2S$ thiadiazole ring is −16.3 kJ/mol, described by the author as a 'substantial' non-covalent binding energy, and one that can be minimized in gas-phase computational models. This comment is what alerted us to Scheiner's approach as of potential value for **3e** – **4e**, reasoning that as a neutral and diamagnetic thiazyl, the 3,4-dihydro-1,2,5-thiadiazole should function as a good model for the neutral chlorothiatriazines. Geometries of our dimers were taken from the X-ray structure of **4c**, since it is the simplest member of our set, and the one with the planar offset that is closest to the average value (0.55 vs. 0.51 Å). (Since we are less interested in theories of bonding and focus instead on modelling real compounds, we have refrained from 'oversimplifying' the models by e.g. replacing all organic substituents with H. Importantly, such 'real life' models require the brilliant capabilities of Grimme's 'D3' [38] and Truhlar's M06-2X [37] dispersion-corrected methods.) For the sake of direct comparison with Scheiner's work, computations were undertaken first with full geometry optimization, followed by a CC calculation to reduce the exaggerated interaction energy (caused by basis set superposition effects, BSSE).[39] Then, to be assured of the best structures for comparison to experiment, they were repeated with a fully CC-corrected geometry optimization (although further changes in geometry were found to be small). In consideration of the demonstrated improvements in CC in DFT from using close-to-basis-set-limit (CBS) wavefunctions,[39] parallel calculations on **4c** were also taken with the highly benchmarked dispersion corrected [38] B3LYP-D3/6-311++D(d,p) method (triple ζ, CBS). The overall BSSE-corrected energy on the geometry optimized structures of the two methods were shown to be within 2 kJ/mol (Table 3), but the computational efficiency (in wall time) of the latter method far outpaced that of M06-2X (consistent with previous experience).[14] Thus, further comparisons of substituent and geometry effects use only the B3LYP-D3 results. The CC-corrected dimer energies for each experimental system, and some additional model configurations, are listed in Table 3. Most interestingly, the *NPA charges* at the CC-optimized dimer geometries (the lines in italic text in Table 2) are altered by the interaction, and notably the N1 values (for 5-CCl_3 compounds) are now higher in magnitude than those of N3, indicating that the charges in the dimers align with the observed $\{^{\delta+}S\cdots N^{\delta-}\}_2$ geometries.

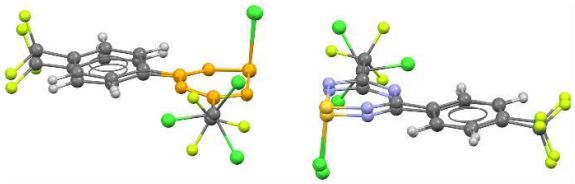

Figure 6. Overlay plot of CC-corrected B3LYP-D3/6-311++D(d,p) optimized dimers of **3e** and **4e**, displaying the difference in ring offsets (overlaid atoms are rendered in orange).

The DFT-computed geometries of the molecules within the optimized dimers are, as expected, in good agreement with those of the experimental structures (Table S8), and as is typical have bonds that are overall a bit longer than the X-ray data. The rings are slightly more puckered towards a boat conformation with, in the case of **4c**, the S1 atom 0.32 Å and N2 0.08 Å out of the mean C1C2N1N3 plane. The offset distance

between two such planes in the computed dimer is only 0.10 Å, so that it has optimized much closer together than in the experimental lattice where this value is 0.55 Å in the case of **4c**. Notably, the plane offsets in the 5-CF_3 (**3c,e**) and 5-H model (**5c**) are larger (Table 3, Fig. 6). In all the minimized dimer structures, the computed geometries of the molecules are in such excellent agreement that a consideration of the inter-molecular properties can be undertaken with considerable confidence (Figs. 6, S10,11).

Table 3. DFT computed interaction energies (kJ/mol) at optimized geometries.

Compound	B3LYP-D3 [a]	M06-2X [b]	d_{calc}(S···N), Å	Offset$_{calc}$, Å [c]	d_{expt}(S···N), Å [d]	Δ$d_{expt-calc}$
$(HC)_2N_2S$ [e]	—	−16.3	3.048	n/a	3.14(10)	+0.094
3c	−30.7	−28.5	3.1002	0.37	n/a	n/a
3e	−31.4	−29.3	3.0985	0.41	3.0473(9)	−0.051
4a	−37.6	−34.5	3.1344	0.07	3.1314(12)	−0.003
4b	−38.0	−35.1	3.1298	0.09	3.1653(9)	+0.036
4c	−38.3	−35.3 [g]	3.1298	0.10	3.3069(12)	+0.177
4d	−38.7	−35.7	3.1286	0.12	3.422(3)	+0.293
4e	−39.1	−35.9	3.1260	0.15	3.211(15) [f]	+0.850
5c	−24.3	−22.1	3.0877	0.37	n/a	n/a
4d-$\{SCl\}_2$ [g]	−13.9	−12.9	n/a	n/a	3.585(4)	n/a

[a] B3LYP-D3/6-311++G(d,p) with CC. [b] M06-2X/Aug-CC-pVDZ with CC at the geometry optimized with B3LYP-D3. [c] Calculated between C1C2N1N3 mean planes. [d] This work, except where noted. [e] Data from ref [2] and the CSD. [f] Average of the S10 and S20 dimers in the unit cell. [g] Computed only at the static crystallographic geometry because the geometry changes with optimization (see text).

The CC-corrected energies at the CC-optimized geometries are presented in Table 3. There is no crystal structure for Scheiner's model system,[2] but a search of 208 structures of 1,2,5-thiadiazoles with $^{\delta+}S\cdots N1^{\delta-}$ short contacts in crystal structures compiled in the CSD, all but one of which are benzo-fused at the 3,4-positions, gives 3.14(10) Å. Thus, the geometry of the $(HC)_2N_2S$ dimer minimizes to slightly less than the experimental distance, within 0.1 Å – an excellent agreement. The 5-CF_3 chlorothiatriazine **3e** optimizes slightly *longer* than experiment, but with an even better agreement within 0.05 Å, and with a computed CC-corrected dimer energy of −31.4 kJ/mol. This is a surprisingly high energy for the putative $\{^{\delta+}S\cdots N1^{\delta-}\}_2$ interaction, double that of $(HC)_2N_2S$ in Scheiner's work.[2] Moving to the 5-CCl_3 chlorothiatriazine **4c**, this optimizes *shorter* than experiment by 0.18 Å with B3LYP-D3/6-311++G(d,p) and by 0.25 Å with M06-2X/Aug-CC-pVDZ, but the energies of −38.3 and −36.5 kJ/mol from the two methods are extremely close. Thereafter, all exemplars, as well as a model 3-phenyl/5-CF_3 system **3c**, were geometry optimized with full CC using the more efficient B3LYP-D3/6-311++G(d,p) method, and the energies were also checked at the same geometries with M06-2X/Aug-CC-pVDZ, (Table 3). The results are most interesting, since for **4a** the agreement of geometry optimization with experiment is within the standard uncertainty of the measurement, and for **4b** the deviation is within 0.04 Å. Notably, these are the structures with the shortest contacts for the CCl_3 series, with $\sum r_{vdW}$ of −0.219 and −0.185 Å, respectively (Table 1). As with the NPA charges, the substituent effects for the comparable series **4a** – **4e** are coherent, and moreover the (small) variations in CC interaction energies correlate quite well with the computed interaction distances (Figs. 7, S10), but the latter are not well correlated with the experimental distances.[40,41]

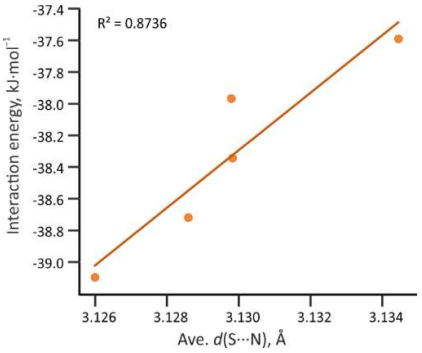

Figure 7. B3LYP-D3/6-311++G(d,p) computed energy vs. distance for the series **4a** – **4e**.

The lack of correlation of the experimental geometry variation by substituent change with either the charges or the dispersion and CC-corrected DFT calculations, and the significant difference in calculated dimer energetics between the CF_3 and CCl_3 series, all point to a likelihood that there are substantial lattice energy effects in these 1-chloro-3-aryl-5-trihalomethyl-1λ^4,2,4,6-thiatriazines beyond those originating from the $\{^{\delta+}S\cdots N^{\delta-}\}_2$ interactions. Consideration of space-filling models, such as that of **4c** at the crystal structure geometry (Fig. 8) points to close intermolecular contacts not only between S and N, but also between Cl2 (from the CCl_3 group) with the ring S atom on the opposite ring. While not as much shortened versus the $\sum r_{vdW}$ as are the S···N contacts, it seems reasonable to propose that these additional dispersive interactions contribute significantly to the total interaction energy. Thus, a better description might be a modified motif $\{^{\delta+}(S,CX_3)\cdots N^{\delta-}\}_2$, yielding a distinct centrosymmetric 'grip' between the interacting monomers.

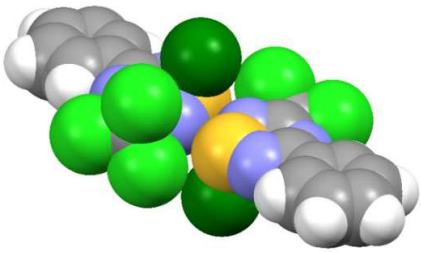

Figure 8. Space filling representations of dimer in the crystal structure of **4c**, showing the $\{^{\delta+}(S,CX_3)\cdots N^{\delta-}\}_2$ 'grip' between rings. The CCl_3 chlorine atoms are rendered light green, while SCl is a darker green for clarity.

To further investigate this possibility, a modified model was computed, named **5c**, wherein the CCl_3 groups in CC-optimized dimer **4c** are replaced by H. At the B3LYP-D3/6-311++G(d,p) level, this has an interaction energy of only −21.9 kJ/mol. This 'amputated' dimer optimizes successfully, with only a slight further shortening of *d*(S···N), to an interaction energy of −24.3 kJ/mol (Fig. S12), hence a loss of some 14 kJ/mol (relative to CCl_3) and 6.5 kJ/mol (relative to CF_3). These key interaction energies have been corroborated by parallel M06-2X/Aug-CC-pVDZ calculations (–22.1 kJ/mol in the geometry-optimized case). This is a strong indication that the CX_3 halogens interact in the dimer geometries, contributing 21-23% (CF_3) or 37-39% (CCl_3) of the total interaction energies (using the two computational models). The stronger 'grip' with CCl_3 may be the reason for the uniform $\{^{\delta+}S\cdots N^{\delta-}\}_2$ motif observed in **4a-4e**, whereas **3b** does not share this geometry with **3e**, (though an argument from two cases obviously holds limited weight).

Interestingly, the experimental geometry of **4d** (Fig. S6) has both the longest interaction distance (with $\sum r_{vdW}$ of +0.072 Å) and largest planar offset (compared e.g. to **3e**, **4a**, **4b** and the DFT optimized geometries). This structure, uniquely, possesses a short $\{^{\delta+}S\cdots Cl^{\delta-}\}_2$ contact (related by symmetry position 2-*x*,2-*y*,-*z*) tangential to the $\{^{\delta+}S\cdots N^{\delta-}\}_2$ motif, which has a similar parallelepiped geometry (Fig. 9, along with numerous other Cl···Cl and Cl···H short contacts). A static computation of this lattice fragment (the normally coloured molecules in Fig. 9) with CC-correction reports -13.9 kJ/mol for this interaction, a sizeable energy contribution that may offset the loss from the particularly long *d*(S···N) in this structure. Attempts to optimize this $\{^{\delta+}S\cdots Cl^{\delta-}\}_2$ dimer failed, since, after first dramatically shortening the interaction distance, the geometry thereafter slowly morphs into something very similar to that in the original $\{^{\delta+}S\cdots N^{\delta-}\}_2$ motif. The important point, however, is that multiple dipolar and dispersive interactions exist simultaneously in the lattice of **4d**, and whilst the geometry of the $\{^{\delta+}S\cdots N^{\delta-}\}_2$ motif persists, it is clearly of lesser energetic importance in this structure. Similarly, short Cl···Cl contacts (Table S7) are found in the crystal structures of **4c** and **4e**, which reasonably accounts for the longer *d*(S···N) values that occur experimentally for these compounds than are predicted by optimization of the lateral contacts (see Fig. S13 and related text for such contacts in CILSAR).[21]

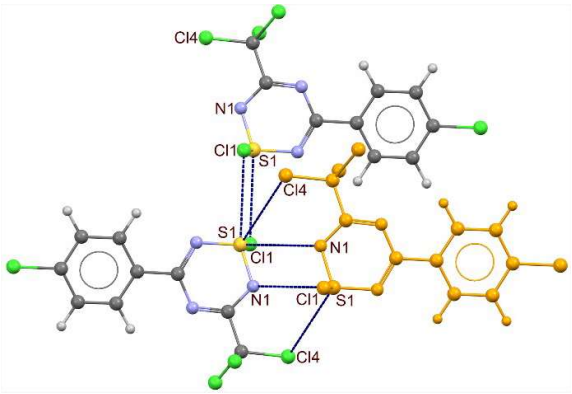

Figure 9 Ball and stick plot of the shortest S···Cl interaction pair (sym code: 2-x,2-y,-z) in the crystal structure of **4d**, oriented off to one side of the $\{^{\delta+}S\cdots N^{\delta-}\}_2$ partner, which is shown false-coloured for clarity (compare Fig. S6).

This Letter presents a short excursus on supramolecular interactions in neutral thiazyl chlorides, focussing on aryl/trihalomethyl-substituted 1-chloro-1λ^4,2,4,6-thiatriazines because of the availability, through the reported synthetic work, of six closely related crystal structures. **4a-e** provide a consistent set containing the $\{^{\delta+}S\cdots N^{\delta-}\}_2$ motif, which is prevalent in known structures of neutral thiazyl chlorides, including the previously published **3e**. The experimental geometries for the three exemplars with the shortest *d*(S···N) relative to the $\sum r_{vdW}$, **3e**, **4a** and **4b** are excellently reproduced by the calculations. However, it is also evident that CX_3 halogen interactions with acceptors contribute substantially to the overall interaction energy, such that the motif encountered specifically in 1-chloro-1λ^4,2,4,6-thiatriazines might perhaps be better described as $\{^{\delta+}(S,CX_3)\cdots N^{\delta-}\}_2$. Within this geometrical pattern, the estimated energy of the $\{^{\delta+}S\cdots N^{\delta-}\}_2$ motif itself, as computed on the 'amputated' models, is −22 to −24 kJ/mol, which seems realistic for this very electron rich ring system.[42] This work highlights the importance of effective, accurate and efficient codes for dispersion

corrected DFT calculations to enable meaningful simulations of complex intermolecular interactions in solid-state molecular structures.

Supporting Information.

The Supporting Information is available online at: _____. Accession Codes: CCDC 2244424-2244429 contain the supplementary crystallographic data for this paper. These data can be obtained free of charge via www.ccdc.cam.ac.uk/data_request/cif, or by emailing data_request@ccdc.cam.ac.uk, or by contacting The Cambridge Crystallographic Data Centre, 12 Union Road, Cambridge CB2 1EZ, UK; fax: +44 1223336033.

Acknowledgements

Research funding for this work was provided by ongoing Discovery Grants from the Natural Sciences and Engineering Research Council of Canada. The funding of the Bruker D8-Apex II diffractometer from the NSERC-C Research Tools and Instruments program, with a generous contribution from the University of Lethbridge, is gratefully acknowledged. Dr. Guanxing Lin is thanked for the ^{15}N NMR data.

References and Notes

1. Tiekink, E. R. T. *CrystEngComm* **2023**, *25*, 9.
2. Scheiner, S. *J. Phys. Chem. A* **2022**, *126*, 1194.
3. Stephaniuk, N. T.; Nascimento, M. A.; Nikoo, S.; Heyer, E.; Watanabe, L. K.; Rawson, J. M. *Chem. Eur. J.* **2022**, *28*, e202103846.
4. Wen, C.; Shi, Y.; Lu, X.; Xu, Z.; Liu, H. *J. Phys. Chem. A* **2021**, *125*, 8572.
5. Nikoo S.; Rawson, J. M. *Cryst. Growth Des*. **2021**, *21*, 4878.
6. Nascimento, M. A.; Heyer, E; Less, R. J.; Pask, C. M.; Arauzo, A.; Campo, J.; Rawson, J. M. *Cryst. Growth Des*. **2020**, *20*, 4313.
7. Galmés, B.; Adrover, J.; Terraneo, G.; Frontera, A.; Resnati, G. *Phys. Chem. Chem. Phys.* **2020**, *22*, 12757.
8. Mills, M. B.; Young, H. K. S.; Wehrle, G.; Verduyn, W. R.; Feng, X.; Boyle, P. D.; Dechambenoit, P.; Johnson, E. R.; Preuss, K. E. *Cryst. Growth Des*. **2021**, *21*, 5669.
9. Mills, M. B.; Wohlhauser, T.; Stein, B.; Verduyn, W. R.; Song, E.; Dechambenoit, P.; Rouzières M, Clérac, R.; Preuss, K. E. *J. Am. Chem. Soc.* **2018**, *140*, 16904.
10. Haynes, D. A.; Rawson, J. M. *Eur. J. Inorg. Chem.* **2018**, 3554.
11. Beldjoudi, Y.; Sun, R.; Arauzo, A.; Campo, J.; Less, R. J.; Rawson, J. M. *Cryst. Growth Des.* **2018**, *18*, 179.
12. Bates, D.; Robertson, C. M.; Leitch, A. A.; Dube, P. A.; Oakley, R. T. *J. Am. Chem. Soc*. **2018**, *140*, 3846.
13. Commonly referred to in the recent literature as 'molecular squares'; see for example [2,4].
14. R. T. Boeré, *ACS Omega*, **2018**, *3*, 18170.
15. Ho, P. C.; Wang, J. Z.; Meloni, F.; Vargas-Baca, I. *Coord. Chem. Rev.* **2020**, *422*, 213464.
16. Boeré, R. T.; Hill, N. D. D. CrystEngComm **2017**, *19*, 3698.
17. Chivers T.; Laitinen, R. S. *Chalcogen-Nitrogen Chemistry* (updated edition); World Scientific: Singapore, **2022**, p.88ff.
18. A CSD search of covalent thiazyl chlorides got 22 hits, of which 11 report having the $\{^{\delta+}S\cdots N^{\delta-}\}_2$ motif; refcodes: CILSAR, COSPIT, DESLIW, ECEBY, EXOVOV, JABRAF, LEDZEZ, LOCZOQ, YAVCON, YAVCUT, ZIJZEX.

19. Groom, C. R.; Bruno, I. J.; Lightfoot, M. P.; Ward, S. C. *Acta Crystallogr., Sect. B: Struct. Sci., Cryst. Eng. Mater.* **2016**, *72*, 171.

20. Chen, S-J.; Behrens, U.; Fischer, E.; Mews, R.; Pauer, F.; Sheldrick, G. M.; Stalke, D.; Stohrer, W.-D. *Chem.Ber.* **1993**, *126*, 2601.

21. Cordes, A. W.; Haynes, P. J.; Josephy, P. D.; Koenig, H.; Oakley, R. T.; Pennington, W. T. *J. Chem. Soc. Chem. Comm.* **1984**, 1021.

22. Ramakrishna, T. V. V.; Elias, A. J.; Vij. A. *Inorg.Chem.* **1999**, *38*, 3022.

23. Boeré, R. T., Roemmele, T. L., Yu, X. *Inorg. Chem*. **2011**, *50*, 5123.

24. Kleemiss, F.; Dolomanov, O. V.; Bodensteiner, M.; Peyerimhoff, N.; Midgley, L.; Bourhis, L. J.; Genoni, A.; Malaspina, L. A.; Jayatilaka, D.; Spencer, J. L.; White, F.; Grundkotter-Stock, B.; Steinhauer, S.; Lentz, D.; Puschmann, H.; Grabowsky, S., *Chem. Sci.* **2020**, *12*, 1675.

25. Boeré, R. T. *Crystals* **2023**, *13*, 293.

26. Hill, N. D. D.; Lilienthal, E.; Bender, C. O.; Boeré, R. T. *J. Org. Chem.* **2022**, *87*, 16213.

27. Marszaukowski, F.; Boeré, R. T.; Wohnrath, K., *Cryst. Growth Des.* **2022**, *22*, 2512.

28. Ibrahim, M. A.; Boeré, R. T. *New J. Chem.* **2022**, *46*, 5479.

29. Boeré, R. T.; Roemmele, T. L.; Suduweli Kondage, S.; Zhou, J.; Parvez, M. *Acta Crystallogr., Sect. C: Cryst. Struct. Commun.* **2011**, *67*, o273.

30. Roemmele, T. L.; Boeré, R. T. *Acta Crystallogr., Sect. E: Struct. Rep. Online* **2011**, *67*, o3137.

31. HAR was employed using NoSpherA2 [24] within Olex2 1.5-*alpha* on all six structures (Section 3 of the Supplementary Information). The first five refined extremely successfully, but **4e** proved challenging due to borderline data quality (twinning and disorder). Nevertheless, all the HAR models represent improvements on the precision of refinements (mean 32.3% improvement on average C–C distances – see Table S5) compared to exactly parallel models in the independent atom model (IAM). For details, see the Experimental and Table S5 in the ESI. The most obvious feature of the HAR, clearly visible in Fig. 3, are the full positional and anisotropic positional refinements of the hydrogen atoms (except for the $C^{10}H_3$ methyl group in **4b**, which is rotationally disordered). Still, even such a disorder would have been difficult to pick out in an IAM model, further validating the impressive performance of NoSpherA2 [25-28]. Full details on the SC-XRD structures and refinement are provided in the SI.

32. Graham, J. B. III; Cordes, A. W.; Oakely, R. T.; Boeré, R. T. *Acta Crystallogr., Sect. C: Cryst. Struct. Commun.* **1985**, *41*, 1835.

33. Boeré, R. T.; Oakely, R. T.; Cordes, A. W. *Acta Crystallogr., Sect. C: Cryst. Struct. Commun.* **1985**, *41*, 1686.

34. Chivers, T.; Richardson, J. F.; Smith, N. R. M. *Inorg. Chem.* **1986**, *25*, 47.

35. Wiegers, G. A.; Vos, A. *Acta Crystallogr.* **1966**, *20*, 192.

36. Macrae, D. F., Edgington, P. R., McCabe, P., Pidcock, E., Shields, G. P., Taylor, R., Towler, M. van de Streek, J. *J. Appl. Cryst.* **2006**, *39*, 453.

37. Zhao, Y., Truhlar, D.G. *Theor. Chem. Account.* **2008**, *120*, 215.

38. Grimme, S.; Hansen, A.; Brandenburg, J. G.; Bannwarth, C. *Chem. Rev.* **2016**, *116*, 5105.

39. Gray, M.; Bowling, P. E.; Herbert, J. M. *J. Chem. Theory Comput.* **2022**, *18*, 6742.

40. A reviewer suggested investigating these interactions by the Quantum Theory of Atoms in Molecules approach. We therefore took the CC-optimized geometry at the B3LYP-D3/6-311++G(d,p) level of theory of **4c** into AIMAll for an AIM analysis.[41] This calculation confirmed the presence of (3,−1) critical points, usually taken as indicative of the presence of 'bonds', for both the (S···N) and (CCl_3···N) type contacts (corresponding to the dashed lines in Fig. 4) with average $\nabla^2\rho$ of 0.035 a.u. for the first and

0.016 a.u. for the second type, corresponding to 'bond' strengths of 8.7 and 2.8 kJ/mol, respectively. So yes, BCPs exist in these optimized lateral dimers. It would, however, take a systematic comparison of these BCP energetics with those at the crystallographic geometries to be able to provide an adequate interpretation of their meanings. If anything, these preliminary results substantiate the importance of dispersion in the contributions of the chloro groups to the intermolecular interactions, since the (CCl_3···N) component is shown to contribute almost 40% of the total energy (see the remaining text), exceeding this AIM estimate of 24% in the absence of dispersion.

41. AIMAll (Version 19.10.12), Todd A. Keith, TK Gristmill Software, Overland Park KS, USA, **2019** (aim.tkgristmill.com).

42. In ref. [2], Scheiner computes interaction energies for hypothetical selenazole dimers, where the CH moieties in the rings are replaced sequentially by one or two nitrogen atoms. It is claimed that for each additional N atom, the interaction energy almost doubles in magnitude. Of course, there is no way to test this experimentally, but our result of a higher interaction energy in the C_2N_3S thiatriazine fits to this prediction.

Graphical Abstract

TOC Graphical Abstract – this is prepared to the 'actual size' for printing, 10.5 x 5 cm at 600 d.p.i.

(also available in 1200 dpi version)

Dispersion in crystal structures of 1-chloro-3-aryl-5-trihalomethyl-1λ⁴,2,4,6-thiatriazines: towards an understanding of the supramolecular organization of covalent thiazyl chlorides

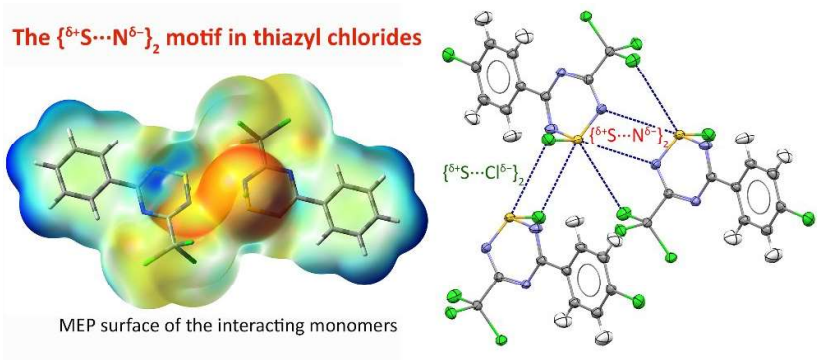

Dispersion in crystal structures of 1-chloro-3-aryl-5-trihalomethyl-1λ⁴,2,4,6-thiatriazines: towards an understanding of the supramolecular organization of covalent thiazyl chlorides

Savini Suduweli Kondage, Tracey L. Roemmele and René T. Boeré

Department of Chemistry and Biochemistry, University of Lethbridge, 4401 University Dr. W, Lethbridge, AB, Canada T1K 3M4 *and* The Canadian Centre for Research in Advanced Fluorine Technologies (C-CRAFT), University of Lethbridge, 4401 University Dr. W, Lethbridge, AB, Canada T1K 3M4

Supplementary Information

Table of Contents

Section 1. Experimental Details and Synthesis

General procedures. Trichloroacetonitrile was obtained commercially and kept under refrigeration prior to use. SCl_2 was distilled from PCl_3 with $CaCl_2$ moisture protection. Triphenylantimony and HCl(g) (Praxair) were obtained commercially and used as received. *Para*-substituted benzamidines were prepared according to literature methods.[1] Unless otherwise indicated, all procedures were performed under an atmosphere of purified N_2 using a drybox, Schlenkware, and vacuum-line techniques. Solvents used were reagent-grade or better. Acetonitrile (HPLC grade) was double-distilled from P_2O_5 and CaH_2. Dichloromethane was distilled from CaH_2. N-heptane was dried by distillation over $LiAlH_4$. Anhydrous ether was dried by distillation from sodium wire. Infrared spectra were obtained as KBr plates and were recorded on a Bomem MB102 Fourier transform spectrometer. Melting points were determined on an Electrothermal melting point apparatus and are uncorrected. EPR spectra (X band) were recorded on a Bruker EMX10 spectrometer as solutions in dichloromethane in 4mm Pyrex glass tubes sealed under vacuum. NMR spectra were acquired at 250.13 (^{1}H) and 62.90 (^{13}C) MHz on a Bruker Tecmag AC250 spectrometer using $CDCl_3$ as the solvent and thus as reference. Mass spectra were recorded by the Mass Spectrometry Center, University of Alberta, Edmonton. Microanalyses were performed by M-H-W Laboratories in Phoenix, AZ. Chlorothiatriazine **3e** was prepared as previously reported, and the original X-ray diffraction intensity data was re-used here for the HAR procedure.[2]

Synthesis of the trichloromethyl imidoylamidines 2a–e.

4–$CH_3OC_6H_4C_3N_3H_3Cl_3$ **2a**. Trichloroacetonitrile (3.93 g, 27.2 mmol) was added dropwise at 15–20 °C to 4–methoxybenzamidine (4.08 g, 27.2 mmol) in 7 mL dried acetonitrile. The mixture was heated at reflux for 1.5 hours, then cooled and rotary evaporated to leave a faint pink solid. All remaining liquids were vacuum filtered off to give 7.69 g of pink solid (26.1 mmol, 96% yield); mp 104–106 °C; ^{1}H NMR (δ, $CDCl_3$): 3.9 (s, OCH_3), 6.5 (s, NH), 7.0 (d, Ph), 7.9 (d, Ph), 9.3 (s, NH), 10.7 (s, NH); ^{13}C NMR (δ, $CDCl_3$): 55.7 (s), 98.2 (s), 114.3 (s), 127.8 (s), 129.4 (s), 163.0 (s), 164.2 (s), 168.2 (s). IR (ν) 3388 (s), 3318 (m), 3136 (w), 3007 (w), 2984 (w), 2938 (w), 2840 (w), 1898 (w), 1618 (sh), 1607 (vs), 1568 (s), 1525 (m), 1492 (vs), 1465 (sh), 1449 (sh), 1439 (m), 1419 (m), 1328 (s), 1312 (m), 1303 (m), 1257 (s), 1184 (m), 1176 (m), 1161 (m), 1142 (s), 1116 (w), 1035 (m), 1023 (sh), 835 (s), 822 (m), 805 (m), 786 (m), 764 (m), 670 (w), 652 (w), 634 (m), 602 (m), 562 (m), 522 (m), 483 (w), 447 (w) cm^{-1}; mass spectrum (*m/e*) 292 ($CH_3OPhC_2N_3H_2CCl_3^+$, 54%), 176 ($CH_3OPhC_2N_3H_3^+$, 91%), 159 ($CH_3OPhC_2N_2^+$, 8%), 134 ($CH_3OPhCNH^+$, 100%). Analysis calculated (found): 40.78 (40.69) %C, 3.42 (3.42) %H, 14.26 (13.02) %N.

4–$CH_3C_6H_4C_3N_3H_3Cl_3$ **2b**. Prepared by the same method reported for **2a** using 4–methylbenzamidine (2.97 g, 22.1 mmol) and trichloroacetonitrile (3.23 g, 22.4 mmol) to give 5.96 g of light pink solid (21.4 mmol, 97% yield); mp 42–44 °C; ^{1}H NMR (δ, $CDCl_3$): 2.4 (s, CH_3), 6.6 (s, NH), 7.2 (d, Ph), 7.8 (d, Ph), 9.3 (s, NH), 10.7 (s, NH); ^{13}C NMR (δ, $CDCl_3$): 21.7 (s), 98.1 (s), 127.5 (s), 129.6 (s) 132.6 (s), 142.6 (s), 164.7 (s), 168.2 (s); IR (ν) 3451 (m), 3419 (m), 3324 (m), 3121 (w), 1624 (vs), 1615 (vs), 1585 (s), 1563 (s), 1523 (s), 1473 (s), 1398 (m), 1327 (s), 1310 (m), 1259 (w), 1185 (m), 1159 (m), 1131 (m), 1115 (m), 1022 (m), 934 (w), 834 (s), 812 (s), 773 (sh), 756 (s), 739 (sh), 697 (w), 670 (m), 647 (m), 580 (m), 539 (m), 520 (m), 456 (w), 449 (w) cm^{-1}; mass spectrum (*m/e*) 276 ($CH_3PhC_2N_3H_2CCl_3^+$, 94%), 215 ($CH_3PhC_2N_2H_2Cl_2^+$, 2%), 160 ($CH_3PhC_2N_3H_3^+$, 97%), 143 ($CH_3PhC_2N_2^+$, 8%), 118 (CH_3PhCNH^+, 100%). Analysis calculated (found): 43.12 (43.20) %C, 3.62 (3.514) %H, 15.08 (15.11) %N.

$C_6H_5C_3N_3H_3Cl_3$ **2c**. Prepared by the same method reported for **2a** using benzamidine (1.02 g, 8.5mmol) and trichloroacetonitrile (1.24 g, 8.6 mmol) to give 2.15 g of solid product (8.1 mmol, 96% yield); mp 68–69 °C; ^{1}H NMR (δ, $CDCl_3$): 6.6 (s, NH), 7.4–7.6 (m, 3H, Ph), 7.9–8.0 (m, 2H, Ph), 9.4 (s, NH), 10.7 (s, NH); ^{13}C NMR (δ, $CDCl_3$): 98.0, 127.6, 129.0, 132.1, 135.5, 164.7, 168.2; IR (ν) 3320 (s), 3284 (s), 3135 (m), 1629 (vs), 1589 (s), 1573 (s), 1508 (s), 1482 (s), 1444 (s), 1326 (s), 1298 (sh), 1180 (sh), 1161 (m), 1073 (w), 1038 (m), 1001 (w), 973 (w), 928 (m), 844 (m), 821 (s), 805 (sh), 780 (m), 765 (m), 713 (s), 694 (s), 651 (m), 575 (m), 615 (w),

521 (w), 454 (w), 420 (w) cm^{-1}; mass spectrum (*m/e*) 262 ($PhC_2N_3H_2CCl_3^+$, 58%), 201 ($PhC_2N_2H_2Cl_2^+$, 2%), 146 ($PhC_2N_3H_3^+$, 99%), 129 ($PhC_2N_2^+$, 6%), 104 ($PhCNH^+$, 100%). Analysis calculated (found): 40.86 (40.78) %C, 3.05 (3.10) %H, 15.88 (15.69) %N.

4–$ClC_6H_4C_3N_3H_3Cl_3$ **2d**. Prepared by the same method reported for **2a** using 4–chlorobenzamidine (4.01 g, 25.9 mmol) and trichloroacetonitrile (3.80 g, 26.3 mmol) to give 7.72 g of light purple solid (25.8 mmol, 99% yield); mp 111–113 °C; ^{1}H NMR (δ, $CDCl_3$): 6.7 (s, NH), 7.4 (d, Ph), 7.9 (d, Ph), 9.4 (s, NH), 10.7 (s, NH); ^{13}C NMR (δ, $CDCl_3$): 97.8 (s), 128.9 (s), 129.2 (s), 133.8 (s), 138.4 (s), 163.6 (s), 167.9 (s). IR (ν) 3442 (m), 3314 (m), 3127 (w), 3056 (w), 1628 (s), 1600 (s), 1583 (s), 1561 (s), 1506 (m), 1483 (sh), 1469 (vs), 1401 (w), 1327 (s), 1302 (w), 1258 (w), 1179 (w), 1158 (s), 1126 (w), 1100 (sh), 1085 (m), 1025 (m), 1014 (m), 970 (w), 934 (w), 848 (s), 813 (s), 803 (m), 762 (s), 742 (m), 734 (m), 676 (w), 648 (m), 623 (m), 576 (m), 529 (m), 476 (w), 458 (w) cm^{-1}; mass spectrum (*m/e*) 298 ($ClPhC_2N_3H_2CCl_3^+$, 83%), 180 ($ClPhC_2N_3H_3^+$, 100%), 163 ($ClPhC_2N_2^+$, 7%), 138 ($ClPhCNH^+$, 86%). Analysis calculated (found): 36.16 (36.20) %C, 2.36 (2.47) %H, 14.05 (14.27) %N.

4–$CF_3C_6H_4C_3N_3H_3Cl_3$ **2e**. Prepared by the same method reported for **2a** using 4–trifluoromethylbenzamidine (3.05 g, 16.2 mmol) and trichloroacetonitrile (2.38 g, 16.5 mmol) to give 5.29 g of light purple solid (15.9 mmol, 98% yield); mp 96–97 °C; ^{1}H NMR (δ, $CDCl_3$): 6.6 (s, NH), 7.7 (d, Ph), 8.1 (d, Ph), 9.5 (s, NH), 10.8 (s, NH); ^{13}C NMR (δ, $CDCl_3$): 97.6 (s), 124.0 (q, 273 Hz), 126.0 (q, 4 Hz), 128.0 (s), 133.8 (q, 33 Hz), 138.9 (s), 163.4 (s), 168.0 (s). IR (ν) 3469 (s), 3322 (s), 3100 (w), 1619 (s), 1587 (s), 1576 (s), 1522 (s), 1484 (s), 1411 (w), 1326 (vs), 1312 (s), 1299 (sh), 1165 (s), 1154 (s), 1120 (s), 1109 (sh), 1068 (s), 1033 (m), 1016 (s), 981 (w), 932 (w), 859 (s), 834 (m), 814 (s), 799 (s), 761 (s), 749 (s), 709 (s), 679 (m), 647 (w), 601 (m), 589 (w), 510 (m), 493 (s), 458 (m), 420 (m), 406 (w) cm^{-1}; mass spectrum (*m/e*) 330 ($CF_3PhC_2N_3H_2CCl_3^+$, 89%), 214 ($CF_3PhC_2N_3H_3^+$, 100%), 197 ($CF_3PhC_2N_2^+$, 8%), 172 (CF_3PhCNH^+, 95%). Analysis calculated (found): 36.12 (36.03) %C, 2.12 (2.19) %H, 12.64 (12.48) %N.

Synthesis of the trichloromethyl imidoylamidine hydrochlorides 3a-e.

4–$CH_3OC_6H_4C_3N_3H_3Cl_3$.HCl **3a**. 200 mL of dried ether was added to a round bottom flask containing the imidoylamidine **1a** (5.92 g, 20.1 mmol). This was stirred and HCl(g) was bubbled through, leaving a white precipitate in solution. This was filtered in air to remove the solvent and dried to leave 6.57 g of white solid (19.8 mmol, 99% yield); dec. 184–186 °C; IR (ν) 3351 (s), 3281 (s), 3120 (s), 3016 (s), 2845 (w), 1690 (s), 1599 (vs), 1504 (m), 1429 (s), 1409 (s), 1316 (m), 1264 (s), 1184 (s), 1160 (s), 1023 (m), 935 (w), 853 (m), 797 (m), 765 (w), 672 (w), 637 (m), 566 (m), 532 (w), 499 (w) cm^{-1}.

4–$CH_3C_6H_4C_3N_3H_3Cl_3$.HCl **3b**. Prepared by the same method as **3a** using **1b** (5.96 g, 21.4 mmol) and HCl(g), to leave 6.62 g of white solid (21.0 mmol, 98% yield); dec. 175–177 °C; IR (ν) 3175 (s), 3103 (s), 3005 (s), 1688 (vs), 1629 (s), 1610 (s), 1560 (m), 1528 (m), 1507 (m), 1435 (s), 1403 (sh), 1379 (sh), 1312 (w), 1263 (w), 1191 (m), 1156 (m), 1120 (w), 1030 (m), 1019 (m), 934 (m), 847 (m), 834 (m), 826 (m), 795 (s), 754 (m), 726 (m), 682 (m), 642 (m), 630 (m), 589 (w), 553 (m), 534 (m), 458 (w), 430 (w) cm^{-1}.

$C_6H_5C_3N_3H_3Cl_3$.HCl **3c**. Prepared by the same method as **3a** using **1c** (6.82 g, 25.8 mmol) and HCl(g), to leave 7.26 g of white powder (24.1 mmol, 94% yield); dec.175–176 °C; IR (ν) 3310 (s), 3127 (s), 3013 (s), 1680 (vs), 1625 (s), 1602 (sh), 1522 (w), 1496 (w), 1448 ms), 1429 (s), 1381 (w), 1185 (w), 1154 (w), 1014 (w), 934 (w), 850 (m), 802 (s), 781 (m), 711 (m), 688 (m), 584 (m), 527 (w), 426 (w) cm^{-1}.

4–$ClC_6H_4C_3N_3H_3Cl_3$.HCl **3d**. Prepared by the same method as **3a** using **1d** (7.71 g, 25.8 mmol) and HCl(g) to leave 8.28 g of white solid (24.7 mmol, 96% yield); dec. 241–243 °C; IR (ν) 3112 (s), 3012 (s), 1683 (vs), 1627 (s), 1593 (s), 1523 (w), 1491 (w), 1438 (s), 1386 (w), 1337 (w), 1182 (w), 1151 (w), 1089 (m), 1031 (w), 1014 (m), 934 (w), 850 (m), 798 (s), 777 (w), 739 (w), 677 (w), 657 (w), 627 (w), 616 (m), 589 (w), 532 (w), 496 (w), 462 (w) cm^{-1}.

4-$CF_3C_6H_4C_3N_3H_3Cl_3$.HCl **3e**. Prepared by the same method as **3a** using using **1e** (5.29 g, 15.9 mmol) and HCl(g) to leave 5.32 g of white solid (14.4 mmol, 91% yield); dec.180–183 °C; IR (ν) 3310 (m), 3128 (s), 2998 (s), 1701 (vs), 1628 (s), 1513 (m), 1439 (s), 1383 (w), 1324 (vs), 1183 (s), 1133 (s), 1118 (s), 1067 (s),

1017 (s), 932 (w), 857 (s), 803 (s), 760 (w), 744 (m), 699 (m), 630 (w), 607 (m), 589 (m), 524 (w), 463 (w), 405 (w) cm^{-1}.

Synthesis of the 1-chloro-5-aryl-3-trichloromethyl-1,2,4,6-thiatriazines 4a-e.

4–$CH_3OC_6H_5C_2N_3SClCCl_3$ **4a**. Freshly distilled SCl_2 (3 mL, 47.2 mmol) in 10 mL acetonitrile was added dropwise to **3a** (2.50 g, 7.6 mmol) in 50 mL acetonitrile under N_2 flow. The temperature of the reaction mixture was gradually raised to 80 °C and was allowed to reflux until the release of hydrogen chloride had ceased (approx. 2 hours). After placing in the freezer overnight orange yellow crystals appeared in solution (1.86 g, 5.2 mmol, 69% yield); mp 90–91 °C; ^{1}H NMR (δ, $CDCl_3$): 3.94 (s, OCH_3), 7.03 (d, phenyl), 8.49 (d, phenyl); mass spectrum (*m/e*) 357 ($CH_3OPhC_3N_3S^{35}Cl_4^+$, 1.1%), 322 ($CH_3OPhC_3N_3S^{35}Cl_3^+$, 31%), 308 ($CH_3OPhC_3N_2S^{35}Cl_3^+$, 0.3%), 189 ($C_3N_2SCl_3$, 1%), 179 ($CH_3OPhCN_2S^+$, 13%), 133 ($CH_3OPhCN^+$, 100%), 103 ($C_7H_5N^+$, 6%), 90 ($C_6H_4N^+$, 10%).

4–$CH_3C_6H_5C_2N_3SClCCl_3$ **4b**. Prepared by the same method as **4c** using **3b** (2.58g, 8.2 mmol) in 60 mL acetonitrile and distilled SCl_2 (3.1 mL, 48.8 mmol) in 10 mL acetonitrile. The crude product was recrystallized from hot heptane to give yellow moisture-sensitive needles (1.98 g, 5.8 mmol, 70% yield); mp 97–99 °C; ^{1}H NMR (δ, $CDCl_3$): 2.48 (s, CH_3), 7.35 (d, phenyl), 8.40 (d, phenyl); mass spectrum (*m/e*) 341 ($CH_3PhC_3N_3S^{35}Cl_4^+$, 2.2%), 306 ($CH_3PhC_3N_3S^{35}Cl_3^+$, 100%), 271 ($CH_3PhC_3N_3S^{35}Cl_2^+$, 13%), 225 ($CH_3PhC_3N_2{}^{35}Cl_2^+$, 2%), 189 ($C_2N_2S^{35}Cl_3^+$, 4%), 163 ($CH_3PhCN_2S^+$, 78%), 143 ($CH_3PhC_2N_2{}^+$, 16%), 117 ($CH_3PhCN^+$, 44%), 89 ($C_7H_5^+$, 18%).

$C_6H_5C_2N_3SClCCl_3$ **4c**. Prepared by the same method using as **4a** using **3c** (2.36 g, 7.8 mmol) in 50 mL acetonitrile and distilled SCl_2 (3.0 mL, 47.2 mmol) in 10 mL acetonitrile. The solution turned clear yellow once all of the SCl_2 was added and was allowed to cool and placed in the freezer overnight. The solvent was removed in vacuo, and the crude product was recrystallized from hot heptane to give dark pink moisture-sensitive plates (2.11 g, 6.4 mmol, 82% yield); mp 91–95 °C; ^{1}H NMR (δ, $CDCl_3$): 7.53–7.60 (m, 2H, Ph), 7.68–7.74 (m, H, Ph), 8.49–8.53 (m, 2H, Ph); mass spectrum (*m/e*) 327 ($PhC_3N_3S^{35}Cl_4^+$, 0.65%), 292 ($PhC_3N_3S^{35}Cl_3^+$, 100%), 189 ($C_2N_2S^{35}Cl_3^+$, 5%), 149 ($PhCN_2S^+$, 71%), 129 ($PhC_2N_2^+$, 33%), 103 ($PhCN^+$, 39%), 76 ($C_6H_4^+$, 22%).

4–$ClC_6H_5C_2N_3SClCCl_3$ **4d**. Prepared by the same method as **4a** using **3d** (3.16 g, 9.4 mmol) in 60 mL acetonitrile and distilled SCl_2 (3.6 mL, 56.7 mmol) in 10 mL acetonitrile. The crude product was recrystallized from hot heptane to give pink crystals (2.37 g, 6.5 mmol, 69% yield); mp 98–99 °C; ^{1}H NMR (δ, $CDCl_3$): 7.53 (d, phenyl), 8.45 (d, phenyl); mass spectrum (*m/e*) 361 ($PhC_3N_3S^{35}Cl_5^+$, 1.1%), 326 ($PhC_3N_3S^{35}Cl_4^+$, 77%), 189 ($C_3N_2SCl_3^+$, 6%), 163 ($PhC_2N_2Cl^+$, 18%), 137 ($PhCNCl^+$, 38%), 102 ($C_7H_4N^+$, 29%).

4–$CF_3C_6H_5C_2N_3SClCCl_3$ **4e**. Prepared by the same method as **4a** using **3e** (2.82 g, 7.7 mmol) in 40 mL dried acetonitrile and distilled SCl_2 (4.80 mL, 75.6 mmol) in 10 mL dried acetonitrile. The mixture was refluxed for 1 hour and allowed to cool to RT, then stored in the freezer overnight which produced yellow, x-ray quality crystals (1.99 g, 5.0 mmol, 65% yield); mp 93–96 °C; ^{1}H NMR (δ, $CDCl_3$): 7.84 (d, phenyl), 8.62 (d, phenyl). mass spectrum (*m/e*) 396 ($CF_3PhC_3N_3S^{35}Cl_4^+$, 0.9%), 361 ($CF_3PhC_3N_3S^{35}Cl_3^+$, 82%), 196 ($CF_3PhC_2N_2{}^+$, 11%), 189 ($C_3N_2SCl_3^+$, 8%), 170 (CF_3PhCN^+, 17%), 102 ($C_7H_4N^+$, 33%).

Section 2. Compiled NMR data

Table S1. ^{1}H NMR of the aryl N-imidoylamidines **2a–e**.[a]

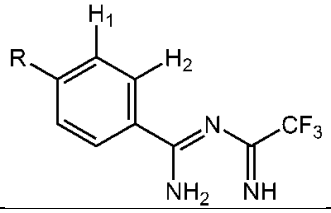

cmpd	H_1	H_2	J_{AB} (Hz)	R	NH	NH	NH
2a	6.96	7.94	9.0	3.86	10.7	9.3	6.5
2b	7.25	7.84	8.4	2.40	10.7	9.3	6.6
2c	m 7.45 – 7.48	m 7.93 – 7.96	—	m 7.42 – 7.56	10.7	9.4	6.6
2d	7.42	7.88	8.9	—	10.7	9.4	6.7
2e	7.73	8.06	8.1	—	10.8	9.5	6.6

[a] All values are in ppm, with reference to TMS.

Table S2. ^{13}C NMR of the aryl imidoylamidines **2a–e**.[a]

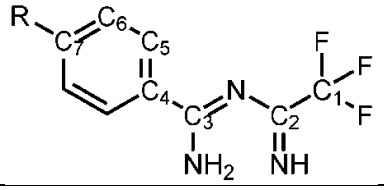

cmpd	C_1	C_2	C_3	C_4	C_5	C_6	C_7	R
2a	98.18	163.02	168.15	127.75	129.36	114.33	164.23	55.71
2b	98.11	164.66	168.17	132.64	127.52	129.62	142.60	21.65
2c	97.99	164.72	168.17	135.48	127.56	128.97	132.07	—
2d	97.78	163.59	167.94	133.83	128.90	129.17	138.39	—
2e	97.62	163.39	168.03	138.90	128.03	126.00 [b]	133.83 [c]	123.97 [d]

[a] All values are in ppm, with reference to TMS. [b] q, $^{3}J_{(F,C)}$ = 3.9 Hz. [c] q, $^{3}J_{(F,C)}$ = 33 Hz. [d] q, $^{3}J_{(F,C)}$ = 273 Hz.

Table S3. ^{1}H NMR of the chlorothiatriazines **4a** – **4e**.

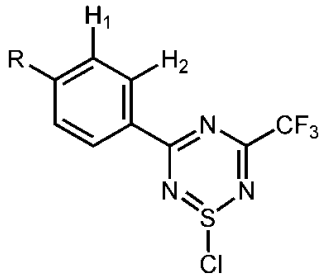

Cmpd	H_1	H_2	R	J_{AB} (Hz)
4a	7.03	8.49	3.94	9.2
4b	7.35	8.40	2.48	8.4
4c	m 7.53 – 7.60	m 8.49 – 8.53	m 7.68 – 7.74	—
4d	7.53	8.45	—	8.9
4e	7.84	8.62	—	8.9

2D NMR data (^{1}H-^{15}N Correlation Spectroscopy)

A sample of **1b** dissolved in $CDCl_3$ was subjected to a detailed multinuclear NMR study in a Varian 500 MHz WB instrument. High resolution ^{1}H, ^{13}C and ^{15}N (HN_gHSQC with and without ^{15}N decoupling) NMR experiments were performed. The ^{15}N reference employed was to external neat nitromethane, and set to the *l*.NH_3 scale as δ = 0. The results are in excellent agreement with the interpretation of the major tautomers in solution being in good correspondence with the observed major locations of the H atoms on N in SC-XRD studies.[3]

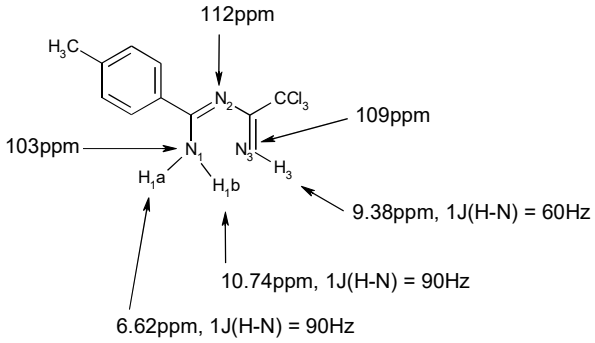

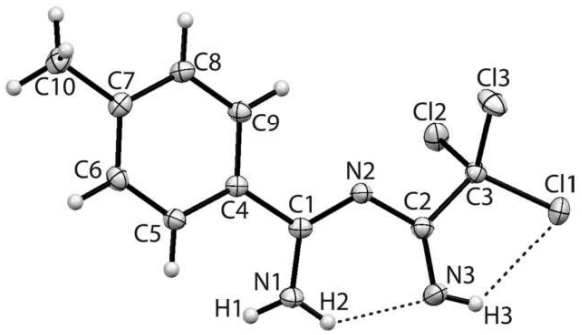

The major evidence for the assignment is provided by the ^{15}N coupled gHSQC spectrum shown below. Additional NMR spectra from this study are included with the archival NMR spectra at the end of this report. In short, H3 is deshielded by interaction with the CCl_3 group, H2 is strongly line broadened in the ^{1}H spectrum from bridging between N1 and N3, and H1 is at the more natural chemical shift expected for an imino NH. The ^{15}N signals correlate in the expected fashion for

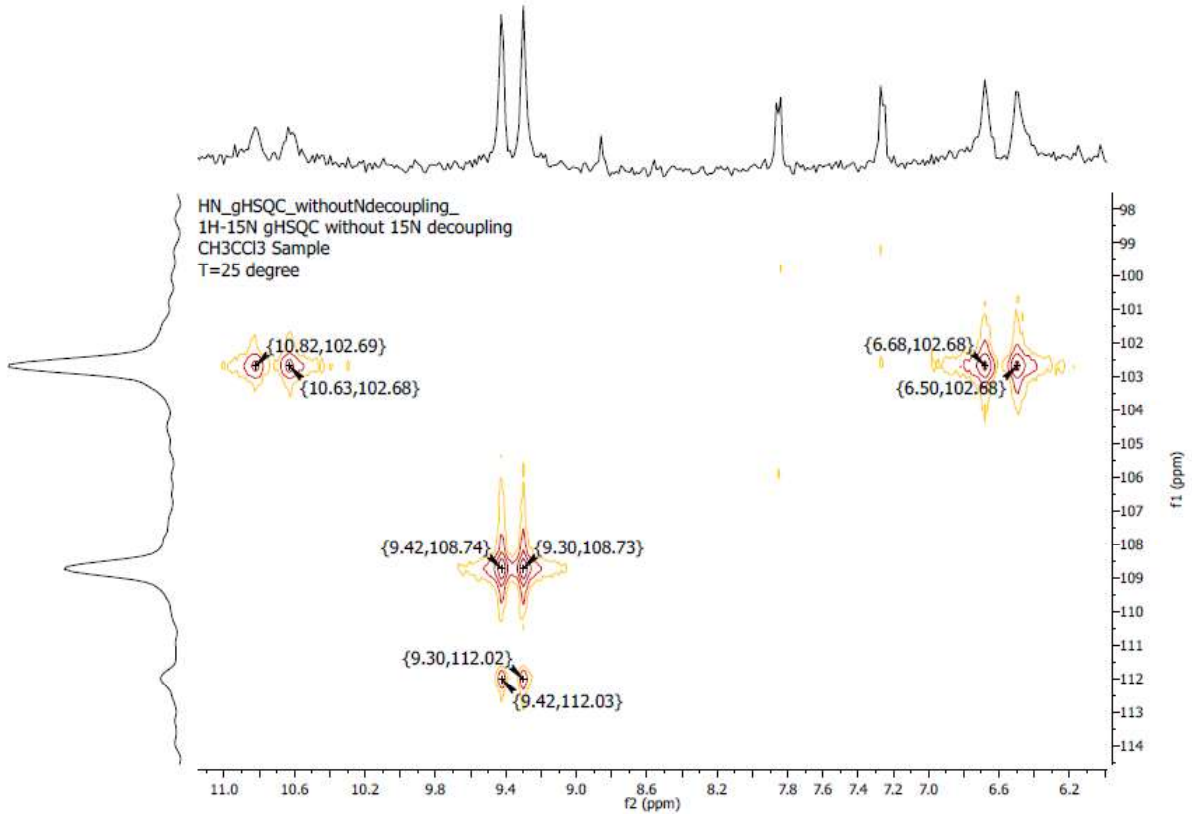

Fig. S1. ^{15}N coupled gHSQC spectrum of **1b** in $CDCl_3$ solution.

Section 3. Details and Additional Information on the X-ray Crystal Structure Determinations

Crystallography. Details of the crystallographic structure determinations for **3e** – **4e** are summarized in Table S4. Crystals for all the samples, irrespective of how the bulk solids were purified, were directly harvested from cold solutions in CH_3CN, immersed in Paratone™ oil, mounted in the oil on fine extruded glass capillaries and cooled directly on the goniometer with the Kryoflex cooling accessory on the Bruker D8-APEX II diffractometer, equipped with the APEX 2 CCD detector. Hemispheres of data were collected, and the intensities harvested, integrated and corrected using SAINT-Plus.[4] Multi-scan absorption corrections were applied using SADABS.[4] All the structures were solved with SHELXTL-2014 [5] in the Olex2 1.5alpha environment.[6] A full refinement in the independent atom model (IAM) was completed using olex2.refine,[7] and this model was archived. HAR was performed using ORCA 5.0 [8] for calculation of the ESD via density functional theory (DFT) first with a double-ζ basis set, after which NoSpherA2 computed aspherical atomic scattering factors on the fly from a Hirshfeld-partitioned ED for the neutral molecular fragments embedded in an electrostatic crystal field by employing cluster charges.[9] Careful release of the H-atom positions, followed by anisotropic refinement, usually with spherical restraints (RIGU or ISOR), occurred in a subsequent olex2.refine multicycle refinement. Once a satisfactory model was established, the HAR procedure was repeated and refined to convergence, with ED calculations at the R2SCAN/def2-TZVP level of theory. HAR worked extremely well for **3e** and **4a-d**. For **4b**, attempted free refinement of the methyl group H atoms immediately failed. A difference map on a model where all the remaining atoms are anisotropically refined provided strong evidence for six H atom positions, rotationally disordered about C10. The final model re-implemented a riding model for the two rotamers, with the C–H distances adjusted to the neutron diffraction value over this temperature range and constraining the isotropic displacements of each set of three hydrogens to the same value. An excellent two-part disorder model could be refined in a 52:48 occupancy ratio. HAR proved challenging for **4e**, and much effort was expended in reviewing the raw data. However, in the end, the original Bruker SAINT twin refinement and twin absorption correction using SADABS (2008) proved the best attainable. Only the first component of the twin data was retained, and the twin law (-1 0 0 0 -1 0 0.533 0.143) was employed in the refinement. Much of the structure was disordered (S–Cl, the CCl_3 chlorine and the CF_3 fluorine atoms. A full twin and disorder HAR was accomplished with NoSpherA2, and the resultant model was carefully assessed for overall quality and consistency. As in previous experience, the model improvement judged on the average precision of the C–C bonds (PLATON) in the case of **4e** (Table S5) of 14.9% is lower, at about half that of the average improvement in this value of 32.2% for all the structures. Nevertheless, the model precision improvement is not negligible, so the HAR was retained over the same model refined in the IAM.

Archival structural data have been deposited under Acquisition Codes 2244424-2244429. These data can be obtained free of charge from The Cambridge Crystallographic Data Centre via their website at www.ccdc.cam.ac.uk/data_request/cif. Data analysis was performed, and illustrations prepared, with Mercury CSD 2022.2.[10]

The crystal structures of **3e** and **4a–d** have only one independent molecule in their unit cells, while **4e** has two independent molecules in the asymmetric units in $P\overline{1}$. The six-membered C_2N_3S ring is effectively planar over the C_2N_3 moiety, with a small 'envelope' tilt angle for the N1,2S component (Fig. 3). In all cases the S-Cl bond is oriented almost perpendicular to the major ring plane. An exception to this is the second component of the disordered S–Cl units modelled for **4e**, for which the S atom is located closer to the plane defined by the C_2N_3 moiety, and the S–Cl bond is tilted outwards at a pronounced angle. We had expected to find evidence for an oxide impurity at S on the opposite side of the ring, by analogy with the planar C_2N_3S ring found in the SC-XRD structure of $Cl_2C_2N_3S(=O)Cl$ (CSD refcode: HANDIK).[11] However, even in the NoSpherA2/HAR, which has exquisite resolution of the residual electron density (ED), there is zero evidence in a final difference map for such an impurity. Notably, the datasets measured for **4e** evidence twinning and

have other substantial disorders, so most likely that is the true cause of these strange S and Cl atom positions. The observed 'normal' S–Cl orientation are consistent with other reports of thiazyl rings bearing covalent chlorides.[12,13,14]

Table S4. Crystallographic data collection and refinement parameters for crystal structures **3e - 4e**.

Parameter	**3e**	**4a**	**4b**	**4c**	**4d**	**4e**
Formula	$C_{10}H_4ClF_6N_3S$	$C_{10}H_7Cl_4N_3OS$	$C_{10}H_7Cl_4N_3S$	$C_9H_5Cl_4N_3S_2$	$C_9H_4Cl_5N_3S$	$C_{10}H_4Cl_4F_3N_3S$
FW (g/mol)	347.672	359.063	343.063	329.036	363.481	397.035
Temp. (K)	173 (1)	173 (1)	173 (1)	173 (1)	173 (1)	173 (1)
Cryst syst	monoclinic	monoclinic	monoclinic	monoclinic	monoclinic	triclinic
Space Grp	$P2_1/c$	$P2_1/c$	$P2_1/c$	$P2_1/n$	$P2_1/n$	$P\bar{1}$
A (Å)	14.5920(14)	5.4833(4)	11.8279(8)	7.411(2)	7.858(7)	5.3976(8)
b (Å)	11.8343(11)	15.7371(13)	5.4047(4)	11.314(3)	5.433(5)	8.9647(14)
c (Å)	7.4331(7)	16.1685(13)	21.1692(15)	15.046(4)	30.80(3)	30.761(5)
A (°)	90	90	90	90	90	90.823(2)
β (°)	94.772(1)	96.804(1)	91.443(1)	93.955(3)	93.686(12)	92.513(2)
γ (°)	90	90	90	90	90	97.992(2)
Volume (Å^3)	1279.1(2)	1385.37(19)	1352.84(17)	1258.6(6)	1312(2)	1472.2(4)
Z	4	4	4	4	4	4
Z'	1	1	1	1	1	2
ρ_{calc} (g/cm^3)	1.805	1.722	1.684	1.736	1.840	1.791
μ (mm^{-1})	0.530	0.998	1.012	1.084	1.246	0.971
F(000)	689.7	723.2	691.1	659.1	723.7	787.3
Cryst.size mm^3	0.17×0.14×0.14	0.34×0.3×0.04	0.30×0.19×0.12	0.28×0.19×0.18	0.31×0.23×0.08	0.42×0.11×0.06
Radiation	Mo Kα (λ = 0.71073)					
2Θ dat. col. (°)	4.44 to 57.66	3.62 to 54.08	3.44 to 57.58	4.5 to 57.46	5.28 to 57.58	3.98 to 50.06
k range	-19 ≤ h ≤ 19	-6 ≤ h ≤ 6	-15 ≤ h ≤ 15	-10 ≤ h ≤ 10	-10 ≤ h ≤ 10	-7 ≤ h ≤ 7
k range	-15 ≤ k ≤ 15	-20 ≤ k ≤ 20	-6 ≤ k ≤ 7	-14 ≤ k ≤ 15	-7 ≤ k ≤ 7	-12 ≤ k ≤ 12
l range	-9 ≤ l ≤ 10	-20 ≤ l ≤ 20	-28 ≤ l ≤ 28	-20 ≤ l ≤ 20	-41 ≤ l ≤ 41	-41 ≤ l ≤ 40
Rfl. collec.	14808	15090	15096	14476	18474	21458
R_{int}/R_{sigma}	0.0221, 0.0178	0.0225, 0.0172	0.0276, 0.0214	0.0169, 0.0131	0.0190, 0.0131	0.0537, 0.0506
Dat/rest/para	3136/90/253	3014/0/235	3333/6/204	3107/0/199	3251/0/199	5145/152/542
GOF on F^2	1.038	1.053	1.026	1.054	1.052	1.027
R_1[a] [I ≥ 2σ(I)]	0.0232	0.0203	0.0205	0.0172	0.0202	0.0434
wR_2 [all data]	0.0465	0.0459	0.0475	0.0401	0.0418	0.1355
Larg.Peak/hol (e Å^{-3})	0.28/-0.28	0.35/-0.32	0.45/-0.44	0.39/-0.31	0.57/-0.49	0.41/-0.29
CCDC	2244424	2244427	2244425	2244428	2244426	2244429

Table S5. Summary of Results and Quality Analysis for NoSpherA2 Refinement of Structures.[a,b]

Structure	C-C bond precision in Å [c]	Deg. impr.	R_1	R_{int}	Data/par. ratio
3e	0.0015 – 0.0021	28.6%	0.0232	0.0221	12.4
4a	0.0018 – 0.0028	35.7%	0.0203	0.0225	12.8
4b	0.0015 – 0.0021	28.6%	0.0205	0.0276	16.3
4c	0.0015 – 0.0020	35.0%	0.0172	0.0169	15.6
4d	0.0015 – 0.0030	33.3%	0.0202	0.0190	16.2
4e	0.0063 – 0.0074	14.9%	0.0434	0.0519	9.5
Average	0.0012 – 0.0019	32.2%			

[c] C-C bond precision taken from PLATON.[15] First value given is C-C bond precision in Å from models refined using NoSpherA2, second value is from parallel refinements in the IAM.

Table S6. Selected interatomic distances and angles in the crystal structures of **3e** – **4e**.[a]

Atom	Atom	Atom	**3e**	**4a**	**4b**	**4c**	**4d**	**4e** (1)	**4e** (2)	Average
Cl1	S1		2.1463(5)	2.1841(5)	2.1742(5)	2.1871(6)	2.1643(15	2.147(9)	2.148(10)	2.171(15)
S1	N1		1.6104(9)	1.6045(10	1.6118(9)	1.6030(9)	1.6147(15	1.625(14)	1.630(14)	1.608(4)
S1	N3		1.6048(8)	1.5867(11	1.5872(9)	1.6001(9)	1.6018(14	1.641(13)	1.630(13)	1.596(8)
C1	N1		1.3263(13	1.3263(15	1.3218(12	1.3318(11	1.3245(18	1.332(6)	1.321(5)	1.326(3)
C1	N2		1.3218(12	1.3137(15	1.3211(12	1.3146(11	1.3234(16	1.346(5)	1.347(5)	1.319(4)
C2	N2		1.3488(12	1.3543(14	1.3490(12	1.3493(11	1.3501(16	1.328(5)	1.320(5)	1.350(2)
C2	N3		1.3301(12	1.3346(15	1.3376(13	1.3330(12	1.3345(17	1.303(6)	1.318(6)	1.334(2)
C1	C3		1.5324(14	1.5401(16	1.5407(13	1.5391(13	1.5409(18	1.547(5)	1.539(6)	1.539(3)
C2	C4		1.4747(13	1.4546(17	1.4648(13	1.4716(12	1.4760(18	1.468(6)	1.472(5)	1.468(8)
N1	S1	Cl1	100.57(4)	100.73(4)	100.47(4)	101.18(3)	99.78(4)	103.5(7)	103.6(7)	100.5(5)
N3	S1	Cl1	102.59(4)	102.17(5)	102.18(4)	100.70(3)	101.83(4)	102.0(7)	102.2(8)	101.9(6)
N3	S1	N1	108.17(5)	109.16(6)	108.91(5)	109.33(4)	108.64(5)	106.0(8)	106.0(8)	108.8(4)
C1	N1	S1	115.27(7)	115.55(8)	115.65(7)	114.97(6)	114.74(8)	117.3(5)	117.0(6)	115.2(3)
C2	N2	C1	117.16(8)	118.07(10	118.05(8)	118.53(8)	117.61(10	117.9(4)	118.1(4)	117.9(5)
C2	N3	S1	118.78(7)	118.52(9)	118.35(7)	118.03(7)	117.38(8)	115.6(5)	115.6(6)	118.2(5)
N2	C1	N1	130.34(9)	129.62(11	129.54(9)	129.55(8)	129.50(11	125.8(4)	126.0(4)	129.7(3)
C3	C1	N1	114.21(9)	113.96(10	114.37(8)	114.92(7)	114.63(10	116.8(4)	116.9(4)	114.4(3)
C3	C1	N2	115.45(9)	116.23(10	115.85(8)	115.48(7)	115.63(9)	117.2(4)	117.0(4)	115.7(3)
N3	C2	N2	126.01(9)	125.41(11	125.53(9)	125.46(8)	126.09(10	129.5(4)	129.0(4)	125.7(3)
C4	C2	N2	117.28(8)	117.33(11	117.64(9)	116.51(8)	116.60(10	115.1(4)	115.9(4)	117.1(4)
C4	C2	N3	116.65(8)	117.22(10	116.76(9)	118.03(8)	117.26(10	115.2(4)	114.9(4)	117.2(5)
N1C1N2C2N3			0.029	0.022	0.022	0.023	0.034	0.027	0.027	0.026(5)
Envelope angle/° [b]			19.40(7)	18.39(8)	19.07(7)	19.51(6)	23.26(8)	26.6(10)	27.2(10)	19.9(17)

[a] The average values are calculated omitting **4e**; errors on the averages are std. dev. [b] Tip angle between N1C1N2C2N3 and N1S1N3 planes.

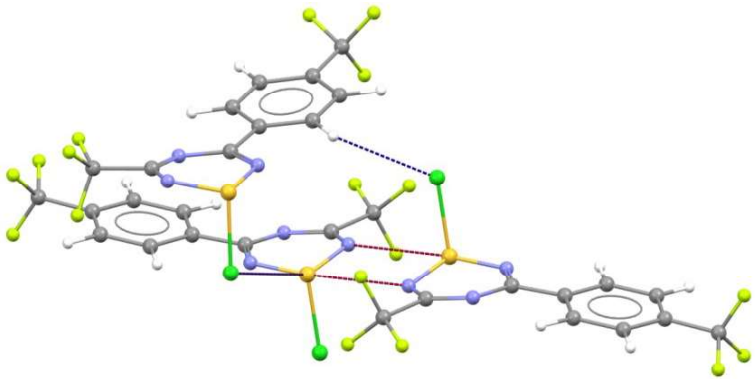

Fig. S2. Key intermolecular interactions in **3e**, drawn as ball and stick representations.

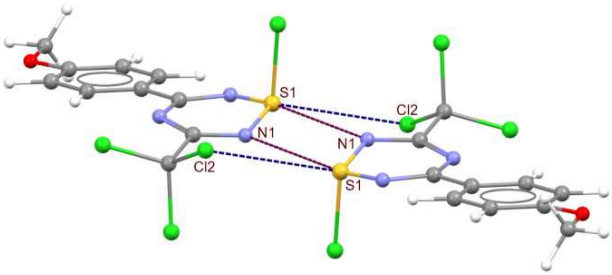

Fig. S3. Key intermolecular interactions in **4a**, drawn as ball and stick representations.

Table S7. All intermolecular contacts in **3e** – **4e** shorter than the $\sum r_{vdW}$.[a]

Atom1	Atom2	Length	Length-VdW	Symm. op. 1	Symm. op. 2
3e-CF3CF3SC					
S1	N1	3.047	-0.303	x,y,z	2-x,1-y,-z
H5	F6	2.46	-0.21	x,y,z	1-x,-1/2+y,1/2-z
S1	Cl1	3.465	-0.085	x,y,z	x,1.5-y,-1/2+z
F1	F5	2.856	-0.084	x,y,z	x,1.5-y,-1/2+z
Cl1	H9	2.913	-0.037	x,y,z	2-x,-1/2+y,1/2-z
Cl1	F2	3.186	-0.034	x,y,z	2-x,1-y,1-z
F4	F5	2.939	-0.001	x,y,z	x,2.5-y,-1/2+z
4a-MeOCCl3SCl					
Cl4	O1	2.901	-0.369	x,y,z	1-x,-y,2-z
C6	H10b	2.635	-0.265	x,y,z	-1+x,y,z
S1	N1	3.131	-0.219	x,y,z	1-x,1-y,2-z
C6	C6	3.185	-0.215	x,y,z	2-x,-y,2-z
Cl3	H8	2.793	-0.157	x,y,z	-1+x,1/2-y,1/2+z
H6	H5	2.268	-0.132	x,y,z	1-x,-y,2-z
H10a	Cl1	2.839	-0.111	x,y,z	1-x,-1/2+y,1.5-z
C9	Cl3	3.347	-0.103	x,y,z	x,1/2-y,-1/2+z
4b-TolCCl3SCl					
S1	N1	3.165	-0.185	x,y,z	1-x,1-y,1-z
H10b	Cl4	2.839	-0.111	x,y,z	-x,-1.5+y,1/2-z
Cl1	C7	3.399	-0.051	x,y,z	-x,1-y,1-z
H10b	C5	2.855	-0.045	x,y,z	-x,-1/2+y,1/2-z
H6	Cl4	2.918	-0.032	x,y,z	-x,-1/2+y,1/2-z
H10b	H5	2.375	-0.025	x,y,z	-x,-1/2+y,1/2-z
C2	Cl4	3.444	-0.006	x,y,z	x,-1+y,z
4c-PhCCl3SCl					
Cl4	Cl3	3.362	-0.138	-x,-y,1-z	-1/2+x,1/2-y,-1/2+z
H9	Cl4	2.814	-0.136	x,y,z	-1/2+x,1/2-y,-1/2+z
S1	N1	3.307	-0.043	x,y,z	-x,-y,1-z
4d-ClCCl3SCl					
Cl1	Cl4	3.347	-0.153	x,y,z	1-x,3-y,-z
Cl1	Cl1	3.405	-0.095	x,y,z	2-x,3-y,-z
Cl3	H8	2.914	-0.036	x,y,z	-1+x,1+y,z
Cl5	Cl2	3.489	-0.011	x,y,z	1.5-x,-1.5+y,1/2-z
C6	H5	2.907	0.007	x,y,z	1.5-x,-1/2+y,1/2-z
H6	H5	2.423	0.023	x,y,z	1.5-x,-1/2+y,1/2-z
Cl1	S1	3.585	0.035	x,y,z	2-x,2-y,-z
H6	Cl2	2.991	0.041	x,y,z	1.5-x,-1/2+y,1/2-z
S1	N1	3.422	0.072	x,y,z	1-x,2-y,-z
C2	Cl2	3.529	0.079	x,y,z	x,-1+y,z
4e-CF3CCl3SCl-S10Mol					
Cl10	Cl10	3.196	-0.304	x,y,z	-1-x,-y,1-z
S10	N12	3.203	-0.147	x,y,z	-x,1-y,1-z
C15	Cl12	3.392	-0.058	x,y,z	x,-1+y,z
Cl12	H15	2.914	-0.036	x,y,z	-1+x,1+y,z
Cl11	C10	3.432	-0.018	x,y,z	-1+x,y,z
Cl11	C13	3.443	-0.007	x,y,z	-1+x,y,z
4e-CF3CCl3SCl-S20mols					
Cl20	Cl20	3.155	-0.345	x,y,z	-x,1-y,-z
S20	N22	3.219	-0.131	x,y,z	1-x,2-y,-z
C25	Cl23	3.335	-0.115	x,y,z	x,-1+y,z
Cl21	C20	3.398	-0.052	x,y,z	-1+x,y,z

[a] Except **4d**, where contacts to +0.8 Å > $\sum r_{vdW}$ are included.

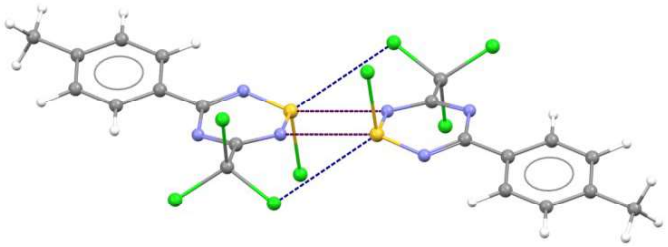

Fig. S4. Key intermolecular interactions in **4b**, drawn as ball and stick representations.

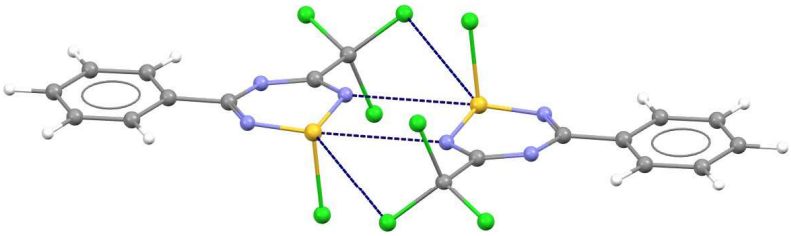

Fig. S5. Key intermolecular interactions in **4c**, drawn as ball and stick representations.

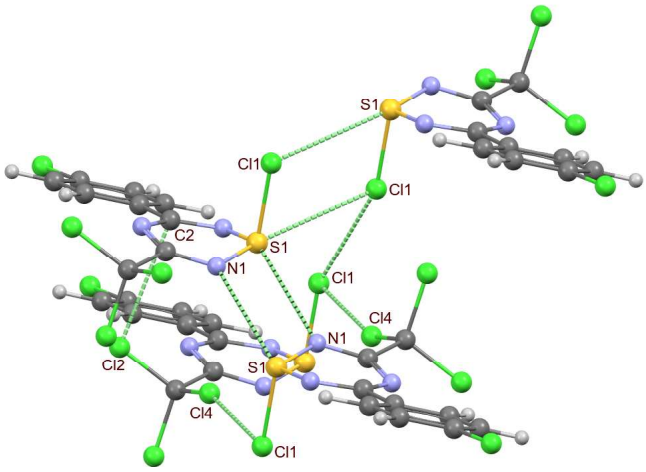

Fig. S6. Key intermolecular interactions in **4d**, drawn as ball and stick representations.

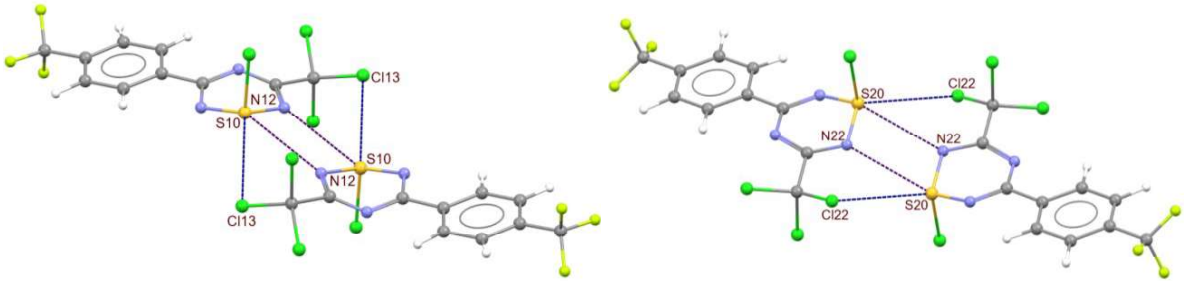

Fig. S7. Key intermolecular interactions in **4e**, drawn as ball and stick representations.

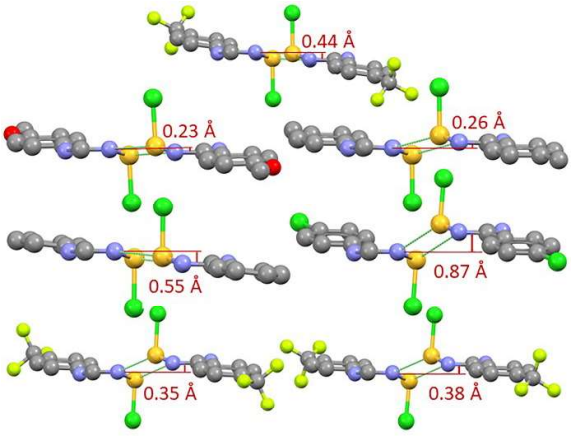

Fig. S8. Plots from the crystal structures of **3e** – **4e**, drawn perpendicular to the C_2N_3 planes, showing the offset distances of each of the interacting dimers. Top row: **3e**. Second row, left: **4a**; right: **4b**. Third row, left: **4c**; right: **4d**. Bottom row, left: **4e**-S10 molecule; right: **4e**-S20 molecule.

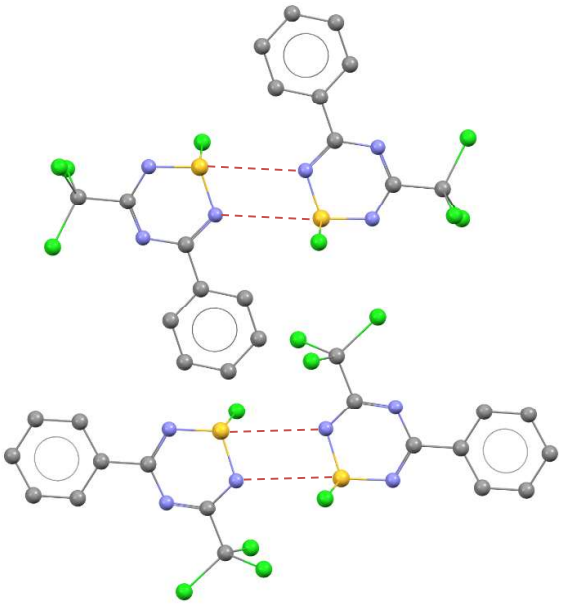

Fig. S9. The two sterically allowed dimer geometries conceivable in **4c**, (ball and stick): lower, the universally observed dimer with the CX_3 group adjacent to the next ring (S1N1); upper, the alternate symmetric orientation (S1N3) with the aryl group adjacent.

Section 4. Computational Chemistry

DFT Computational Methods. The geometries obtained from the SC-XRD HAR (ignoring minor components from disorder and using the first (S^{10}) molecule for **4e** were optimised in the gas phase using the well-known B3LYP functional [16,17] and the near CBS triple-ζ 6-311++G(d,p) basis set. NPA charges were calculated using normal bond order analysis. Minimum geometries were verified using harmonic vibrational analysis. The use of Grimme's D3 correction for dispersion, an attractive effect which is not readily accounted for by the bare B3LYP functional was applied in all cases.[18-20] Dimer geometries based on 'double $^{\delta+}S\cdots N^{\delta-}$' interactions were optimized first for two systems, namely the (model only) **3c** and **4c**, using the crystallographic dimer geometry obtained from **4c** as a starting point. Counterpoise corrections (CC) using the Boys–Bernardi [21] protocol were applied in two ways: first, the energy of the optimized dimer was calculated; then, the geometry was also re-optimized with CC, leading in all cases to a somewhat longer interaction distance, but quite comparable corrected interaction energies. The dimer models were evaluated both at the B3LYP-D3/6-311++G(d,p) and the M062X/aug-cc-VDZ levels of theory, the latter method chosen to match the models developed by Scheiner on 1,2,5-thiadiazole $\{^{\delta+}S\cdots N^{\delta-}\}_2$ dimers.[22] Based on the success with these first systems, all the structures under study were geometry optimized using B3LYP-D3/6-311++G(d,p)-CC, and were also computed for energy comparisons using M062X/aug-cc-VDZ-CC. Additional models were then computed for an 'amputated' model in which the CX_3 groups are replaced by H. A static (X-ray geometry) calculation on an $\{^{\delta+}S\cdots Cl^{\delta-}\}$ motif was additionally calculated with B3LYP-D3/6-311++G(d,p)-CC for **4d**, but this was not stable towards isolation as a 'free' dimer; instead the components re-organize towards the more stable $\{^{\delta+}S\cdots N^{\delta-}\}_2$ dimer geometry. The dimers optimized to well-defined minima but tended to have one small imaginary frequency for a 'hinge' motion at the monomer intersections; in the crystal lattice itself that motion would be countered by the full lattice interactions. Computed geometries are presented in Figs. S10, S12 and are tabulated in Table S8. ESP surfaces are presented in Fig. 11. All calculations were performed using Gaussian 16W on an AMD Ryzen Threadripper 16-core 3.75 Hz PC under Windows 10.[23]

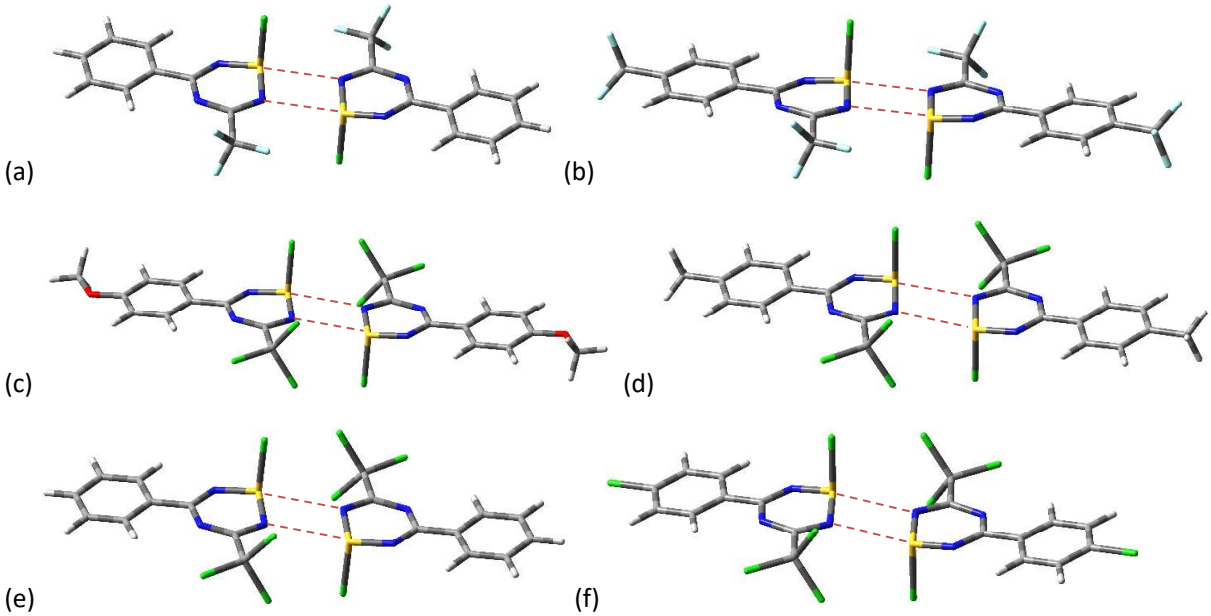

Figure S10. Optimized DFT computed geometries on model systems of (a) **3c** (b) **3e**, (c) **4a**, (d) **4b**, (e) **4c**, (f) **4d** from B3LYP-D3/6-311++D(d,p)-CC calculations.

Table S8. Selected interatomic distances and angles from computation compared to crystal structures.[a]

Atom	Atom	Atom	**3e**	**4a**	**4b**	**4c**	**4d**	**4e** (1)	**4e** (2)
Cl1	S1		2.1463(5)	2.1841(5)	2.1742(5)	2.1871(6)	2.1643(15)	2.147(9)	2.148(10)
			2.254	2.293	2.276	2.271	2.268	2.260	2.260
S1	N1		1.6104(9)	1.6045(10)	1.6118(9)	1.6030(9)	1.6147(15)	1.625(14)	1.630(14)
			1.647	1.628	1.645	1.645	1.646	1.646	1.646
S1	N3		1.6048(8)	1.5867(11)	1.5872(9)	1.6001(9)	1.6018(14)	1.641(13)	1.630(13)
			1.616	1.619	1.607	1.609	1.610	1.612	1.612
C1	N1		1.3263(13)	1.3263(15)	1.3218(12)	1.3318(11)	1.3245(18)	1.332(6)	1.321(5)
			1.319	1.332	1.318	1.318	1.318	1.317	1.317
C1	N2		1.3218(12)	1.3137(15)	1.3211(12)	1.3146(11)	1.3234(16)	1.346(5)	1.347(5)
			1.329	1.314	1.328	1.329	1.330	1.332	1.332
C2	N2		1.3488(12)	1.3543(14)	1.3490(12)	1.3493(11)	1.3501(16	1.328(5)	1.320(5)
			1.344	1.358	1.342	1.341	1.340	1.338	1.338
C2	N3		1.3301(12)	1.3346(15)	1.3376(13)	1.3330(12)	1.3345(17)	1.303(6)	1.318(6)
			1.344	1.340	1.352	1.350	1.350	1.347	1.347
C1	C3		1.5324(14)	1.5401(16)	1.5407(13)	1.5391(13)	1.5409(18)	1.547(5)	1.539(6)
			1.540	1.551	1.550	1.549	1.549	1.549	1.549
C2	C4		1.4747(13)	1.4546(17)	1.4648(13)	1.4716(12)	1.4760(18)	1.468(6)	1.472(5)
			1.476	1.461	1.467	1.471	1.470	1.476	1.476
N1	S1	Cl1	100.57(4)	100.73(4)	100.47(4)	101.18(3)	99.78(4)	103.5(7)	103.6(7)
			100.62	101.11	100.07	100.17	100.18	100.38	100.38
N3	S1	Cl1	102.59(4)	102.17(5)	102.18(4)	100.70(3)	101.83(4)	102.0(7)	102.2(8)
			103.49	101.59	104.09	103.98	103.94	103.77	103.77
N3	S1	N1	108.17(5)	109.16(6)	108.91(5)	109.33(4)	108.64(5)	106.0(8)	106.0(8)
			108.26	107.87	108.63	108.55	108.51	108.38	108.38
C1	N1	S1	115.27(7)	115.55(8)	115.65(7)	114.97(6)	114.74(8)	117.3(5)	117.0(6)
			114.73	115.64	115.04	115.09	115.15	115.25	115.25
C2	N2	C1	117.16(8)	118.07(10)	118.05(8)	118.53(8)	117.61(10)	117.9(4)	118.1(4)
			118.44	118.87	119.31	119.26	119.20	119.10	119.10
C2	N3	S1	118.78(7)	118.52(9)	118.35(7)	118.03(7)	117.38(8)	115.6(5)	115.6(6)
			117.70	118.27	117.48	117.43	117.33	117.20	117.20
N2	C1	N1	130.34(9)	129.62(11)	129.54(9)	129.55(8)	129.50(11)	125.8(4)	126.0(4)
			130.35	129.27	129.46	129.40	129.35	129.24	129.24
C3	C1	N1	114.21(9)	113.96(10)	114.37(8)	114.92(7)	114.63(10)	116.8(4)	116.9(4)
			115.79	113.44	116.42	116.46	116.49	116.58	116.58
C3	C1	N2	115.45(9)	116.23(10)	115.85(8)	115.48(7)	115.63(9)	117.2(4)	117.0(4)
			113.83	117.29	114.13	114.14	114.16	114.17	114.17
N3	C2	N2	126.01(9)	125.41(11)	125.53(9)	125.46(8)	126.09(10)	129.5(4)	129.0(4)
			125.65	125.24	125.09	125.25	125.40	125.70	125.70
C4	C2	N2	117.28(8)	117.33(11)	117.64(9)	116.51(8)	116.60(10)	115.1(4)	115.9(4)
			117.53	117.10	117.76	117.67	117.58	117.42	117.42
C4	C2	N3	116.65(8)	117.22(10)	116.76(9)	118.03(8)	117.26(10)	115.2(4)	114.9(4)
			116.75	117.62	117.09	117.01	116.96	116.82	116.82
Envelope angle/°			19.40(7)	18.39(8)	19.07(7)	19.51(6)	23.26(8)	26.6(10)	27.2(10)
			19.29	19.29	19.32	19.39	19.47	19.60	19.60

[a] X-ray data (equivalent to Table S6) are in red text. Computed values are presented in the second rows in black and are taken from the B3LYP-D3/6-311++D(d,p) calculations.

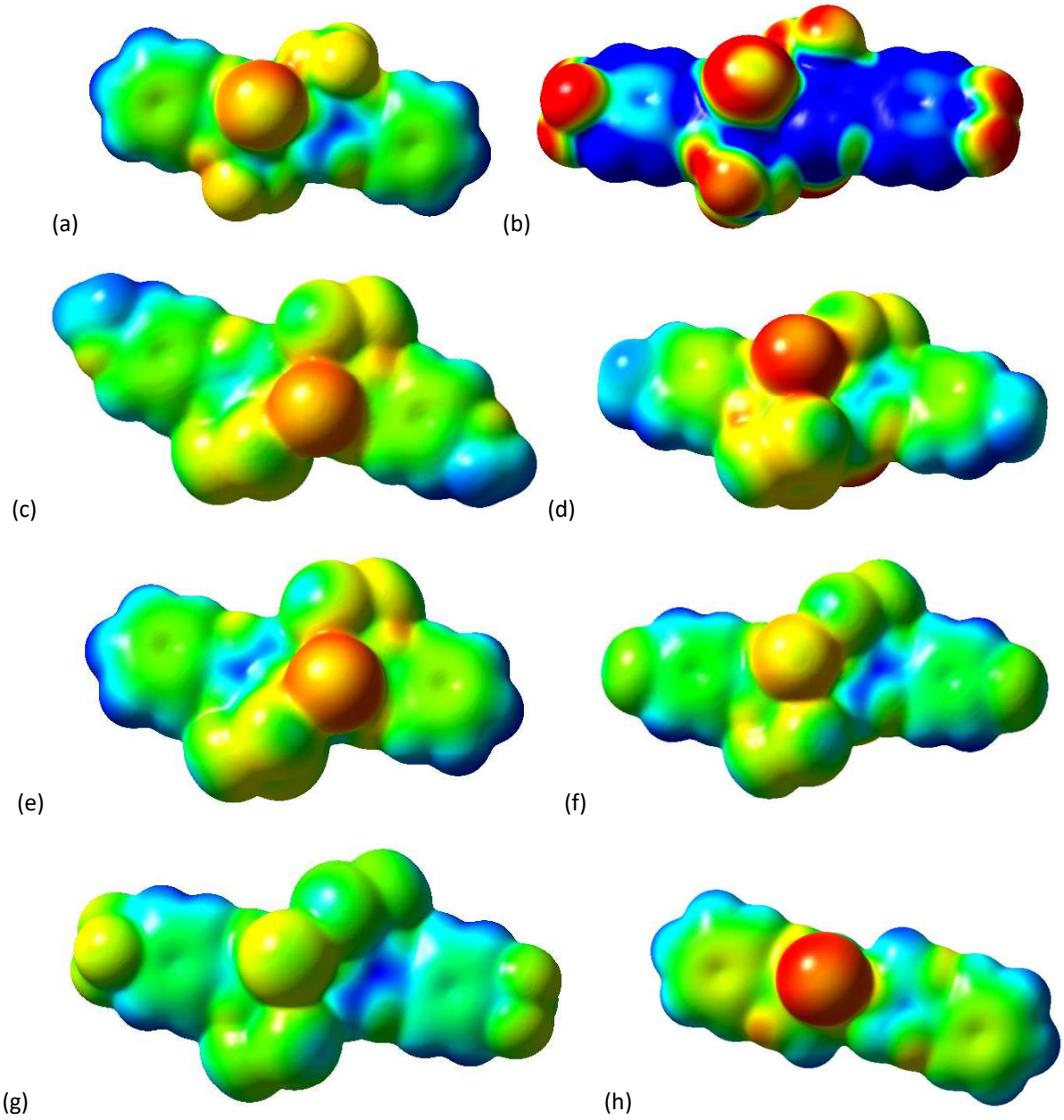

Figure S11. ESP surface plots computed at the B3LYP-D3/6-311++G(d,p) level of theory at the CC-optimized dimer geometry for (a) **3c**, (b) **3e**, (c) **4a**, (d) **4b**, (e) **4c**, (f) **4d**, (g) **4e**, (h) **5c**. Surfaces drawn in GaussView 6 (plot isovalues 0.004).[24]

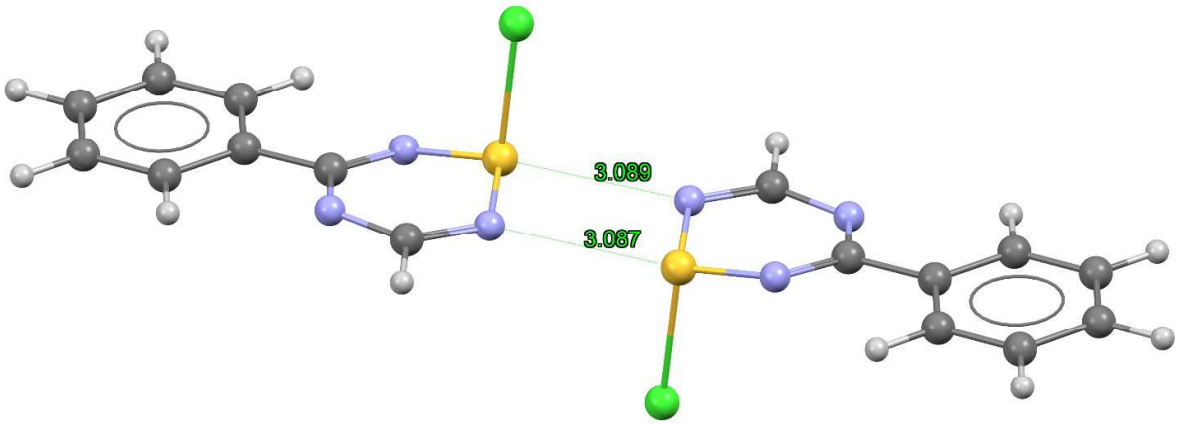

Fig. S12. Ball and stick plot of the optimized 'amputated' model **5c** with an H atom in place of the CX_3 groups. The calculated intermolecular S···N distances (Å) are shown (B3LYP-D3/6-311++G(d,p)-CC).

Since −24.3 kJ/mol as computed for the 'amputated' dimer, after optimization, is still large compared to the energy of $\{^{\delta+}S\cdots N1^{\delta-}\}_2$ interaction, we cannot rule out that that Cl1 (i.e. attached to S1) also has a significant interaction with neighbouring molecules (as it clearly does in the case of **4d** (Fig. S6). Further evidence for such interactions is found from the lattice structure of $Ph_2C_2N_3SCl$ (CSD refcode CILSAR, Fig. S13).[25] This long-known symmetrically substituted chlorothiatriazine displays a helical interaction (which is polymeric, along a 2_1 screw) consisting of a chain of $\{^{\delta+}S\cdots N1^{\delta-}\}_2$ contacts of 3.309(4) and 3.297(4) Å, further supported by $^{\delta+}S\cdots Cl^{\delta-}$ at 3.455(2) Å, all somewhat less than the $\sum r_{vdW}$ and of a comparable magnitude as in **4c** but considerably weaker than in **3e**.

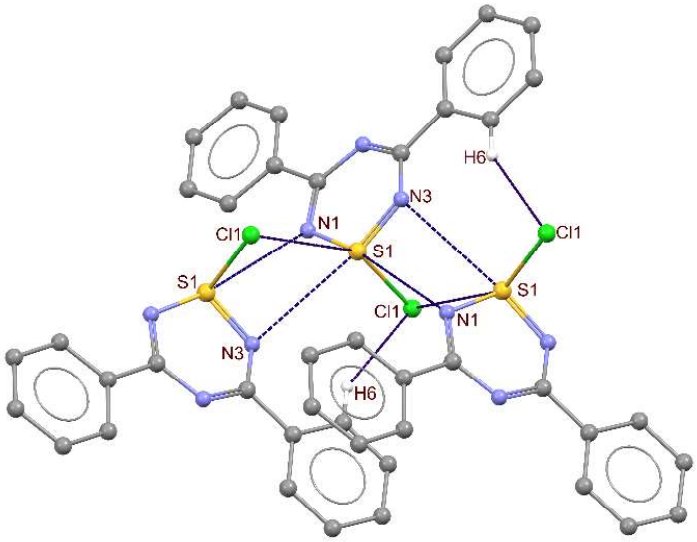

Figure S13. Intermolecular interactions in CILSAR,[25] showing the combined of $^{\delta+}S\cdots N^{\delta-}$ and $^{\delta+}S\cdots Cl^{\delta-}$ interactions.

References to the Supporting Information

1. Boeré, R. T.; Oakley, R.T.; Reed, R.W. *J. Organomet. Chem.* **1987**, *331*, 161.

2. Boeré, R. T., Roemmele, T. L., Yu, Xin (2011). *Inorg. Chem*. **50**, 5123.

3. Roemmele, T. L.; Boeré, R. T. *Acta Crystallogr., Sect. E:Struct. Rep. Online* **2011**, *67*, o3137.

4. Bruker (2008). *APEX2*, *SAINT-Plus* and *SADABS*. Bruker AXS Inc., Madison Wisconsin, USA.

5. Sheldrick, G., *Acta Crystallogr., Sect. A: Found. Adv.* **2015**, *71*, 3.

6. Dolomanov, O. V.; Bourhis, L. J.; Gildea, R. J.; Howard, J. A. K.; Puschmann, H., *J. Appl. Crystallogr.* **2009,** *42* (2), 339.

7. Bourhis, L. J.; Dolomanov, O. V.; Gildea, R. J.; Howard, J. A. K.; Puschmann, H., *Acta Crystallogr A Found Adv* **2015,** *71*, 59-75.

8. Neese, F., *WIREs Computational Molecular Science* **2022,** *12*, e1606.

9. Kleemiss, F.; Dolomanov, O. V.; Bodensteiner, M.; Peyerimhoff, N.; Midgley, L.; Bourhis, L. J.; Genoni, A.; Malaspina, L. A.; Jayatilaka, D.; Spencer, J. L.; White, F.; Grundkotter-Stock, B.; Steinhauer, S.; Lentz, D.; Puschmann, H.; Grabowsky, S., *Chem. Sci.* **2020,** *12*, 1675-1692.

10. C. F. Macrae, I. Sovago, S. J. Cottrell, P. T. A. Galek, P. McCabe, E. Pidcock, M. Platings, G. P. Shields, J. S. Stevens, M. Towler and P. A. Wood, J. Appl. Crystallogr., **2020**, *53*, 226.

11. Clark, T.J.; Lough, A.J.; Chivers, T.; Manners, I. *Acta Crystallogr., Sect. E: Struct. Rep. Online* **2004***, 60***,** o2402.

12. Chen, S -J.; Behrens, U.; Fischer, E.; Mews, R.; Pauer, F.; Sheldrick, G. M.; Stalke, D.; Stohrer, W.-D. *Chem.Ber.* **1993**, *126***,** 2601.

13. Graham, J. B. III; Cordes, A. W.; Oakely, R. T.; Boeré, R. T. *Acta Crystallogr., Sect. C: Cryst. Struct. Commun.* **1985**, *41*, 1835.

14. Boeré, R. T.; Oakely, R. T.; Cordes, A. W. *Acta Crystallogr., Sect. C: Cryst. Struct. Commun.* **1985**, *41*, 1686.

15. Spek, A. L., *J. Appl. Cryst.* **2002,** *36*, 7.

16. A. D. Becke, *J. Chem. Phys.* **1993**, *98*, 5648.

17. C. Lee, W. Yang, R. G. Parr, *Phys. Rev. B.* **1988**, *37*, 785.

18. S. Grimme, J. Antony, S. Ehrlich, H. Krieg, *J. Chem. Phys.* **2010**, *132*, 154104.

19. J. Antony, S. Grimme, *Phys. Chem. Chem. Phys.* **2006**, *8*, 5287.

20. L. Goerigk, S. Grimme, *Phys. Chem. Chem. Phys.* **2011**, *13*, 6670.

21. Gray, M.; Bowling, P. E.; Herbert, J. M. *J. Chem. Theory Comput.* **2022**, *18*, 6742.

22. Scheiner, S. *J. Phys. Chem. A* **2022**, *126*, 1194.

23. Gaussian 16, Revision C.01, M. J. Frisch, G. W. Trucks, H. B. Schlegel, G. E. Scuseria, M. A. Robb, J. R. Cheeseman, G. Scalmani, V. Barone, G. A. Petersson, H. Nakatsuji, X. Li, M. Caricato, A. V. Marenich, J. Bloino, B. G. Janesko, R. Gomperts, B. Mennucci, H. P. Hratchian, J. V. Ortiz, A. F. Izmaylov, J. L. Sonnenberg, D. Williams-Young, F. Ding, F. Lipparini, F. Egidi, J. Goings, B. Peng, A. Petrone, T. Henderson, D. Ranasinghe, V. G. Zakrzewski, J. Gao, N. Rega, G. Zheng, W. Liang, M. Hada, M. Ehara, K. Toyota, R. Fukuda, J. Hasegawa, M. Ishida, T. Nakajima, Y. Honda, O. Kitao, H. Nakai, T. Vreven, K. Throssell, J. A. Montgomery, Jr., J. E. Peralta, F. Ogliaro, M. J. Bearpark, J. J. Heyd, E. N. Brothers, K. N. Kudin, V. N. Staroverov, T. A. Keith, R. Kobayashi, J. Normand, K. Raghavachari, A. P. Rendell, J. C. Burant, S. S. Iyengar, J. Tomasi, M. Cossi, J. M. Millam, M. Klene, C. Adamo, R. Cammi, J. W. Ochterski, R. L. Martin, K. Morokuma, O. Farkas, J. B. Foresman, and D. J. Fox, Gaussian, Inc., Wallingford CT, 2016.

24. GaussView, Version 6.1.1, Roy Dennington, Todd Keith, and John Millam, Semichem Inc., Shawnee Mission, KS, 2019.

25. Cordes, A. W.; Haynes, P. J.; Josephy, P. D.; Koenig, H.; Oakley, R. T.; Pennington, W. T. *J. Chem. Soc. Chem. Comm.* **1984**, 1021.

Detailed Crystal Structure Reports

3e

Table 1 Crystal data and structure refinement for 3e.

Identification code	rb0672a
Empirical formula	$C_{10}H_4ClF_6N_3S$
Formula weight	347.672
Temperature/K	273.15
Crystal system	monoclinic
Space group	$P2_1/c$
a/Å	14.5920(14)
b/Å	11.8343(11)
c/Å	7.4331(7)
α/°	90
β/°	94.772(1)
γ/°	90
Volume/Å^3	1279.1(2)
Z	4
ρ_{calc}g/cm^3	1.805
μ/mm^{-1}	0.530
F(000)	689.7
Crystal size/mm^3	0.17 × 0.14 × 0.14
Radiation	Mo Kα (λ = 0.71073)
2Θ range for data collection/°	4.44 to 57.66
Index ranges	-19 ≤ h ≤ 19, -15 ≤ k ≤ 15, -9 ≤ l ≤ 10
Reflections collected	14808
Independent reflections	3136 [R_{int} = 0.0221, R_{sigma} = 0.0178]
Data/restraints/parameters	3136/90/253
Goodness-of-fit on F^2	1.038
Final R indexes [I>=2σ (I)]	R_1 = 0.0232, wR_2 = 0.0435
Final R indexes [all data]	R_1 = 0.0317, wR_2 = 0.0465
Largest diff. peak/hole / e Å^{-3}	0.28/-0.28

Table 2 Fractional Atomic Coordinates (×10^4) and Equivalent Isotropic Displacement Parameters (Å^2×10^3) for 3e. U_{eq} is defined as 1/3 of the trace of the orthogonalised U_{IJ} tensor.

Atom	*x*	*y*	*z*	U(eq)
Cl1	10364.8(2)	6313.9(3)	3239.9(5)	47.59(9)
S1	9585.50(18)	6431.8(2)	667.6(4)	30.99(7)
F1	6960.1(5)	4142.6(6)	1908.5(14)	70.6(3)
F2	8247.9(7)	3652.3(6)	3216.1(11)	65.2(2)
F3	7976.7(6)	3405.2(6)	384.8(10)	54.2(2)
N1	9034.8(6)	5251.8(7)	635.6(12)	30.4(2)
N2	7785.1(6)	6126.3(7)	2024.8(11)	26.62(18)

Table 2 Fractional Atomic Coordinates (×10^4) and Equivalent Isotropic Displacement Parameters (Å^2×10^3) for 3e. U_{eq} is defined as 1/3 of the trace of the orthogonalised U_{IJ} tensor.

Atom	*x*	*y*	*z*	U(eq)
N3	8872.6(6)	7430.2(7)	987.0(13)	33.4(2)
C1	8255.5(7)	5267.1(8)	1435.2(13)	26.2(2)
C2	8081.5(6)	7174.4(8)	1658.6(13)	23.6(2)
C3	7844.9(8)	4095.6(9)	1723.5(16)	35.7(3)
C4	7454.4(6)	8123.3(8)	1941.7(13)	22.9(2)
C5	6583.0(7)	7914.3(9)	2516.9(15)	29.8(2)
C6	5976.6(8)	8805.4(10)	2704.4(16)	35.5(3)
C7	6246.0(7)	9901.4(9)	2316.9(14)	32.7(2)
C8	7117.4(8)	10118.5(9)	1769.7(15)	32.3(2)
C9	7724.4(8)	9229.3(8)	1583.5(14)	28.4(2)
C10	5585.4(9)	10864.8(11)	2455.7(19)	46.5(3)
F4	5566(2)	11528(3)	1065(4)	97.8(13)
F5	5710(2)	11420(2)	3880(3)	92.3(7)
F6	4699.3(10)	10480.7(14)	2383(6)	95.6(7)
F4A	5147(4)	11124(5)	1035(5)	95(2)
F5A	6071.3(19)	11874(2)	2891(6)	80.1(10)
F6A	5068(3)	10785(3)	3746(6)	82.7(10)

Table 3 Anisotropic Displacement Parameters (Å^2×10^3) for 3e. The Anisotropic displacement factor exponent takes the form: $-2\pi^2[h^2a^{*2}U_{11}+2hka^*b^*U_{12}+\ldots]$.

Atom	U_{11}	U_{22}	U_{33}	U_{12}	U_{13}	U_{23}
Cl1	32.41(15)	49.18(18)	59.4(2)	11.62(13)	-6.67(13)	-20.69(15)
S1	28.70(14)	24.40(13)	41.40(15)	5.42(10)	12.10(11)	0.13(11)
F1	48.8(5)	30.8(4)	135.3(8)	-10.3(3)	25.7(5)	-4.7(5)
F2	102.5(7)	37.3(4)	52.8(5)	-10.5(4)	-11.5(4)	16.4(4)
F3	79.4(6)	27.4(4)	56.2(5)	-6.4(3)	7.1(4)	-13.0(3)
N1	32.7(5)	24.6(4)	34.3(5)	5.1(4)	5.1(4)	-6.2(4)
N2	28.4(4)	20.3(4)	31.8(4)	1.7(3)	6.0(4)	0.1(3)
N3	28.8(5)	22.2(4)	51.2(6)	4.8(4)	15.5(4)	4.6(4)
C1	29.5(5)	19.8(5)	29.3(5)	2.1(4)	1.4(4)	-1.7(4)
C2	23.7(5)	20.6(5)	27.1(5)	3.0(4)	4.4(4)	0.0(4)
C3	41.7(6)	21.3(5)	43.8(7)	-0.9(5)	1.8(5)	-0.8(5)
C4	21.7(5)	19.7(5)	27.4(5)	2.0(4)	2.2(4)	-1.1(4)
C5	23.5(5)	24.8(5)	41.6(6)	1.7(4)	6.8(4)	0.9(5)
H5	44(9)	31(8)	80(11)	-14(7)	15(8)	4(8)
C6	24.9(6)	33.2(6)	49.2(7)	6.1(5)	8.6(5)	0.2(5)
H6	33(8)	58(10)	100(13)	3(7)	27(9)	9(9)
C7	31.7(6)	29.2(6)	37.3(6)	11.4(4)	4.3(5)	-1.3(4)
C8	35.6(6)	21.0(5)	41.0(6)	6.5(4)	6.6(5)	0.5(4)
H8	55(10)	29(8)	89(12)	6(7)	23(8)	5(8)
C9	27.8(6)	20.5(5)	37.3(6)	1.6(4)	6.1(4)	-0.4(4)
H9	40(9)	41(9)	80(11)	-4(7)	31(8)	5(8)

Table 3 Anisotropic Displacement Parameters ($Å^2×10^3$) for 3e. The Anisotropic displacement factor exponent takes the form: $-2π^2[h^2a^{*2}U_{11}+2hka^*b^*U_{12}+…]$.

Atom	U_{11}	U_{22}	U_{33}	U_{12}	U_{13}	U_{23}
C10	45.4(7)	39.3(7)	55.4(8)	21.3(6)	6.7(6)	-1.2(6)
F4	113(3)	77.1(19)	109(3)	67.1(16)	47(2)	52.9(18)
F5	95.8(18)	93.5(18)	83.7(15)	60.8(14)	-16.0(12)	-49.9(13)
F6	34.7(8)	51.5(10)	202(3)	20.1(7)	15.6(13)	-5.7(15)
F4A	110(4)	107(4)	60(2)	82(3)	-45(3)	-32(3)
F5A	63.5(17)	37.5(13)	140(3)	21.0(11)	12(2)	-22.7(16)
F6A	89(2)	70(2)	97(2)	47.2(18)	57(2)	18.4(17)

Table 4 Bond Lengths for 3e.

Atom	Atom	Length/Å	Atom	Atom	Length/Å
Cl1	S1	2.1463(5)	C4	C9	1.3989(14)
S1	N1	1.6104(9)	C5	C6	1.3912(14)
S1	N3	1.6048(8)	C6	C7	1.3923(16)
F1	C3	1.3109(14)	C7	C8	1.3908(15)
F2	C3	1.3204(13)	C7	C10	1.5021(15)
F3	C3	1.3140(13)	C8	C9	1.3897(14)
N1	C1	1.3263(13)	C10	F4	1.296(3)
N2	C1	1.3218(12)	C10	F5	1.247(2)
N2	C2	1.3488(12)	C10	F6	1.367(2)
N3	C2	1.3301(12)	C10	F4A	1.227(4)
C1	C3	1.5324(14)	C10	F5A	1.412(3)
C2	C4	1.4747(13)	C10	F6A	1.272(3)
C4	C5	1.3968(14)			

Table 5 Bond Angles for 3e.

Atom	Atom	Atom	Angle/˚	Atom	Atom	Atom	Angle/˚
N1	S1	Cl1	100.57(4)	C10	C7	C8	119.17(10)
N3	S1	Cl1	102.59(4)	C9	C8	C7	119.67(10)
N3	S1	N1	108.17(5)	C8	C9	C4	119.84(10)
C1	N1	S1	115.27(7)	F4	C10	C7	112.11(18)
C2	N2	C1	117.16(8)	F5	C10	C7	114.17(13)
C2	N3	S1	118.78(7)	F5	C10	F4	110.5(2)
N2	C1	N1	130.34(9)	F6	C10	C7	110.80(12)
C3	C1	N1	114.21(9)	F6	C10	F4	102.24(19)
C3	C1	N2	115.45(9)	F6	C10	F5	106.2(2)
N3	C2	N2	126.01(9)	F4A	C10	C7	115.0(2)
C4	C2	N2	117.28(8)	F4A	C10	F4	35.7(3)
C4	C2	N3	116.65(8)	F4A	C10	F5	128.9(2)
F2	C3	F1	107.60(10)	F4A	C10	F6	68.0(3)
F3	C3	F1	108.25(10)	F5A	C10	C7	110.16(14)
F3	C3	F2	107.83(9)	F5A	C10	F4	69.4(2)
C1	C3	F1	112.10(9)	F5A	C10	F5	47.52(16)

Table 5 Bond Angles for 3e.

Atom	Atom	Atom	Angle/˚	Atom	Atom	Atom	Angle/˚
C1	C3	F2	108.97(9)	F5A	C10	F6	138.16(15)
C1	C3	F3	111.91(9)	F5A	C10	F4A	101.6(3)
C5	C4	C2	120.02(9)	F6A	C10	C7	114.80(15)
C9	C4	C2	119.83(9)	F6A	C10	F4	132.2(2)
C9	C4	C5	120.13(9)	F6A	C10	F5	56.8(2)
C6	C5	C4	119.95(10)	F6A	C10	F6	52.2(2)
C7	C6	C5	119.50(10)	F6A	C10	F4A	111.6(3)
C8	C7	C6	120.89(10)	F6A	C10	F5A	102.0(3)
C10	C7	C6	119.93(10)				

Table 6 Torsion Angles for 3e.

A	B	C	D	Angle/˚	A	B	C	D	Angle/˚
Cl1	S1	N1	C1	85.73(6)	N3	C2	C4	C5	175.31(9)
Cl1	S1	N3	C2	-87.19(6)	N3	C2	C4	C9	-2.87(11)
S1	N1	C1	N2	11.23(10)	C2	C4	C5	C6	-177.07(10)
S1	N1	C1	C3	-168.37(7)	C2	C4	C9	C8	177.01(10)
S1	N3	C2	N2	-3.73(10)	C4	C5	C6	C7	-0.07(12)
S1	N3	C2	C4	179.46(7)	C4	C9	C8	C7	0.20(12)
F1	C3	C1	N1	-157.71(10)	C5	C6	C7	C8	-0.91(14)
F1	C3	C1	N2	22.63(11)	C5	C6	C7	C10	177.98(11)
F2	C3	C1	N1	83.30(10)	C6	C7	C8	C9	0.84(13)
F2	C3	C1	N2	-96.36(10)	C6	C7	C10	F4	-133.6(2)
F3	C3	C1	N1	-35.86(11)	C6	C7	C10	F5	99.8(2)
F3	C3	C1	N2	144.48(9)	C6	C7	C10	F6	-20.0(2)
N1	C1	N2	C2	5.91(13)	C6	C7	C10	F4A	-94.7(4)
N2	C2	C4	C5	-1.78(11)	C6	C7	C10	F5A	151.2(2)
N2	C2	C4	C9	-179.97(9)	C6	C7	C10	F6A	36.8(3)

Table 7 Hydrogen Atom Coordinates (Å×10^4) and Isotropic Displacement Parameters (Å^2×10^3) for 3e.

Atom	*x*	*y*	*z*	U(eq)
H5	6397(9)	7064(11)	2809(19)	51(4)
H6	5294(9)	8654(11)	3120(20)	63(5)
H8	7322(9)	10975(11)	1480(20)	57(4)
H9	8409(9)	9384(11)	1155(19)	52(4)

Table 8 Atomic Occupancy for 3e.

Atom	*Occupancy*	Atom	*Occupancy*	Atom	*Occupancy*
F4	0.610000	F5	0.610000	F6	0.610000
F4A	0.390000	F5A	0.390000	F6A	0.390000

4a

Table 1 Crystal data and structure refinement for 4A.

Identification code	RB06052
Empirical formula	$C_{10}H_7Cl_4N_3OS$
Formula weight	359.063
Temperature/K	173.15
Crystal system	monoclinic
Space group	$P2_1/c$
a/Å	5.4833(4)
b/Å	15.7371(13)
c/Å	16.1685(13)
α/°	90
β/°	96.804(1)
γ/°	90
Volume/Å^3	1385.37(19)
Z	4
ρ_{calc}g/cm^3	1.722
μ/mm^{-1}	0.998
F(000)	723.2
Crystal size/mm^3	0.34 × 0.3 × 0.04
Radiation	Mo Kα (λ = 0.71073)
2Θ range for data collection/°	3.62 to 54.08
Index ranges	-6 ≤ h ≤ 6, -20 ≤ k ≤ 20, -20 ≤ l ≤ 20
Reflections collected	15090
Independent reflections	3014 [R_{int} = 0.0225, R_{sigma} = 0.0172]
Data/restraints/parameters	3014/0/235
Goodness-of-fit on F^2	1.053
Final R indexes [I>=2σ (I)]	R_1 = 0.0203, wR_2 = 0.0429
Final R indexes [all data]	R_1 = 0.0285, wR_2 = 0.0459
Largest diff. peak/hole / e Å^{-3}	0.35/-0.32

Table 2 Fractional Atomic Coordinates (×10^4) and Equivalent Isotropic Displacement Parameters (Å^2×10^3) for 4A. U_{eq} is defined as 1/3 of the trace of the orthogonalised U_{IJ} tensor.

Atom	*x*	*y*	*z*	U(eq)
Cl2	780.2(6)	3926.3(2)	11110.0(2)	33.21(8)
Cl3	5270.7(6)	3260.1(3)	11986.16(19)	39.54(9)
Cl4	1631.4(6)	2136.9(2)	11158.4(2)	37.01(9)
Cl1	3010.4(7)	4198.0(3)	8367.2(2)	51.04(11)
S1	6207.3(6)	4133.6(2)	9309.2(2)	31.02(8)
O1	10711.9(18)	-532.9(6)	8536.7(6)	39.7(2)
N1	4898(2)	4012.7(7)	10137.7(6)	32.2(2)
N2	5086.5(18)	2503.2(6)	10001.6(6)	27.4(2)
N3	7436(2)	3262.1(7)	9089.5(7)	33.7(3)

Table 2 Fractional Atomic Coordinates (×10^4) and Equivalent Isotropic Displacement Parameters (Å^2×10^3) for 4A. U_{eq} is defined as 1/3 of the trace of the orthogonalised U_{IJ} tensor.

Atom	*x*	*y*	*z*	U(eq)
C1	4418(2)	3216.2(8)	10332.4(7)	25.1(3)
C2	6684(2)	2547.7(8)	9425.3(7)	25.8(3)
C3	3044(2)	3129.6(8)	11105.5(7)	26.2(3)
C4	7735(2)	1753.8(8)	9172.4(7)	25.7(3)
C9	9566(2)	1754.7(9)	8639.4(8)	29.0(3)
C8	10612(2)	1001.5(8)	8408.9(8)	29.5(3)
C7	9810(2)	232.8(8)	8709.2(7)	29.3(3)
C6	7979(3)	226.3(9)	9241.7(9)	34.7(3)
C5	6959(2)	977.6(9)	9472.8(8)	31.3(3)
C10	12496(3)	-588.4(12)	7968.9(11)	39.0(3)

Table 3 Anisotropic Displacement Parameters (Å^2×10^3) for 4A. The Anisotropic displacement factor exponent takes the form: $-2\pi^2[h^2a^{*2}U_{11}+2hka^*b^*U_{12}+\ldots]$.

Atom	U_{11}	U_{22}	U_{33}	U_{12}	U_{13}	U_{23}
Cl2	25.49(16)	38.77(18)	37.52(18)	3.83(13)	12.76(13)	0.97(14)
Cl3	27.10(16)	67.4(2)	24.26(16)	1.30(16)	3.63(12)	-3.52(15)
Cl4	41.76(19)	34.59(17)	38.49(18)	-5.89(14)	20.61(15)	-1.21(14)
Cl1	46.8(2)	67.2(3)	39.3(2)	6.44(19)	5.64(17)	15.50(18)
S1	32.89(17)	30.65(17)	32.39(17)	-1.07(13)	15.77(13)	1.82(13)
O1	47.0(6)	34.4(5)	41.5(5)	2.8(4)	21.2(5)	-1.5(4)
N1	37.7(6)	30.9(6)	31.2(6)	0.1(5)	16.7(5)	-0.5(5)
N2	27.1(5)	31.0(6)	26.4(5)	-2.0(4)	12.2(4)	-2.2(4)
N3	35.1(6)	33.6(6)	36.4(6)	-1.7(5)	20.3(5)	-0.1(5)
C1	23.5(6)	30.7(7)	22.5(6)	-1.4(5)	8.1(5)	-1.5(5)
C2	24.1(6)	31.3(7)	23.4(6)	-1.9(5)	8.6(5)	-2.0(5)
C3	22.8(6)	34.0(7)	22.8(6)	-0.4(5)	7.3(5)	-1.6(5)
C4	24.0(6)	32.6(7)	21.9(6)	-0.9(5)	8.2(5)	-1.9(5)
C9	29.7(7)	33.2(7)	26.4(6)	-1.5(6)	12.8(5)	0.1(5)
H9	48(10)	41(10)	48(11)	-2(8)	31(9)	-2(8)
C8	29.9(7)	34.9(7)	26.0(6)	0.6(5)	13.0(5)	-2.0(5)
H8	46(10)	57(11)	48(10)	14(9)	31(9)	-4(8)
C7	30.7(7)	33.2(7)	25.9(6)	0.1(5)	11.5(5)	-2.3(5)
C6	37.8(7)	32.4(8)	37.6(7)	-1.6(6)	20.0(6)	0.7(6)
H6	89(14)	43(11)	76(14)	-8(10)	55(12)	-1(10)
C5	31.4(7)	33.7(7)	31.9(7)	-1.2(6)	17.4(6)	-1.5(5)
H5	59(12)	46(11)	75(14)	-1(9)	24(11)	-7(10)
C10	38.1(9)	41.7(10)	39.7(9)	4.5(7)	14.5(7)	-7.1(8)
H10a	84(15)	118(19)	41(12)	29(13)	12(11)	-1(12)
H10b	46(11)	102(17)	60(13)	-11(12)	19(10)	-12(11)
H10c	124(19)	49(13)	94(16)	9(13)	55(14)	-8(12)

Table 4 Bond Lengths for 4A.

Atom	Atom	Length/Å	Atom	Atom	Length/Å
Cl2	C3	1.7647(12)	N2	C2	1.3543(14)
Cl3	C3	1.7745(12)	N3	C2	1.3346(15)
Cl4	C3	1.7502(12)	C1	C3	1.5401(16)
Cl1	S1	2.1841(5)	C2	C4	1.4546(17)
S1	N1	1.6045(10)	C4	C9	1.3983(16)
S1	N3	1.5867(11)	C4	C5	1.3993(17)
O1	C7	1.3442(15)	C9	C8	1.3868(18)
O1	C10	1.4215(16)	C8	C7	1.3938(17)
N1	C1	1.3263(15)	C7	C6	1.3980(17)
N2	C1	1.3137(15)	C6	C5	1.3783(18)

Table 5 Bond Angles for 4A.

Atom	Atom	Atom	Angle/˚	Atom	Atom	Atom	Angle/˚
N1	S1	Cl1	100.73(4)	Cl4	C3	Cl3	109.30(7)
N3	S1	Cl1	102.17(5)	C1	C3	Cl2	110.64(8)
N3	S1	N1	109.16(6)	C1	C3	Cl3	106.54(8)
C10	O1	C7	119.16(11)	C1	C3	Cl4	112.36(8)
C1	N1	S1	115.55(8)	C9	C4	C2	120.64(11)
C2	N2	C1	118.07(10)	C5	C4	C2	120.36(11)
C2	N3	S1	118.52(9)	C5	C4	C9	118.99(12)
N2	C1	N1	129.62(11)	C8	C9	C4	120.97(12)
C3	C1	N1	113.96(10)	C7	C8	C9	119.39(12)
C3	C1	N2	116.23(10)	C8	C7	O1	124.54(11)
N3	C2	N2	125.41(11)	C6	C7	O1	115.46(12)
C4	C2	N2	117.33(11)	C6	C7	C8	119.99(12)
C4	C2	N3	117.22(10)	C5	C6	C7	120.31(13)
Cl3	C3	Cl2	109.39(6)	C6	C5	C4	120.33(12)
Cl4	C3	Cl2	108.57(6)				

Table 6 Torsion Angles for 4A.

A	B	C	D	Angle/˚	A	B	C	D	Angle/˚
Cl2	C3	C1	N1	40.10(9)	O1	C7	C6	C5	178.75(12)
Cl2	C3	C1	N2	-144.45(8)	N1	C1	N2	C2	6.81(16)
Cl3	C3	C1	N1	-78.70(9)	N2	C2	C4	C9	-174.06(11)
Cl3	C3	C1	N2	96.74(9)	N2	C2	C4	C5	4.71(13)
Cl4	C3	C1	N1	161.63(9)	N3	C2	C4	C9	3.85(14)
Cl4	C3	C1	N2	-22.92(10)	N3	C2	C4	C5	-177.38(11)
Cl1	S1	N1	C1	87.65(7)	C2	C4	C9	C8	178.69(12)
Cl1	S1	N3	C2	-87.41(7)	C2	C4	C5	C6	-179.14(12)
S1	N1	C1	N2	8.26(12)	C4	C9	C8	C7	0.46(15)
S1	N1	C1	C3	-177.04(9)	C4	C5	C6	C7	0.42(15)
S1	N3	C2	N2	-5.95(12)	C9	C8	C7	C6	-0.39(15)
S1	N3	C2	C4	176.33(9)	C8	C7	C6	C5	-0.05(15)

Table 7 Hydrogen Atom Coordinates (Å×10^4) and Isotropic Displacement Parameters (Å^2×10^3) for 4A.

Atom	*x*	*y*	*z*	U(eq)
H9	10190(30)	2348(10)	8421(9)	44(4)
H8	12050(30)	1022(10)	8005(9)	48(5)
H6	7400(30)	-374(10)	9461(11)	66(6)
H5	5580(30)	998(10)	9890(10)	59(5)
H10a	11750(40)	-332(13)	7376(11)	80(7)
H10b	14150(30)	-252(13)	8207(11)	68(6)
H10c	12890(40)	-1226(13)	7937(12)	86(7)

4b

Table 1 Crystal data and structure refinement for 4b.

Identification code	rb06042
Empirical formula	$C_{10}H_7Cl_4N_3S$
Formula weight	343.063
Temperature/K	173.15
Crystal system	monoclinic
Space group	$P2_1/c$
a/Å	11.8279(8)
b/Å	5.4047(4)
c/Å	21.1692(15)
α/°	90
β/°	91.443(1)
γ/°	90
Volume/Å^3	1352.84(17)
Z	4
ρ_{calc}g/cm^3	1.684
μ/mm^{-1}	1.012
F(000)	691.1
Crystal size/mm^3	0.3 × 0.19 × 0.12
Radiation	Mo Kα (λ = 0.71073)
2Θ range for data collection/°	3.44 to 57.58
Index ranges	-15 ≤ h ≤ 15, -6 ≤ k ≤ 7, -28 ≤ l ≤ 28
Reflections collected	15096
Independent reflections	3333 [R_{int} = 0.0276, R_{sigma} = 0.0214]
Data/restraints/parameters	3333/6/204
Goodness-of-fit on F^2	1.026
Final R indexes [I>=2σ (I)]	R_1 = 0.0205, wR_2 = 0.0462
Final R indexes [all data]	R_1 = 0.0257, wR_2 = 0.0475
Largest diff. peak/hole / e Å^{-3}	0.45/-0.44

Table 2 Fractional Atomic Coordinates (×10^4) and Equivalent Isotropic Displacement Parameters (Å^2×10^3) for 4b. U_{eq} is defined as 1/3 of the trace of the orthogonalised U_{IJ} tensor.

Atom	*x*	*y*	*z*	U(eq)
S1	3428.7(2)	3812.6(5)	5016.14(13)	27.76(7)
Cl1	2632.0(3)	6598.0(7)	5597.53(14)	47.55(10)
Cl2	4930.3(2)	9915.8(5)	3909.53(14)	32.09(8)
Cl3	4785.1(3)	5833.4(5)	3037.44(14)	34.98(8)
Cl4	3026.0(2)	9513.3(5)	3059.17(13)	29.54(7)
N1	4031.1(7)	5550.0(18)	4505.2(4)	27.6(2)
N2	2382.6(7)	5368.4(15)	3829.7(4)	21.31(18)
N3	2369.5(7)	2494.3(17)	4686.8(4)	28.1(2)
C1	3403.0(8)	6146.2(18)	4002.8(5)	19.5(2)
C2	1928.0(8)	3489.4(19)	4157.2(5)	20.8(2)
C3	4000.9(8)	7818.8(18)	3525.6(5)	20.3(2)
C4	892.4(8)	2351.6(19)	3898.0(5)	21.9(2)
C5	360.0(9)	3324(2)	3356.1(5)	25.5(2)
C6	-602.4(9)	2201(2)	3102.3(5)	29.0(2)
C7	-1056.6(9)	90(2)	3380.9(5)	28.8(2)
C8	-521.2(10)	-870(2)	3924.1(6)	29.8(3)
C9	442.1(9)	239(2)	4181.4(6)	26.3(2)
C10	-2109.1(10)	-1110(3)	3108.6(6)	42.5(3)

Table 3 Anisotropic Displacement Parameters (Å^2×10^3) for 4b. The Anisotropic displacement factor exponent takes the form: $-2\pi^2[h^2a^{*2}U_{11}+2hka^*b^*U_{12}+\ldots]$.

Atom	U_{11}	U_{22}	U_{33}	U_{12}	U_{13}	U_{23}
S1	23.61(14)	33.99(16)	25.37(14)	-8.05(11)	-5.54(10)	10.72(11)
Cl1	57.8(2)	54.6(2)	30.61(17)	-13.66(17)	8.86(14)	-9.04(14)
Cl2	32.65(15)	23.49(14)	39.77(16)	-10.23(11)	-6.42(12)	5.10(11)
Cl3	41.97(17)	25.64(14)	38.24(16)	6.49(12)	19.13(13)	2.87(12)
Cl4	26.38(14)	29.33(14)	32.79(15)	1.26(11)	-1.95(11)	11.41(11)
N1	20.7(5)	35.2(5)	26.7(5)	-7.7(4)	-3.4(4)	10.4(4)
N2	18.6(4)	22.5(4)	22.7(4)	-4.1(3)	-1.6(3)	4.3(3)
N3	26.5(5)	29.4(5)	28.1(5)	-8.9(4)	-5.0(4)	10.0(4)
C1	17.0(5)	20.1(5)	21.4(5)	-2.8(4)	0.1(4)	3.1(4)
C2	18.2(5)	22.2(5)	22.0(5)	-3.9(4)	-0.0(4)	1.8(4)
C3	19.2(5)	17.8(5)	24.1(5)	-0.6(4)	2.3(4)	2.5(4)
C4	18.9(5)	23.7(5)	23.0(5)	-4.2(4)	0.7(4)	-0.1(4)
C5	23.3(6)	27.4(6)	25.8(6)	-4.2(4)	-2.5(4)	1.9(5)
H5	60(10)	52(10)	32(9)	-12(8)	-12(7)	16(7)
C6	24.6(6)	33.9(6)	28.2(6)	-5.1(5)	-5.3(4)	-3.4(5)
H6	56(10)	63(11)	66(11)	-6(9)	-38(8)	27(9)
C7	21.8(5)	33.9(6)	30.8(6)	-7.1(5)	0.9(4)	-7.4(5)
C8	25.9(6)	31.8(6)	31.8(6)	-11.5(5)	3.1(5)	-1.5(5)
H8	53(10)	62(10)	37(8)	-33(8)	6(7)	9(8)
C9	24.7(6)	26.4(6)	27.7(6)	-9.0(4)	1.0(5)	2.8(5)

Table 3 Anisotropic Displacement Parameters ($Å^2×10^3$) for 4b. The Anisotropic displacement factor exponent takes the form: $-2π^2[h^2a^{*2}U_{11}+2hka^*b^*U_{12}+…]$.

Atom	U_{11}	U_{22}	U_{33}	U_{12}	U_{13}	U_{23}
H9	37(9)	75(12)	36(9)	-10(8)	-8(7)	12(8)
C10	30.4(7)	52.0(8)	44.8(8)	-15.5(6)	-3.1(6)	-12.7(6)

Table 4 Bond Lengths for 4b.

Atom	Atom	Length/Å	Atom	Atom	Length/Å
S1	Cl1	2.1742(5)	C1	C3	1.5407(13)
S1	N1	1.6118(9)	C2	C4	1.4648(13)
S1	N3	1.5872(9)	C4	C5	1.3971(14)
Cl2	C3	1.7630(10)	C4	C9	1.4011(14)
Cl3	C3	1.7687(10)	C5	C6	1.3862(15)
Cl4	C3	1.7568(10)	C6	C7	1.3981(16)
N1	C1	1.3218(12)	C7	C8	1.3985(16)
N2	C1	1.3211(12)	C7	C10	1.5054(15)
N2	C2	1.3490(12)	C8	C9	1.3867(15)
N3	C2	1.3376(13)			

Table 5 Bond Angles for 4b.

Atom	Atom	Atom	Angle/˚	Atom	Atom	Atom	Angle/˚
N1	S1	Cl1	100.47(4)	Cl4	C3	Cl3	109.53(5)
N3	S1	Cl1	102.18(4)	C1	C3	Cl2	111.48(7)
N3	S1	N1	108.91(5)	C1	C3	Cl3	106.45(7)
C1	N1	S1	115.65(7)	C1	C3	Cl4	111.64(7)
C2	N2	C1	118.05(8)	C5	C4	C2	120.33(9)
C2	N3	S1	118.35(7)	C9	C4	C2	120.33(9)
N2	C1	N1	129.54(9)	C9	C4	C5	119.32(10)
C3	C1	N1	114.37(8)	C6	C5	C4	120.15(11)
C3	C1	N2	115.85(8)	C7	C6	C5	120.95(11)
N3	C2	N2	125.53(9)	C8	C7	C6	118.60(10)
C4	C2	N2	117.64(9)	C10	C7	C6	120.85(11)
C4	C2	N3	116.76(9)	C10	C7	C8	120.54(11)
Cl3	C3	Cl2	109.23(5)	C9	C8	C7	120.87(11)
Cl4	C3	Cl2	108.47(5)	C8	C9	C4	120.10(11)

Table 6 Torsion Angles for 4b.

A	B	C	D	Angle/˚	A	B	C	D	Angle/˚
S1	N1	C1	N2	-6.20(10)	N2	C2	C4	C5	-4.69(11)
S1	N1	C1	C3	179.68(7)	N2	C2	C4	C9	173.64(9)
S1	N3	C2	N2	8.39(10)	N3	C2	C4	C5	178.19(10)
S1	N3	C2	C4	-174.74(8)	N3	C2	C4	C9	-3.48(11)
Cl2	C3	C1	N1	-34.74(8)	C2	C4	C5	C6	178.23(10)
Cl2	C3	C1	N2	150.29(7)	C2	C4	C9	C8	-178.26(10)
Cl3	C3	C1	N1	84.28(7)	C4	C5	C6	C7	-0.03(13)

Table 6 Torsion Angles for 4b.

A	B	C	D	Angle/˚	A	B	C	D	Angle/˚
Cl3	C3	C1	N2	-90.68(7)	C4	C9	C8	C7	0.07(13)
Cl4	C3	C1	N1	-156.23(7)	C5	C6	C7	C8	0.19(13)
Cl4	C3	C1	N2	28.80(8)	C5	C6	C7	C10	179.33(11)
N1	C1	N2	C2	-8.51(13)	C6	C7	C8	C9	-0.21(12)

Table 7 Hydrogen Atom Coordinates (Å×10^4) and Isotropic Displacement Parameters (Å^2×10^3) for 4b.

Atom	*x*	*y*	*z*	U(eq)
H5	702(12)	4940(30)	3145(6)	48(4)
H6	-1028(12)	3040(30)	2685(7)	62(5)
H8	-867(11)	-2510(30)	4143(6)	50(4)
H9	845(11)	-530(30)	4594(6)	49(4)
H10a	-2822(5)	130(20)	3161(13)	51(8)
H10b	-1996(10)	-1500(50)	2612(3)	51(8)
H10c	-2267(14)	-2820(30)	3357(10)	51(8)
H10d	-2770(9)	-1050(50)	3454(6)	50(8)
H1	-2386(16)	-120(40)	2687(9)	50(8)
H2	-1929(7)	-3017(17)	2989(14)	50(8)

Table 8 Atomic Occupancy for 4b.

Atom	*Occupancy*	Atom	*Occupancy*	Atom	*Occupancy*
H10a	0.52(3)	H10b	0.52(3)	H10c	0.52(3)
H10d	0.48(3)	H1	0.48(3)	H2	0.48(3)

4c

Table 1 Crystal data and structure refinement for 4c.

Identification code	rb06051
Empirical formula	$C_9H_5Cl_4N_3S$
Formula weight	329.036
Temperature/K	173.15
Crystal system	monoclinic
Space group	$P2_1/n$
a/Å	7.411(2)
b/Å	11.314(3)
c/Å	15.046(4)
α/°	90
β/°	93.955(3)
γ/°	90
Volume/Å^3	1258.6(6)
Z	4
ρ_{calc}g/cm^3	1.736
μ/mm^{-1}	1.084
F(000)	659.1

Crystal size/mm^3	0.28 × 0.19 × 0.18
Radiation	MoKα (λ = 0.71073)
2Θ range for data collection/°	4.5 to 57.46
Index ranges	-10 ≤ h ≤ 10, -14 ≤ k ≤ 15, -20 ≤ l ≤ 20
Reflections collected	14476
Independent reflections	3107 [R_{int} = 0.0169, R_{sigma} = 0.0131]
Data/restraints/parameters	3107/0/199
Goodness-of-fit on F^2	1.054
Final R indexes [I>=2σ (I)]	R_1 = 0.0172, wR_2 = 0.0382
Final R indexes [all data]	R_1 = 0.0215, wR_2 = 0.0401
Largest diff. peak/hole / e Å^{-3}	0.39/-0.31

Table 2 Fractional Atomic Coordinates (×10^4) and Equivalent Isotropic Displacement Parameters (Å^2×10^3) for 4c. U_{eq} is defined as 1/3 of the trace of the orthogonalised U_{IJ} tensor.

Atom	*x*	*y*	*z*	U(eq)
Cl1	3354.0(4)	723.3(2)	4120.78(19)	41.28(7)
Cl2	-67.5(4)	991.6(2)	7277.58(17)	37.63(7)
Cl3	2090.3(4)	3077.1(2)	7564.93(16)	41.80(7)
Cl4	3732.6(4)	928.0(2)	6979.88(19)	42.45(7)
S1	708.6(3)	1476.8(2)	4350.34(15)	26.91(6)
N1	637.0(11)	1283.3(7)	5402.7(5)	27.79(17)
N2	2064.3(10)	3158.8(6)	5676.7(5)	25.15(16)
N3	1067.3(11)	2843.8(7)	4154.6(5)	30.67(18)
C1	1439.5(12)	2124.1(7)	5907.8(6)	23.31(17)
C3	1748.1(13)	1811.7(8)	6902.3(6)	26.36(19)
C4	2235.5(11)	4743.3(8)	4625.7(6)	24.01(18)
C5	2866.9(13)	5490.7(9)	5318.6(7)	29.9(2)
C6	3357.1(15)	6645.7(9)	5131.7(8)	34.7(2)
C7	3220.1(14)	7059.3(9)	4259.7(8)	36.3(2)
C8	2596.9(15)	6314.0(9)	3568.0(8)	36.8(2)
C9	2099.0(14)	5160.6(9)	3749.1(7)	30.4(2)
C2	1765.2(11)	3511.7(8)	4822.6(6)	23.27(17)

Table 3 Anisotropic Displacement Parameters (Å^2×10^3) for 4c. The Anisotropic displacement factor exponent takes the form: $-2\pi^2[h^2a^{*2}U_{11}+2hka^*b^*U_{12}+\ldots]$.

Atom	U_{11}	U_{22}	U_{33}	U_{12}	U_{13}	U_{23}
Cl1	37.64(14)	35.19(14)	51.87(16)	3.04(10)	9.33(11)	-11.83(11)
Cl2	41.52(15)	38.39(14)	33.91(13)	-9.96(11)	9.31(10)	4.14(10)
Cl3	70.8(2)	27.42(12)	26.59(12)	-8.24(12)	-0.94(11)	-2.52(9)
Cl4	38.68(15)	39.85(15)	48.60(16)	10.30(11)	1.52(11)	15.40(12)
S1	30.01(12)	23.46(11)	26.85(11)	-1.98(9)	-0.94(9)	-3.16(9)
N1	33.4(4)	21.1(4)	28.8(4)	-4.3(3)	2.4(3)	-2.0(3)
N2	29.5(4)	20.9(4)	24.9(4)	-3.2(3)	0.2(3)	0.9(3)
N3	39.8(5)	24.2(4)	27.1(4)	-1.4(3)	-3.9(3)	0.6(3)
C1	26.1(4)	19.5(4)	24.4(4)	-0.4(3)	2.7(3)	-0.1(3)

Table 3 Anisotropic Displacement Parameters ($Å^2×10^3$) for 4c. The Anisotropic displacement factor exponent takes the form: $-2π^2[h^2a^{*2}U_{11}+2hka*b*U_{12}+…]$.

Atom	U_{11}	U_{22}	U_{33}	U_{12}	U_{13}	U_{23}
C3	31.6(5)	20.6(4)	27.0(4)	-1.0(4)	2.3(4)	1.8(3)
C4	24.7(4)	20.4(4)	27.2(4)	1.7(3)	3.9(3)	1.8(3)
C5	36.5(5)	22.8(5)	30.9(5)	-3.6(4)	5.8(4)	-0.4(4)
H5	76(10)	41(8)	44(8)	-11(7)	3(7)	2(7)
C6	40.6(6)	22.7(5)	41.9(6)	-5.2(4)	10.1(5)	-2.7(4)
H6	86(11)	30(8)	69(10)	-14(8)	14(9)	-1(7)
C7	38.1(6)	23.7(5)	48.4(6)	-0.1(4)	13.1(5)	7.3(4)
H7	78(11)	35(9)	83(11)	-1(8)	12(9)	10(8)
C8	42.3(6)	31.3(5)	37.7(6)	2.0(4)	8.2(5)	11.1(5)
H8	113(13)	63(10)	32(8)	1(9)	3(8)	18(7)
C9	34.3(5)	28.2(5)	28.8(5)	1.3(4)	2.7(4)	4.6(4)
H9	66(10)	55(9)	45(8)	-10(8)	-9(7)	9(7)
C2	23.8(4)	20.3(4)	25.6(4)	1.1(3)	1.1(3)	1.0(3)

Table 4 Bond Lengths for 4c.

Atom	Atom	Length/Å	Atom	Atom	Length/Å
Cl1	S1	2.1871(6)	N3	C2	1.3330(12)
Cl2	C3	1.7593(10)	C1	C3	1.5391(13)
Cl3	C3	1.7530(10)	C4	C5	1.3977(13)
Cl4	C3	1.7756(10)	C4	C9	1.3979(13)
S1	N1	1.6030(9)	C4	C2	1.4716(12)
S1	N3	1.6001(9)	C5	C6	1.3903(14)
N1	C1	1.3318(11)	C6	C7	1.3900(16)
N2	C1	1.3146(11)	C7	C8	1.3933(16)
N2	C2	1.3493(11)	C8	C9	1.3883(15)

Table 5 Bond Angles for 4c.

Atom	Atom	Atom	Angle/˚	Atom	Atom	Atom	Angle/˚
N1	S1	Cl1	101.18(3)	C1	C3	Cl3	111.80(6)
N3	S1	Cl1	100.70(3)	C1	C3	Cl4	105.07(6)
N3	S1	N1	109.33(4)	C9	C4	C5	119.88(9)
C1	N1	S1	114.97(6)	C2	C4	C5	119.63(8)
C2	N2	C1	118.53(8)	C2	C4	C9	120.47(8)
C2	N3	S1	118.03(7)	C6	C5	C4	119.76(10)
N2	C1	N1	129.55(8)	C7	C6	C5	120.29(10)
C3	C1	N1	114.92(7)	C8	C7	C6	120.00(10)
C3	C1	N2	115.48(7)	C9	C8	C7	120.08(10)
Cl3	C3	Cl2	109.40(5)	C8	C9	C4	119.98(10)
Cl4	C3	Cl2	109.28(5)	N3	C2	N2	125.46(8)
Cl4	C3	Cl3	109.62(5)	C4	C2	N2	116.51(8)
C1	C3	Cl2	111.56(6)	C4	C2	N3	118.03(8)

Table 6 Torsion Angles for 4c.

A	B	C	D	Angle/˚	A	B	C	D	Angle/˚
Cl1	S1	N1	C1	84.63(5)	S1	N3	C2	C4	175.03(6)
Cl1	S1	N3	C2	-86.53(5)	N1	C1	N2	C2	5.89(11)
Cl2	C3	C1	N1	-37.44(7)	N2	C2	C4	C5	-3.15(10)
Cl2	C3	C1	N2	144.99(6)	N2	C2	C4	C9	175.21(8)
Cl3	C3	C1	N1	-160.30(6)	N3	C2	C4	C5	176.13(8)
Cl3	C3	C1	N2	22.13(7)	N3	C2	C4	C9	-5.52(10)
Cl4	C3	C1	N1	80.87(6)	C4	C5	C6	C7	0.06(11)
Cl4	C3	C1	N2	-96.71(6)	C4	C9	C8	C7	-0.48(11)
S1	N1	C1	N2	10.18(9)	C5	C6	C7	C8	-0.28(12)
S1	N1	C1	C3	-166.98(6)	C6	C7	C8	C9	0.49(12)
S1	N3	C2	N2	-5.77(9)					

Table 7 Hydrogen Atom Coordinates (Å×10^4) and Isotropic Displacement Parameters (Å^2×10^3) for 4c.

Atom	*x*	*y*	*z*	U(eq)
H5	2977(19)	5150(11)	5971(9)	54(4)
H6	3850(20)	7219(11)	5647(9)	61(4)
H7	3600(20)	7956(11)	4120(9)	65(4)
H8	2480(20)	6619(13)	2906(8)	69(5)
H9	1622(19)	4577(12)	3235(8)	56(4)

4d

Table 1 Crystal data and structure refinement for 4d.

Identification code	rb10028
Empirical formula	$C_9H_4Cl_5N_3S$
Formula weight	363.481
Temperature/K	173.15
Crystal system	monoclinic
Space group	$P2_1/n$
a/Å	7.858(7)
b/Å	5.433(5)
c/Å	30.80(3)
α/°	90
β/°	93.686(12)
γ/°	90
Volume/Å^3	1312(2)
Z	4
ρ_{calc}g/cm^3	1.840
μ/mm^{-1}	1.246
F(000)	723.7
Crystal size/mm^3	0.305 × 0.227 × 0.078
Radiation	Mo Kα (λ = 0.71073)

2Θ range for data collection/°	5.28 to 57.58
Index ranges	-10 ≤ h ≤ 10, -7 ≤ k ≤ 7, -41 ≤ l ≤ 41
Reflections collected	18474
Independent reflections	3251 [R_{int} = 0.0190, R_{sigma} = 0.0131]
Data/restraints/parameters	3251/0/199
Goodness-of-fit on F^2	1.052
Final R indexes [I>=2σ (I)]	R_1 = 0.0202, wR_2 = 0.0410
Final R indexes [all data]	R_1 = 0.0224, wR_2 = 0.0418
Largest diff. peak/hole / e Å^{-3}	0.57/-0.49

Table 2 Fractional Atomic Coordinates (×10^4) and Equivalent Isotropic Displacement Parameters (Å^2×10^3) for 4d. U_{eq} is defined as 1/3 of the trace of the orthogonalised U_{IJ} tensor.

Atom	*x*	*y*	*z*	U(eq)
Cl1	9104.1(4)	12607.0(6)	259.82(10)	31.35(8)
Cl2	4676.3(4)	15105.9(5)	1445.93(9)	25.28(7)
Cl3	2537.5(4)	11104.6(6)	1102.88(11)	28.18(7)
Cl4	3473.4(5)	15092.7(6)	547.86(10)	33.79(8)
Cl5	11075.0(4)	4557.2(6)	2772.74(10)	31.90(8)
S1	7430.5(4)	9504.4(6)	344.95(9)	23.35(7)
N1	5730.4(13)	10944(2)	468.9(3)	26.7(2)
N2	6769.6(12)	11015.2(18)	1217.0(3)	20.51(19)
N3	8287.1(13)	8252.0(19)	776.3(3)	25.9(2)
C1	5724.3(14)	11639(2)	880.9(4)	19.3(2)
C2	7904.0(14)	9199(2)	1157.7(4)	19.8(2)
C3	4180.8(14)	13224(2)	988.5(4)	19.6(2)
C4	8739.3(14)	8094(2)	1554.1(4)	19.4(2)
C5	8446.0(15)	9088(2)	1961.3(4)	22.7(2)
C6	9175.0(15)	8018(2)	2339.6(4)	24.4(2)
C7	10178.9(14)	5926(2)	2304.4(4)	22.2(2)
C8	10491.7(16)	4914(2)	1902.4(4)	25.6(2)
C9	9777.2(15)	6012(2)	1525.4(4)	24.2(2)

Table 3 Anisotropic Displacement Parameters (Å^2×10^3) for 4d. The Anisotropic displacement factor exponent takes the form: -2π^2[h^{2}a*^{2}U_{11}+2hka*b*U_{12}+…].

Atom	U_{11}	U_{22}	U_{33}	U_{12}	U_{13}	U_{23}
Cl1	31.24(16)	34.38(17)	28.79(16)	2.67(13)	4.72(12)	6.10(13)
Cl2	26.43(14)	23.62(14)	25.36(14)	3.96(11)	-1.62(11)	-8.21(11)
Cl3	20.53(13)	24.51(14)	39.50(17)	0.15(11)	2.05(12)	-4.72(12)
Cl4	47.92(19)	26.20(15)	26.22(15)	12.34(14)	-5.65(13)	2.69(12)
Cl5	32.49(16)	36.45(17)	26.18(15)	6.59(13)	-2.59(12)	8.82(13)
S1	26.10(14)	27.21(15)	16.65(13)	6.26(12)	0.71(10)	-4.67(11)
N1	23.6(5)	37.3(6)	18.7(5)	7.3(4)	-3.3(4)	-7.3(4)
N2	22.3(5)	21.8(5)	17.2(5)	6.0(4)	-1.0(4)	-2.3(4)

Table 3 Anisotropic Displacement Parameters ($Å^2×10^3$) for 4d. The Anisotropic displacement factor exponent takes the form: $-2π^2[h^2a^{*2}U_{11}+2hka^*b^*U_{12}+…]$.

Atom	U_{11}	U_{22}	U_{33}	U_{12}	U_{13}	U_{23}
N3	33.4(5)	24.7(5)	19.7(5)	10.6(4)	3.6(4)	-1.2(4)
C1	19.3(5)	20.1(5)	18.3(5)	2.9(4)	-0.6(4)	-2.7(4)
C2	21.4(5)	19.4(5)	18.8(5)	3.6(4)	1.3(4)	-0.6(4)
C3	20.0(5)	18.6(5)	19.8(5)	3.9(4)	-1.9(4)	-2.3(4)
C4	19.1(5)	20.2(5)	18.9(5)	3.9(4)	1.8(4)	0.6(4)
C5	26.0(6)	22.8(6)	19.4(6)	6.3(5)	1.2(4)	-0.4(4)
H5	59(12)	38(11)	43(11)	21(10)	3(9)	3(9)
C6	27.7(6)	26.2(6)	19.1(6)	5.2(5)	0.5(5)	0.4(5)
H6	69(13)	63(14)	27(10)	24(11)	-6(9)	-1(10)
C7	19.9(5)	25.1(6)	21.6(6)	1.5(4)	0.5(4)	4.0(5)
C8	25.8(6)	26.2(6)	24.7(6)	9.2(5)	2.2(5)	3.0(5)
H8	41(11)	48(12)	43(11)	24(10)	3(8)	3(9)
C9	26.1(6)	25.6(6)	21.1(6)	9.5(5)	2.7(5)	0.7(5)
H9	71(13)	45(12)	22(9)	17(10)	3(9)	-5(8)

Table 4 Bond Lengths for 4d.

Atom	Atom	Length/Å	Atom	Atom	Length/Å
Cl1	S1	2.1643(15)	N3	C2	1.3345(17)
Cl2	C3	1.7639(16)	C1	C3	1.5409(18)
Cl3	C3	1.7822(16)	C2	C4	1.4760(18)
Cl4	C3	1.7563(16)	C4	C5	1.3980(19)
Cl5	C7	1.7317(16)	C4	C9	1.4009(18)
S1	N1	1.6147(15)	C5	C6	1.3919(19)
S1	N3	1.6018(14)	C6	C7	1.3921(19)
N1	C1	1.3245(18)	C7	C8	1.391(2)
N2	C1	1.3234(16)	C8	C9	1.3913(19)
N2	C2	1.3501(16)			

Table 5 Bond Angles for 4d.

Atom	Atom	Atom	Angle/˚	Atom	Atom	Atom	Angle/˚
N1	S1	Cl1	99.78(4)	Cl4	C3	Cl3	109.20(6)
N3	S1	Cl1	101.83(4)	C1	C3	Cl2	111.06(7)
N3	S1	N1	108.64(5)	C1	C3	Cl3	105.77(8)
C1	N1	S1	114.74(8)	C1	C3	Cl4	111.80(8)
C2	N2	C1	117.61(10)	C5	C4	C2	119.66(10)
C2	N3	S1	117.38(8)	C9	C4	C2	120.38(10)
N2	C1	N1	129.50(11)	C9	C4	C5	119.92(11)
C3	C1	N1	114.63(10)	C6	C5	C4	120.46(11)
C3	C1	N2	115.63(9)	C7	C6	C5	118.73(11)
N3	C2	N2	126.09(10)	C6	C7	Cl5	119.21(9)
C4	C2	N2	116.60(10)	C8	C7	Cl5	119.09(9)
C4	C2	N3	117.26(10)	C8	C7	C6	121.70(11)

Table 5 Bond Angles for 4d.

Atom	Atom	Atom	Angle/˚	Atom	Atom	Atom	Angle/˚
Cl3	C3	Cl2	110.01(6)	C9	C8	C7	119.24(11)
Cl4	C3	Cl2	108.96(6)	C8	C9	C4	119.93(11)

Table 6 Torsion Angles for 4d.

A	B	C	D	Angle/˚	A	B	C	D	Angle/˚
Cl1	S1	N1	C1	-81.17(7)	S1	N3	C2	C4	-178.02(8)
Cl1	S1	N3	C2	82.42(7)	N1	C1	N2	C2	-8.72(15)
Cl2	C3	C1	N1	-154.66(9)	N2	C2	C4	C5	-5.49(12)
Cl2	C3	C1	N2	30.39(9)	N2	C2	C4	C9	172.41(10)
Cl3	C3	C1	N1	86.02(9)	N3	C2	C4	C5	177.03(11)
Cl3	C3	C1	N2	-88.93(8)	N3	C2	C4	C9	-5.07(13)
Cl4	C3	C1	N1	-32.73(10)	C2	C4	C5	C6	177.74(11)
Cl4	C3	C1	N2	152.33(8)	C2	C4	C9	C8	-176.88(11)
Cl5	C7	C6	C5	-179.32(9)	C4	C5	C6	C7	-0.89(14)
Cl5	C7	C8	C9	-179.85(10)	C4	C9	C8	C7	-0.78(14)
S1	N1	C1	N2	-11.47(12)	C5	C6	C7	C8	1.15(15)
S1	N1	C1	C3	174.44(8)	C6	C7	C8	C9	-0.32(14)
S1	N3	C2	N2	4.76(12)					

Table 7 Hydrogen Atom Coordinates (Å×10^4) and Isotropic Displacement Parameters (Å^2×10^3) for 4d.

Atom	*x*	*y*	*z*	U(eq)
H5	7640(20)	10690(30)	1977(5)	47(5)
H6	8970(20)	8770(40)	2655(5)	54(5)
H8	11290(20)	3290(30)	1886(5)	44(5)
H9	10020(20)	5260(30)	1203(5)	46(5)

Structure Report 4e

PLATON

3.6 Angstrom Coordination Sphere Around Atom I = S10 [ARU = 1555.01] 0.03800 0.29130 0.47970 -0.8050 2.2812 14.7387

Nr	d(I,J)	To	Atom J	Symm_Oper. on Atom J	ARU(J)	Type	Phi	Mu	X	Y	Z	XO	YO	ZO
9	3.203(15)	.<	N12_b	[-x,1-y,1-z = 2566.01]		92.67	38.53	0.09880	0.57790	0.54464	-0.9216	4.7842	16.7340	

3.6 Angstrom Coordination Sphere Around Atom I = S20 [ARU = 1555.02] 0.54500 0.79320 0.02080 1.9250 7.0285 0.6391

Nr	d(I,J)	To	Atom J	Symm_Oper. on Atom J	ARU(J)	Type	Phi	Mu	X	Y	Z	XO	YO	ZO
9	3.219(15)	.<	N22_b	[1-x,2-y,-z = 2675.02]		91.58	-38.27	0.58050	1.07310	-0.04408	1.8552	9.5546	-1.3544	

Least Squares Planes – from Mercury

N10-C10-N11-C11-N12 N10-C10-N11-C11-N12 0.347 Å (is below the accuracy for Platon auto calc).

N20-C20-N21-C21-N22 N20-C20-N21-C21-N22 0.383 Å (not calc in Platon)

These two planes are centrosymetrically co-planar.

Table 1 Crystal data and structure refinement for 4e.

Identification code	rb10059-twin
Empirical formula	$C_{10}H_4Cl_4F_3N_3S$
Formula weight	397.035
Temperature/K	173.15
Crystal system	triclinic
Space group	P-1
a/Å	5.3976(8)
b/Å	8.9647(14)
c/Å	30.761(5)
α/°	90.823(2)
β/°	92.513(2)
γ/°	97.992(2)
Volume/Å^3	1472.2(4)
Z	4
ρ_{calc}g/cm^3	1.791
μ/mm^{-1}	0.971
F(000)	787.3
Crystal size/mm^3	0.419 × 0.108 × 0.062
Radiation	Mo Kα (λ = 0.71073)
2Θ range for data collection/°	3.98 to 50.06
Index ranges	-7 ≤ h ≤ 7, -12 ≤ k ≤ 12, -41 ≤ l ≤ 40
Reflections collected	21458
Independent reflections	5145 [R_{int} = 0.0537, R_{sigma} = 0.0506]
Data/restraints/parameters	5145/152/542
Goodness-of-fit on F^2	1.027
Final R indexes [I>=2σ (I)]	R_1 = 0.0434, wR_2 = 0.1271
Final R indexes [all data]	R_1 = 0.0511, wR_2 = 0.1355
Largest diff. peak/hole / e Å^{-3}	0.41/-0.29

Table 2 Fractional Atomic Coordinates (×10^4) and Equivalent Isotropic Displacement Parameters (Å^2×10^3) for 4e. U_{eq} is defined as 1/3 of the trace of the orthogonalised U_{IJ} tensor.

Atom	*x*	*y*	*z*	U(eq)
Cl10	-2780(30)	1377(18)	4990(4)	50.4(17)
Cl11	-5211(18)	4301(12)	3505(3)	35.1(9)
Cl12	-892(18)	6446(11)	3708(4)	43.6(16)
Cl13	-4917(9)	6024(12)	4299(4)	39.9(12)
S10	380(30)	2913(15)	4797(5)	34.6(17)
F10	5350(20)	-2699(11)	2856(2)	82(3)
F11	1935(13)	-2604(11)	2475(3)	77(3)
F12	5045(17)	-931(7)	2422(2)	57.0(19)
N10	1524(7)	1991(4)	4412.9(12)	33.0(9)
N11	-1382(6)	2790(4)	3890.4(11)	25.5(7)
N12	-988(8)	4221(4)	4553.6(13)	36.3(9)
C10	355(7)	1931(5)	4021.2(14)	24.7(9)

Table 2 Fractional Atomic Coordinates (×10^4) and Equivalent Isotropic Displacement Parameters (Å^2×10^3) for 4e. U_{eq} is defined as 1/3 of the trace of the orthogonalised U_{IJ} tensor.

Atom	*x*	*y*	*z*	U(eq)
C11	-1784(8)	3914(5)	4152.0(14)	26.1(9)
C12	-3206(7)	5112(5)	3935.1(15)	27.8(9)
C13	1173(8)	917(4)	3694.7(13)	23.9(9)
C14	3055(8)	46(5)	3800.2(14)	27.4(9)
C15	3903(9)	-850(5)	3484.2(15)	30.2(9)
C16	2855(9)	-871(5)	3060.1(14)	29.8(9)
C17	952(10)	-32(5)	2958.3(15)	36.7(11)
C18	103(9)	865(5)	3272.3(14)	32.4(10)
C19	3794(11)	-1801(6)	2712.3(16)	40.4(12)
Cl20	2230(20)	6341(17)	12(4)	50.4(17)
Cl21	450(20)	9540(15)	1481(4)	36.1(11)
Cl22	370(8)	11116(11)	681(3)	39.5(12)
Cl23	4651(14)	11643(9)	1282(4)	45.4(15)
S20	5450(30)	7932(16)	208(5)	36.5(18)
F20	8000(40)	2000(16)	2295(7)	66(4)
F21	11700(20)	2990(30)	2236(8)	78(5)
F22	9410(60)	3910(20)	2685(4)	73(5)
N20	6804(7)	7088(4)	599.2(12)	32.1(9)
N21	4105(6)	7953(4)	1108.1(11)	25.1(7)
N22	4195(8)	9269(4)	440.8(13)	40.2(10)
C20	5797(8)	7080(4)	983.0(13)	23.7(8)
C21	3572(8)	9029(5)	846.2(14)	26.7(9)
C22	2246(8)	10260(5)	1051.7(15)	29.1(10)
C23	6727(8)	6095(4)	1312.9(13)	24.2(9)
C24	8553(8)	5208(5)	1214.1(14)	26.8(9)
C25	9474(9)	4308(5)	1533.3(15)	31.7(10)
C26	8533(9)	4307(5)	1946.8(14)	31.1(10)
C27	6698(10)	5179(5)	2045.9(15)	37.9(11)
C28	5777(9)	6078(5)	1730.7(14)	32.5(10)
C29	9455(10)	3316(5)	2290.0(16)	40.2(12)
F12a	3940(90)	-1180(40)	2345(8)	66(9)
F11a	2420(60)	-3100(30)	2686(15)	75(9)
F10a	5950(40)	-2190(40)	2806(12)	64(9)
F22a	10470(50)	4078(18)	2628(8)	65(5)
F21a	11200(50)	2560(30)	2158(6)	73(5)
F20a	7570(40)	2340(30)	2424(9)	76(5)
S20a	5860(50)	8100(30)	242(7)	32(3)
Cl	2880(70)	6551(19)	-70(7)	51(4)
Cl1	-2110(60)	1600(20)	5068(8)	47(4)
S10a	760(50)	3090(30)	4758(7)	31(3)
Cl2	-920(60)	6610(40)	3834(16)	39(6)
Cl3	-5420(60)	4490(40)	3511(12)	35.1(9)

Table 2 Fractional Atomic Coordinates (×10^4) and Equivalent Isotropic Displacement Parameters (Å^2×10^3) for 4e. U_{eq} is defined as 1/3 of the trace of the orthogonalised U_{IJ} tensor.

Atom	*x*	*y*	*z*	U(eq)
Cl4	-4980(40)	5740(30)	4379(8)	39.9(12)
Cl5	230(30)	10770(30)	592(6)	39.5(12)
Cl6	210(80)	9660(60)	1466(15)	36.1(11)
Cl7	4600(60)	11770(30)	1140(12)	45(5)

Table 3 Anisotropic Displacement Parameters (Å^2×10^3) for 4e. The Anisotropic displacement factor exponent takes the form: -2π^2[h^{2}a*^{2}U$_{11}$+2hka*b*U$_{12}$+…].

Atom	U_{11}	U_{22}	U_{33}	U_{12}	U_{13}	U_{23}
Cl10	55(4)	63(4)	37(3)	21(2)	7(2)	15(2)
Cl11	30.8(17)	33(2)	42.8(7)	12.1(13)	-10.1(11)	4.4(14)
Cl12	24.9(13)	35(2)	71(4)	3.6(14)	2(2)	20(2)
Cl13	34.6(7)	47(2)	44(2)	25.6(12)	-3.3(11)	-0.1(19)
S10	45(3)	36(3)	25(3)	20(2)	-9(2)	-3(2)
F10	151(7)	71(5)	42(3)	77(5)	8(4)	-2(3)
F11	70(4)	74(5)	79(5)	-11(3)	19(3)	-50(4)
F12	66(4)	56(3)	49(3)	4(3)	24(3)	-6(2)
N10	40(2)	36(2)	26(2)	20.6(17)	-8.3(17)	-4.2(16)
N11	26.2(17)	22.8(18)	28.5(19)	8.7(14)	-4.3(15)	-0.8(14)
N12	47(2)	31(2)	33(2)	18.2(18)	-11.1(18)	-7.0(17)
C10	24(2)	25(2)	26(2)	6.4(16)	-1.7(17)	0.3(17)
C11	25(2)	24(2)	30(2)	7.6(17)	-1.7(17)	3.6(18)
C12	18.6(19)	23(2)	43(3)	7.8(16)	-2.9(18)	2.1(18)
C13	26(2)	23(2)	24(2)	8.5(17)	-2.1(17)	3.9(16)
C14	27(2)	30(2)	28(2)	11.2(18)	-1.9(18)	2.9(18)
H14	72(16)	72(16)	71(16)	30(9)	-5(9)	-9(9)
C15	35(2)	29(2)	29(2)	12.5(19)	-1.7(19)	0.3(18)
H15	72(16)	72(16)	71(16)	30(9)	-5(9)	-9(9)
C16	40(2)	26(2)	25(2)	9.9(19)	4.5(19)	1.2(18)
C17	51(3)	40(3)	23(2)	20(2)	-4(2)	-2(2)
H17	72(16)	72(16)	71(16)	30(9)	-5(9)	-9(9)
C18	40(3)	33(2)	26(2)	17(2)	-7(2)	-1.0(19)
H18	72(16)	72(16)	71(16)	30(9)	-5(9)	-9(9)
C19	59(3)	32(3)	33(3)	15(2)	10(2)	-3(2)
Cl20	55(3)	62(3)	36(3)	21(2)	-7(2)	-15(2)
Cl21	33(2)	38(2)	39.4(12)	13.3(14)	8.0(16)	-1.6(11)
Cl22	35.9(8)	45(2)	44(2)	24.7(13)	6.0(11)	5.4(19)
Cl23	24.1(12)	33.4(18)	78(4)	2.5(10)	2(2)	-22(2)
S20	49(4)	40(3)	26(3)	23(3)	9(2)	6(2)
F20	86(8)	35(5)	74(8)	3(4)	-21(5)	23(4)
F21	40(5)	106(10)	92(9)	20(5)	-8(4)	55(7)

Table 3 Anisotropic Displacement Parameters ($Å^2×10^3$) for 4e. The Anisotropic displacement factor exponent takes the form: $-2π^2[h^2a^{*2}U_{11}+2hka^*b^*U_{12}+…]$.

Atom	U_{11}	U_{22}	U_{33}	U_{12}	U_{13}	U_{23}
F22	128(13)	64(6)	32(4)	36(7)	-10(6)	8(4)
N20	39(2)	37(2)	25.3(19)	19.5(17)	6.8(16)	3.8(16)
N21	25.3(17)	24.0(17)	27.1(19)	6.8(14)	2.9(15)	0.8(14)
N22	57(3)	33(2)	37(2)	24(2)	13(2)	10.9(18)
C20	25(2)	24(2)	23(2)	8.3(16)	1.0(17)	1.3(16)
C21	25(2)	23(2)	33(2)	7.5(17)	-0.0(18)	0.7(18)
C22	21(2)	24(2)	44(3)	6.8(17)	4.0(19)	-1.2(19)
C23	27(2)	22(2)	24(2)	6.4(16)	-1.4(17)	0.8(16)
C24	31(2)	25(2)	26(2)	9.4(17)	3.2(18)	1.0(17)
H24	48(14)	48(13)	43(13)	22(8)	14(8)	12(8)
C25	36(2)	28(2)	34(2)	13.4(19)	-1(2)	3.9(19)
H25	48(14)	48(13)	43(13)	22(8)	14(8)	12(8)
C26	40(2)	25(2)	29(2)	10.9(19)	-6(2)	0.3(18)
C27	55(3)	37(3)	25(2)	18(2)	2(2)	2(2)
H27	48(14)	48(13)	43(13)	22(8)	14(8)	12(8)
C28	41(3)	36(2)	24(2)	17(2)	4.1(19)	1.8(19)
H28	48(14)	48(13)	43(13)	22(8)	14(8)	12(8)
C29	56(3)	31(3)	34(3)	11(2)	-9(2)	7(2)
F12a	99(18)	71(13)	35(10)	34(9)	8(8)	1(7)
F11a	83(14)	51(12)	89(17)	4(7)	15(8)	-34(8)
F10a	26(10)	90(18)	76(15)	7(7)	13(7)	-25(8)
F22a	85(10)	48(5)	58(8)	11(5)	-37(6)	1(5)
F21a	109(12)	66(8)	56(6)	60(7)	-3(6)	7(5)
F20a	68(7)	71(10)	84(11)	-10(6)	-17(6)	48(7)
S20a	50(6)	29(4)	20(3)	19(4)	-4(3)	1(2)
Cl	75(9)	47(4)	33(5)	19(4)	-21(5)	-12(3)
Cl1	68(9)	45(4)	35(6)	18(5)	18(5)	12(3)
S10a	49(6)	26(4)	21(3)	17(4)	4(3)	3(2)
Cl2	22(5)	21(5)	72(15)	0(4)	-10(8)	15(8)
Cl3	30.8(17)	33(2)	42.8(7)	12.1(13)	-10.1(11)	4.4(14)
Cl4	34.6(7)	47(2)	44(2)	25.6(12)	-3.3(11)	-0.1(19)
Cl5	35.9(8)	45(2)	44(2)	24.7(13)	6.0(11)	5.4(19)
Cl6	33(2)	38(2)	39.4(12)	13.3(14)	8.0(16)	-1.6(11)
Cl7	34(6)	29(5)	72(13)	-2(4)	19(8)	-15(8)

Table 4 Bond Lengths for 4e.

Atom	Atom	Length/Å	Atom	Atom	Length/Å
Cl10	S10	2.147(9)	Cl21	C22	1.750(10)
Cl11	C12	1.755(8)	Cl22	C22	1.748(6)
Cl12	C12	1.778(9)	Cl23	C22	1.781(8)
Cl13	C12	1.747(6)	S20	N20	1.630(14)
S10	N10	1.625(14)	S20	N22	1.630(13)

Table 4 Bond Lengths for 4e.

Atom	Atom	Length/Å	Atom	Atom	Length/Å
S10	N12	1.641(13)	F20	C29	1.325(15)
F10	C19	1.310(8)	F21	C29	1.303(15)
F11	C19	1.333(8)	F22	C29	1.324(13)
F12	C19	1.338(7)	N20	C20	1.321(5)
N10	C10	1.332(6)	N20	S20a	1.55(2)
N10	S10a	1.55(2)	N21	C20	1.347(5)
N11	C10	1.346(5)	N21	C21	1.320(5)
N11	C11	1.328(5)	N22	C21	1.318(6)
N12	C11	1.303(6)	N22	S20a	1.60(2)
N12	S10a	1.59(2)	C20	C23	1.472(5)
C10	C13	1.468(6)	C21	C22	1.539(6)
C11	C12	1.547(5)	C22	Cl5	1.846(17)
C12	Cl2	1.73(3)	C22	Cl6	1.76(3)
C12	Cl3	1.76(3)	C22	Cl7	1.73(3)
C12	Cl4	1.826(19)	C23	C24	1.391(6)
C13	C14	1.395(6)	C23	C28	1.404(6)
C13	C18	1.396(6)	C24	C25	1.397(6)
C14	C15	1.385(6)	C25	C26	1.390(7)
C15	C16	1.398(6)	C26	C27	1.386(7)
C16	C17	1.383(6)	C26	C29	1.502(6)
C16	C19	1.495(6)	C27	C28	1.389(6)
C17	C18	1.381(6)	C29	F22a	1.293(16)
C19	F12a	1.27(2)	C29	F21a	1.309(17)
C19	F11a	1.29(2)	C29	F20a	1.331(17)
C19	F10a	1.28(2)	S20a	Cl	2.157(17)
Cl20	S20	2.148(10)	Cl1	S10a	2.165(16)

Table 5 Bond Angles for 4e.

Atom	Atom	Atom	Angle/˚	Atom	Atom	Atom	Angle/˚
N10	S10	Cl10	103.5(7)	C20	N20	S20	117.0(6)
N12	S10	Cl10	102.0(7)	S20a	N20	S20	9.2(12)
N12	S10	N10	106.0(8)	S20a	N20	C20	118.5(10)
C10	N10	S10	117.3(5)	C21	N21	C20	118.1(4)
S10a	N10	S10	9.6(11)	C21	N22	S20	115.6(6)
S10a	N10	C10	117.8(10)	S20a	N22	S20	9.4(11)
C11	N11	C10	117.9(4)	S20a	N22	C21	115.3(9)
C11	N12	S10	115.6(5)	N21	C20	N20	126.0(4)
S10a	N12	S10	9.6(11)	C23	C20	N20	116.9(4)
S10a	N12	C11	115.1(9)	C23	C20	N21	117.0(4)
N11	C10	N10	125.8(4)	N22	C21	N21	129.0(4)
C13	C10	N10	116.8(4)	C22	C21	N21	115.9(4)
C13	C10	N11	117.2(4)	C22	C21	N22	114.9(4)
N12	C11	N11	129.5(4)	Cl22	C22	Cl21	109.6(4)

Table 5 Bond Angles for 4e.

Atom	Atom	Atom	Angle/˚	Atom	Atom	Atom	Angle/˚
C12	C11	N11	115.1(4)	Cl23	C22	Cl21	106.7(7)
C12	C11	N12	115.2(4)	Cl23	C22	Cl22	109.3(4)
Cl12	C12	Cl11	107.5(6)	C21	C22	Cl21	110.7(5)
Cl13	C12	Cl11	109.5(4)	C21	C22	Cl22	113.8(5)
Cl13	C12	Cl12	109.7(4)	C21	C22	Cl23	106.4(4)
C11	C12	Cl11	110.6(5)	Cl5	C22	Cl21	111.2(7)
C11	C12	Cl12	106.2(4)	Cl5	C22	Cl22	12.7(5)
C11	C12	Cl13	113.2(5)	Cl5	C22	Cl23	119.3(6)
Cl2	C12	Cl11	119.4(15)	Cl5	C22	C21	102.3(7)
Cl2	C12	Cl12	13.5(14)	Cl6	C22	Cl21	6.0(16)
Cl2	C12	Cl13	98.5(14)	Cl6	C22	Cl22	103.8(14)
Cl2	C12	C11	105.3(13)	Cl6	C22	Cl23	108(2)
Cl3	C12	Cl11	7.2(11)	Cl6	C22	C21	115.5(16)
Cl3	C12	Cl12	106.7(15)	Cl6	C22	Cl5	106.0(16)
Cl3	C12	Cl13	103.4(12)	Cl7	C22	Cl21	120.4(13)
Cl3	C12	C11	117.3(11)	Cl7	C22	Cl22	97.7(12)
Cl3	C12	Cl2	118(2)	Cl7	C22	Cl23	14.8(11)
Cl4	C12	Cl11	111.2(8)	Cl7	C22	C21	104.1(11)
Cl4	C12	Cl12	118.2(7)	Cl7	C22	Cl5	106.4(12)
Cl4	C12	Cl13	11.1(6)	Cl7	C22	Cl6	121(2)
Cl4	C12	C11	102.9(9)	C24	C23	C20	120.4(4)
Cl4	C12	Cl2	106.1(14)	C28	C23	C20	119.3(4)
Cl4	C12	Cl3	106.0(14)	C28	C23	C24	120.3(4)
C14	C13	C10	120.5(4)	C25	C24	C23	120.0(4)
C18	C13	C10	119.3(4)	C26	C25	C24	119.3(4)
C18	C13	C14	120.1(4)	C27	C26	C25	121.0(4)
C15	C14	C13	120.1(4)	C29	C26	C25	119.9(4)
C16	C15	C14	119.4(4)	C29	C26	C27	119.1(4)
C17	C16	C15	120.4(4)	C28	C27	C26	120.1(4)
C19	C16	C15	120.1(4)	C27	C28	C23	119.4(4)
C19	C16	C17	119.5(4)	F21	C29	F20	105.4(10)
C18	C17	C16	120.4(4)	F22	C29	F20	105.8(10)
C17	C18	C13	119.6(4)	F22	C29	F21	108.0(11)
F11	C19	F10	109.1(6)	C26	C29	F20	110.9(9)
F12	C19	F10	105.4(6)	C26	C29	F21	114.2(9)
F12	C19	F11	103.9(5)	C26	C29	F22	111.9(8)
C16	C19	F10	114.1(5)	F22a	C29	F20	125.8(11)
C16	C19	F11	112.3(5)	F22a	C29	F21	84.8(10)
C16	C19	F12	111.3(5)	F22a	C29	F22	26.5(9)
F12a	C19	F10	123.5(16)	F22a	C29	C26	112.3(9)
F12a	C19	F11	77.2(19)	F21a	C29	F20	86.2(11)
F12a	C19	F12	28.3(19)	F21a	C29	F21	21.9(11)
F12a	C19	C16	114.2(14)	F21a	C29	F22	124.6(11)

Table 5 Bond Angles for 4e.

Atom	Atom	Atom	Angle/˚	Atom	Atom	Atom	Angle/˚
F11a	C19	F10	77.7(17)	F21a	C29	C26	113.3(10)
F11a	C19	F11	37.6(18)	F21a	C29	F22a	104.7(11)
F11a	C19	F12	133.5(18)	F20a	C29	F20	24.8(11)
F11a	C19	C16	109.0(14)	F20a	C29	F21	124.0(12)
F11a	C19	F12a	111.6(19)	F20a	C29	F22	83.6(10)
F10a	C19	F10	24.5(14)	F20a	C29	C26	110.6(10)
F10a	C19	F11	126.3(16)	F20a	C29	F22a	107.4(11)
F10a	C19	F12	83.6(16)	F20a	C29	F21a	108.1(12)
F10a	C19	C16	113.8(16)	N22	S20a	N20	111.3(14)
F10a	C19	F12a	107(2)	Cl	S20a	N20	100.4(12)
F10a	C19	F11a	100.7(18)	Cl	S20a	N22	98.3(12)
N20	S20	Cl20	103.6(7)	N12	S10a	N10	112.3(14)
N22	S20	Cl20	102.2(8)	Cl1	S10a	N10	99.7(12)
N22	S20	N20	106.0(8)	Cl1	S10a	N12	98.0(12)

Table 6 Torsion Angles for 4e.

A	B	C	D	Angle/˚	A	B	C	D	Angle/˚
Cl10	S10	N10	C10	78.1(8)	Cl20	S20	N20	C20	-77.3(8)
Cl10	S10	N10	S10a	173(3)	Cl20	S20	N20	S20a	-179(3)
Cl10	S10	N12	C11	-81.3(9)	Cl20	S20	N22	C21	81.0(9)
Cl10	S10	N12	S10a	-171(3)	Cl20	S20	N22	S20a	171(3)
Cl11	C12	C11	N11	29.1(5)	Cl21	C22	C21	N21	-28.6(6)
Cl11	C12	C11	N12	-156.2(5)	Cl21	C22	C21	N22	156.6(6)
Cl12	C12	C11	N11	-87.2(6)	Cl22	C22	C21	N21	-152.5(4)
Cl12	C12	C11	N12	87.6(6)	Cl22	C22	C21	N22	32.7(4)
Cl13	C12	C11	N11	152.3(4)	Cl23	C22	C21	N21	87.0(5)
Cl13	C12	C11	N12	-32.9(4)	Cl23	C22	C21	N22	-87.7(5)
S10	N10	C10	N11	13.6(8)	S20	N20	C20	N21	-14.8(8)
S10	N10	C10	C13	-171.3(7)	S20	N20	C20	C23	169.3(7)
S10	N10	S10a	N12	-101(8)	S20	N20	S20a	N22	96(8)
S10	N10	S10a	Cl1	2(8)	S20	N20	S20a	Cl	-7(9)
S10	N12	C11	N11	-9.6(8)	S20	N22	C21	N21	9.5(8)
S10	N12	C11	C12	176.5(7)	S20	N22	C21	C22	-176.6(7)
S10	N12	S10a	N10	105(7)	S20	N22	S20a	N20	-104(8)
S10	N12	S10a	Cl1	1(8)	S20	N22	S20a	Cl	0(8)
F10	C19	C16	C15	8.8(8)	F20	C29	C26	C25	-92.9(12)
F10	C19	C16	C17	-171.4(8)	F20	C29	C26	C27	85.4(12)
F11	C19	C16	C15	133.7(7)	F21	C29	C26	C25	26.1(15)
F11	C19	C16	C17	-46.6(8)	F21	C29	C26	C27	-155.6(14)
F12	C19	C16	C15	-110.3(6)	F22	C29	C26	C25	149.2(16)
F12	C19	C16	C17	69.5(7)	F22	C29	C26	C27	-32.5(16)
N10	C10	N11	C11	8.2(5)	N20	C20	N21	C21	-7.6(5)
N10	C10	C13	C14	1.3(5)	N20	C20	C23	C24	-1.0(5)

Table 6 Torsion Angles for 4e.

A	B	C	D	Angle/˚	A	B	C	D	Angle/˚
N10	C10	C13	C18	-176.8(4)	N20	C20	C23	C28	178.0(4)
N10	S10a	N12	C11	9.3(19)	N20	S20a	N22	C21	-10.2(19)
N11	C10	C13	C14	176.9(4)	N21	C20	C23	C24	-177.3(4)
N11	C10	C13	C18	-1.2(5)	N21	C20	C23	C28	1.8(5)
N11	C11	N12	S10a	1.0(12)	N21	C21	N22	S20a	-1.0(12)
N11	C11	C12	Cl2	-101.1(17)	N21	C21	C22	Cl5	-147.1(7)
N11	C11	C12	Cl3	32.0(16)	N21	C21	C22	Cl6	-33(2)
N11	C11	C12	Cl4	147.9(8)	N21	C21	C22	Cl7	102.2(14)
N12	C11	C12	Cl2	73.6(18)	N22	C21	C22	Cl5	38.1(7)
N12	C11	C12	Cl3	-153.3(16)	N22	C21	C22	Cl6	153(2)
N12	C11	C12	Cl4	-37.3(9)	N22	C21	C22	Cl7	-72.6(14)
C10	C13	C14	C15	-176.7(4)	C20	C23	C24	C25	178.2(4)
C10	C13	C18	C17	176.8(4)	C20	C23	C28	C27	-178.4(4)
C13	C14	C15	C16	-0.0(5)	C23	C24	C25	C26	0.4(5)
C13	C18	C17	C16	-0.2(5)	C23	C28	C27	C26	-0.2(5)
C14	C15	C16	C17	-1.4(5)	C24	C25	C26	C27	0.2(5)
C14	C15	C16	C19	178.4(4)	C24	C25	C26	C29	178.4(4)
C15	C16	C17	C18	1.5(5)	C25	C26	C27	C28	-0.3(5)
C15	C16	C19	F12a	-141(3)	C25	C26	C29	F22a	120.6(15)
C15	C16	C19	F11a	94(2)	C25	C26	C29	F21a	2.1(15)
C15	C16	C19	F10a	-18.0(19)	C25	C26	C29	F20a	-119.4(18)

Table 7 Hydrogen Atom Coordinates (Å×10^4) and Isotropic Displacement Parameters (Å^2×10^3) for 4e.

Atom	*x*	*y*	*z*	U(eq)
H14	3820(100)	20(50)	4140(20)	70(9)
H15	5400(90)	-1510(50)	3580(20)	70(9)
H17	450(100)	-100(60)	2630(20)	70(9)
H18	-1300(110)	1460(60)	3140(20)	70(9)
H24	9220(80)	5250(50)	901(17)	44(7)
H25	10710(100)	3550(60)	1441(17)	44(7)
H27	5900(70)	5230(40)	2374(17)	44(7)
H28	4300(80)	6770(50)	1812(16)	44(7)

Table 8 Atomic Occupancy for 4e.

Atom	*Occupancy*	Atom	*Occupancy*	Atom	*Occupancy*
Cl10	0.65(5)	Cl11	0.79(5)	Cl12	0.79(5)
Cl13	0.79(5)	S10	0.65(5)	F10	0.81(2)
F11	0.81(2)	F12	0.81(2)	Cl20	0.64(5)
Cl21	0.79(3)	Cl22	0.79(3)	Cl23	0.79(3)
S20	0.64(5)	F20	0.54(5)	F21	0.54(5)
F22	0.54(5)	F12a	0.19(2)	F11a	0.19(2)
F10a	0.19(2)	F22a	0.46(5)	F21a	0.46(5)

Table 8 Atomic Occupancy for 4e.

Atom	*Occupancy*	Atom	*Occupancy*	Atom	*Occupancy*
F20a	0.46(5)	S20a	0.36(5)	Cl	0.36(5)
Cl1	0.35(5)	S10a	0.35(5)	Cl2	0.21(5)
Cl3	0.21(5)	Cl4	0.21(5)	Cl5	0.21(3)
Cl6	0.21(3)	Cl7	0.21(3)		

Archive of Computational Data – Cartesian Coordinates of Optimized Geometries

3e_B3LYP-D3/6-311++G(d,p)_Monomer

Cl	-2.907600	-2.709200	1.261300
S	-2.644900	-1.824600	-0.794900
F	-2.891000	2.886100	-0.742400
F	-3.251600	2.332300	1.333100
F	-4.721600	1.853800	-0.193200
N	-3.436100	-0.392100	-0.612200
N	-1.383100	0.646600	0.082000
N	-1.059500	-1.520900	-0.874900
C	-2.687000	0.599600	-0.170800
C	-0.614300	-0.376500	-0.328400
C	-3.413900	1.937400	0.059200
C	0.849100	-0.212100	-0.230600
C	1.390300	1.014200	0.181500
H	0.725800	1.833600	0.419500
C	2.766400	1.170000	0.278100
H	3.187900	2.117200	0.589100
C	3.607200	0.103200	-0.040100
C	3.078600	-1.122000	-0.448300
H	3.740900	-1.942600	-0.692400
C	1.703200	-1.279100	-0.545400
H	1.281800	-2.225400	-0.856600
C	5.098900	0.254800	0.117800
F	5.782500	-0.523600	-0.749300
F	5.499100	-0.099700	1.363600
F	5.503700	1.528300	-0.076700

4a_B3LYP-D3/6-311++G(d,p)_Monomer

Cl	-4.379700	-0.778700	0.483900
Cl	-2.138900	-2.600100	0.938900
Cl	-2.680400	-1.558200	-1.768700
Cl	-1.319800	3.318300	-1.205400
S	-1.188700	2.360500	0.861700
O	5.790700	-1.213000	-0.311100
N	-2.255800	1.123200	0.667600
N	-0.463600	-0.291600	-0.051100
N	0.295400	1.755200	0.925600
C	-1.729500	-0.002000	0.224900
C	0.505900	0.551300	0.341100
C	-2.713100	-1.176500	-0.009500
C	1.891100	0.117700	0.185400
C	2.951600	0.989000	0.472100
H	2.733100	1.994700	0.806900
C	4.270300	0.584900	0.319400
H	5.067000	1.280900	0.541300
C	4.547500	-0.715700	-0.126700
C	3.491700	-1.596900	-0.416600
H	3.733200	-2.595400	-0.758800
C	2.184300	-1.186400	-0.262900
H	1.368300	-1.861700	-0.483400
C	6.920200	-0.382600	-0.042000
H	6.923800	0.501300	-0.687800
H	6.943100	-0.074300	1.008200
H	7.793000	-0.994700	-0.259700

4b_B3LYP-D3/6-311++G(d,p)_Monomer

S	0.853000	2.363300	0.858100
Cl	0.983800	3.313200	-1.206100
Cl	4.067900	-0.752200	0.490200
Cl	1.839700	-2.592000	0.932600
Cl	2.381100	-1.536900	-1.770200
N	1.927500	1.131100	0.676200
N	0.149600	-0.293700	-0.057200
N	-0.630300	1.747200	0.911900
C	1.413200	0.004400	0.224500
C	-0.825500	0.540100	0.336200
C	2.406400	-1.161700	-0.009600
C	-2.212700	0.087500	0.187400
C	-2.486700	-1.218600	-0.249200
H	-1.662500	-1.885300	-0.466200
C	-3.799100	-1.643400	-0.393500
H	-3.997700	-2.656200	-0.727400
C	-4.873000	-0.788200	-0.111100
C	-4.590000	0.512600	0.327100
H	-5.407400	1.189500	0.551500
C	-3.282100	0.949800	0.476300
H	-3.075500	1.958800	0.808200
C	-6.295100	-1.244900	-0.305100
H	-6.627700	-1.030600	-1.326800
H	-6.394600	-2.321000	-0.147500
H	-6.977100	-0.731400	0.376000

4c_B3LYP-D3/6-311++G(d,p)_Monomer

Cl	0.296400	3.321200	1.165400
Cl	3.808500	-0.373300	-0.552700
Cl	1.804700	-2.473800	-0.896300

Cl	2.282100	-1.297800	1.768500
S	0.239900	2.335700	-0.880300
N	1.456500	1.241500	-0.709300
N	-0.123000	-0.371700	0.085000
N	-1.161400	1.545400	-0.892500
C	1.090900	0.069900	-0.229200
C	2.220700	-0.965000	0.000500
C	-2.519800	-0.284600	-0.120300
C	-2.618200	-1.611400	0.328600
H	-1.712400	-2.166600	0.533000
C	-3.867500	-2.193700	0.503000
H	-3.940400	-3.218100	0.848900
C	-5.025200	-1.462500	0.232000
H	-5.998600	-1.919600	0.370300
C	-4.932700	-0.143000	-0.213800
H	-5.832000	0.425700	-0.418600
C	-3.687200	0.446300	-0.391500
H	-3.605000	1.471200	-0.728500
C	-1.196700	0.333000	-0.300100

4d_B3LYP-D3/6-311++G(d,p)_Monomer

Cl	1.452700	3.284600	-1.220400
Cl	2.573800	-1.628500	-1.770800
Cl	1.985000	-2.641900	0.938400
Cl	4.313900	-0.935600	0.479500
Cl	-6.260400	-0.917100	-0.224000
S	1.285900	2.363000	0.844700
N	2.285500	1.068000	0.667000
N	0.425500	-0.254800	-0.052400
N	-0.232000	1.831600	0.910800
C	1.707100	-0.029000	0.221800
C	-0.494700	0.635100	0.344600
C	2.630200	-1.250900	-0.011600
C	-1.908900	0.257700	0.210000
C	-2.253800	-1.033200	-0.219700
H	-1.468400	-1.742800	-0.444100
C	-3.585900	-1.396500	-0.354200
H	-3.858800	-2.390300	-0.684200
C	-4.578200	-0.463300	-0.055500
C	-4.258400	0.825000	0.371900
H	-5.045900	1.533600	0.592100
C	-2.924000	1.180800	0.504400
H	-2.658900	2.178800	0.827100

4e_B3LYP-D3/6-311++G(d,p)_Monomer

Cl	2.142200	3.248600	1.241700
Cl	3.010000	-1.708800	1.772600
Cl	4.808900	-1.094700	-0.454500
Cl	2.399700	-2.674800	-0.949500
S	1.958300	2.358700	-0.827500
F	-5.949600	-0.195700	1.377100
F	-6.295000	0.214600	-0.729300
F	-5.799700	-1.803200	-0.078400
N	0.413600	1.904400	-0.914000
N	0.954400	-0.217600	0.041700
N	2.886800	1.010800	-0.652500
C	0.088600	0.719000	-0.363100
C	2.250500	-0.056900	-0.218100
C	3.106500	-1.326000	0.016600
C	-1.350400	0.407300	-0.254300
C	-2.311600	1.380600	-0.561400
H	-1.991700	2.365400	-0.874300
C	-3.663100	1.082700	-0.454600
H	-4.408100	1.830900	-0.692500
C	-4.059700	-0.190700	-0.044800
C	-3.110900	-1.165700	0.265200
H	-3.430600	-2.151600	0.577400
C	-1.759100	-0.868900	0.158900
H	-1.010500	-1.614900	0.389400
C	-5.525900	-0.496000	0.124300

5c_B3LYP-D3/6-311++G(d,p)_Monomer

Cl	-2.877600	-1.299500	1.120100
S	-2.260600	-0.279400	-0.835500
N	-2.591100	1.288400	-0.496300
N	-0.344000	1.590700	0.314400
N	-0.657600	-0.474400	-0.860900
C	-1.596000	1.970900	0.061000
C	1.531500	0.118700	-0.078000
C	2.410900	1.067500	0.466000
H	2.019400	2.023400	0.787300
C	3.764000	0.774500	0.587000
H	4.438900	1.511100	1.007200
C	4.252700	-0.463800	0.168400
H	5.308500	-0.690600	0.265800
C	3.382800	-1.412400	-0.371400
H	3.760500	-2.376600	-0.690900
C	2.029000	-1.125500	-0.496200
H	1.345800	-1.858800	-0.903700
C	0.093500	0.424000	-0.197200
H	-1.846400	2.996800	0.322900

3c_B3LYP-D3/6-311++G(d,p)-CC_Dimer

Cl	-1.530100	1.469000	2.165300
S	-1.700900	0.975900	-0.042100
N	-1.380400	-0.643900	0.012900
N	-3.725700	-1.113900	0.247400
N	-3.272700	1.154400	-0.352000
C	-2.435600	-1.416600	0.178800
C	-2.147100	-2.925500	0.279600
C	-5.549600	0.409000	-0.171900
C	-6.474000	-0.639000	-0.034700
H	-6.111000	-1.642900	0.140500
C	-7.835800	-0.379800	-0.125600
H	-8.546400	-1.191200	-0.020000
C	-8.287400	0.920900	-0.353600
H	-9.351000	1.120000	-0.423000
C	-7.372900	1.966800	-0.489700

H	-7.724500	2.977300	-0.661400
C	-6.009700	1.715900	-0.400200
H	-5.293300	2.521100	-0.495600
C	-4.107700	0.137900	-0.067800
F	-2.669500	-3.421600	1.414100
F	-0.835000	-3.192800	0.275100
F	-2.708300	-3.574700	-0.757300
Cl	1.519800	-1.464500	-2.158000
S	1.701500	-0.975100	0.049500
N	1.381700	0.645000	-0.001400
N	3.726200	1.113800	-0.246700
N	3.274700	-1.155200	0.351400
C	2.436600	1.417200	-0.171400
C	2.148600	2.926500	-0.268400
C	5.551100	-0.410900	0.161200
C	6.475500	0.636700	0.021200
H	6.112300	1.641200	-0.150500
C	7.837600	0.376500	0.104900
H	8.548100	1.187600	-0.002800
C	8.289500	-0.924900	0.328500
H	9.353200	-1.124800	0.392300
C	7.375000	-1.970400	0.467300
H	7.726800	-2.981500	0.635700
C	6.011500	-1.718500	0.385100
H	5.295100	-2.523400	0.482600
C	4.109000	-0.138800	0.064700
F	0.836800	3.194600	-0.257000
F	2.715400	3.573700	0.766700
F	2.665600	3.423900	-1.404700

3e_B3LYP-D3/6-311++G(d,p)-CC_Dimer

Cl	-1.584800	1.317100	2.204500
S	-1.768800	0.848900	0.006000
N	-1.327300	-0.743800	0.019000
N	-3.621100	-1.394200	0.317100
N	-3.362100	0.910700	-0.258000
C	-2.313300	-1.597700	0.207100
C	-1.908400	-3.081700	0.275600
C	-5.567500	-0.014700	-0.040300
C	-6.400600	-1.134300	0.098400
H	-5.957500	-2.109200	0.249800
C	-7.779700	-0.987300	0.038200
H	-8.425500	-1.850100	0.138000
C	-8.332000	0.277700	-0.164500
C	-7.512100	1.398500	-0.301100
H	-7.951900	2.374900	-0.458200
C	-6.133200	1.252800	-0.241300
H	-5.487400	2.114600	-0.342100
C	-4.101900	-0.172300	0.028400
F	-2.360800	-3.630400	1.414800
F	-0.580300	-3.246000	0.232600
F	-2.446700	-3.754900	-0.757200
C	-9.830100	0.445400	-0.174200
F	-10.461800	-0.657800	-0.630300
F	-10.220000	1.482800	-0.946400
F	-10.305600	0.683500	1.073000
Cl	1.577100	-1.313100	-2.195400
S	1.769000	-0.847600	0.003300
N	1.328200	0.745400	-0.006400
N	3.621200	1.394900	-0.312000
N	3.363100	-0.910500	0.261700
C	2.313900	1.598900	-0.197100
C	1.909600	3.083200	-0.262600
C	5.568200	0.014000	0.037200
C	6.401400	1.133300	-0.103300
H	5.958300	2.108600	-0.252100
C	7.780600	0.985500	-0.048000
H	8.426500	1.848100	-0.149100
C	8.332900	-0.280000	0.151500
C	7.512900	-1.400500	0.289800
H	7.952800	-2.377300	0.444300
C	6.134000	-1.254000	0.234900
H	5.488000	-2.115600	0.337100
C	4.102400	0.172400	-0.026200
F	0.581700	3.248000	-0.215300
F	2.451400	3.754900	0.769300
F	2.358800	3.633100	-1.402600
C	9.831100	-0.448400	0.155800
F	10.464900	0.654000	0.611100
F	10.223000	-1.486900	0.925400
F	10.302000	-0.685200	-1.093400

4a_B3LYP-D3/6-311++G(d,p)-CC_Dimer

Cl	-1.615800	1.018500	2.587000
Cl	-0.986400	-3.320600	-1.312300
Cl	-3.371200	-4.124200	0.178200
Cl	-0.970900	-3.293100	1.635700
S	-1.731000	0.891800	0.300300
N	-1.376800	-0.678300	0.054800
N	-3.683900	-1.266800	0.273600
N	-3.317100	1.089200	0.043200
C	-2.399500	-1.524000	0.166300
C	-1.971100	-3.014600	0.158500
C	-5.551000	0.222800	-0.010600
C	-6.431800	-0.876400	-0.060300
H	-6.026400	-1.877600	0.001200
C	-7.791600	-0.680400	-0.184500
H	-8.480600	-1.514700	-0.224600
C	-8.312900	0.621800	-0.262800
C	-7.448000	1.725300	-0.212900
H	-7.828200	2.735800	-0.265100
C	-6.081800	1.518500	-0.088900
H	-5.411600	2.367000	-0.042100
C	-4.111300	0.013100	0.121400
O	-9.657100	0.707600	-0.381200
C	-10.268100	1.994700	-0.464700
H	-9.918500	2.542300	-1.345900
H	-11.336200	1.807400	-0.554200

H	-10.075100	2.583500	0.437700
Cl	1.603900	-1.011900	-2.579400
Cl	0.986400	3.316500	1.327700
Cl	3.372500	4.124000	-0.158500
Cl	0.973000	3.297600	-1.620500
S	1.730500	-0.891400	-0.293000
N	1.377800	0.678200	-0.042000
N	3.683900	1.266900	-0.270500
N	3.317900	-1.089700	-0.044000
C	2.400100	1.524000	-0.156100
C	1.972100	3.014600	-0.143200
C	5.552200	-0.223800	0.000200
C	6.433500	0.875100	0.048300
H	6.028000	1.876500	-0.008500
C	7.793900	0.678400	0.164900
H	8.483300	1.512600	0.203700
C	8.315300	-0.624000	0.237100
C	7.449900	-1.727200	0.188700
H	7.830200	-2.737900	0.236300
C	6.083100	-1.519800	0.072300
H	5.412500	-2.368100	0.026800
C	4.111900	-0.013400	-0.123800
O	9.660000	-0.710400	0.348400
C	10.271200	-1.997900	0.425400
H	11.339800	-1.810900	0.509800
H	9.926100	-2.547600	1.306900
H	10.073500	-2.584300	-0.477600

4b_B3LYP-D3/6-311++G(d,p)-CC_Dimer

Cl	-1.562800	1.144100	2.554800
Cl	-1.188500	-3.268900	-1.282000
Cl	-3.624900	-3.894700	0.210600
Cl	-1.182900	-3.190200	1.665500
S	-1.668800	1.006200	0.275600
N	-1.417400	-0.583500	0.036100
N	-3.756900	-1.021600	0.255200
N	-3.242600	1.303800	0.012900
C	-2.491200	-1.362300	0.159200
C	-2.157900	-2.876600	0.178500
C	-5.526900	0.579800	-0.076700
C	-6.466800	-0.461600	-0.125600
H	-6.124400	-1.484800	-0.045400
C	-7.816400	-0.175800	-0.276600
H	-8.532000	-0.990200	-0.316800
C	-8.269700	1.145300	-0.381000
C	-7.323500	2.179000	-0.333500
H	-7.654600	3.208900	-0.414300
C	-5.972400	1.907200	-0.183800
H	-5.251600	2.713400	-0.142300
C	-4.099100	0.280700	0.083500
C	-9.738800	1.452300	-0.509000
H	-10.282500	0.624800	-0.969400
H	-10.179200	1.626800	0.479000
H	-9.908400	2.351600	-1.105500
Cl	1.550900	-1.136400	-2.548900
Cl	1.188300	3.265300	1.296100
Cl	3.626700	3.894600	-0.191300
Cl	1.186300	3.195200	-1.651600
S	1.668100	-1.005400	-0.269800
N	1.418500	0.583800	-0.024700
N	3.757100	1.021600	-0.253700
N	3.242900	-1.304300	-0.015300
C	2.492000	1.362400	-0.150300
C	2.159300	2.876900	-0.164200
C	5.528100	-0.581600	0.064000
C	6.468700	0.459200	0.111500
H	6.126300	1.482800	0.036600
C	7.819000	0.172300	0.254300
H	8.535100	0.986200	0.293500
C	8.272200	-1.149400	0.351800
C	7.325300	-2.182500	0.305800
H	7.656400	-3.212800	0.381300
C	5.973500	-1.909600	0.164200
H	5.252100	-2.715300	0.123800
C	4.099600	-0.281300	-0.087700
C	9.741800	-1.457400	0.470900
H	10.177100	-1.627700	-0.520100
H	10.288200	-0.632100	0.932200
H	9.914200	-2.359300	1.062600

4c_B3LYP-D3/6-311++G(d,p)-CC_Dimer

Cl	1.532800	-1.279500	2.512900
Cl	1.379100	3.202900	-1.269700
Cl	3.853600	3.662100	0.221700
Cl	1.378500	3.087800	1.676600
S	1.607400	-1.112700	0.239600
N	1.449500	0.492800	0.025400
N	3.814200	0.786100	0.210500
N	3.157700	-1.499800	-0.055100
C	2.569500	1.204000	0.140500
C	2.328200	2.735300	0.182300
C	5.481300	-0.914200	-0.175500
C	6.476000	0.074800	-0.232500
H	6.191800	1.114000	-0.134400
C	7.805800	-0.287500	-0.410600
H	8.571100	0.478600	-0.454600
C	8.154600	-1.632800	-0.533800
H	9.193100	-1.912400	-0.671500
C	7.169200	-2.620400	-0.476100
H	7.441400	-3.665400	-0.566800
C	5.838100	-2.266700	-0.298400
H	5.068000	-3.025000	-0.245000
C	4.073000	-0.530900	0.015100
Cl	-1.522200	1.271600	-2.509600
Cl	-1.378000	-3.199500	1.280800
Cl	-3.855600	-3.662000	-0.204000
Cl	-1.383100	-3.092600	-1.665800
S	-1.606700	1.111900	-0.236200

N	-1.450400	-0.493200	-0.016700
N	-3.814500	-0.785800	-0.210500
N	-3.157900	1.500500	0.051000
C	-2.570200	-1.204100	-0.133800
C	-2.329700	-2.735600	-0.170400
C	-5.482400	0.916600	0.161900
C	-6.477900	-0.071600	0.218100
H	-6.193800	-1.111400	0.125400
C	-7.808400	0.292000	0.388400
H	-8.574200	-0.473500	0.431800
C	-8.157000	1.638100	0.504600
H	-9.196000	1.918700	0.636100
C	-7.170900	2.624900	0.447700
H	-7.443000	3.670400	0.532900
C	-5.839100	2.269800	0.277900
H	-5.068400	3.027500	0.225100
C	-4.073400	0.531900	-0.020600

4c_M06-2X/Aug-CC-pVDZ-CC_Dimer

Cl	0.000000	0.000000	0.000000
Cl	5.600000	0.000000	0.000000
Cl	5.065000	2.841000	0.000000
Cl	3.633000	1.112000	-1.842000
S	1.380000	-0.539000	1.604000
N	2.816000	-0.291000	0.865000
N	2.689000	2.040000	1.397000
N	1.141000	0.701000	2.640000
C	3.181000	0.985000	0.786000
C	4.343000	1.238000	-0.204000
C	1.492000	2.989000	3.261000
C	2.210000	4.182000	3.102000
H	2.971000	4.243000	2.328000
C	1.940000	5.267000	3.931000
H	2.497000	6.194000	3.807000
C	0.959000	5.166000	4.918000
H	0.749000	6.018000	5.564000
C	0.242000	3.979000	5.077000
H	-0.526000	3.903000	5.845000
C	0.505000	2.891000	4.251000
H	-0.051000	1.963000	4.361000
C	1.777000	1.837000	2.377000
Cl	4.784000	-3.320000	0.883000
Cl	-0.815000	-3.320000	0.880000
Cl	-0.282000	-6.161000	0.876000
Cl	1.151000	-4.436000	2.721000
S	3.405000	-2.781000	-0.722000
N	1.969000	-3.029000	0.016000
N	2.097000	-5.361000	-0.517000
N	3.645000	-4.021000	-1.758000
C	1.604000	-4.306000	0.093000
C	0.442000	-4.560000	1.082000
C	3.297000	-6.310000	-2.379000
C	2.579000	-7.503000	-2.221000
H	1.816000	-7.564000	-1.448000
C	2.850000	-8.588000	-3.049000
H	2.293000	-9.515000	-2.927000
C	3.833000	-8.487000	-4.035000
H	4.043000	-9.338000	-4.681000
C	4.549000	-7.299000	-4.193000
H	5.318000	-7.224000	-4.960000
C	4.285000	-6.211000	-3.368000
H	4.841000	-5.283000	-3.478000
C	3.010000	-5.158000	-1.496000

4d_B3LYP-D3/6-311++G(d,p)-CC_Dimer

Cl	-1.573400	1.070700	2.563200
Cl	-1.086400	-3.300100	-1.295200
Cl	-3.489800	-4.017100	0.208600
Cl	-1.063600	-3.239800	1.653000
S	-1.697900	0.946800	0.293400
N	-1.398000	-0.632400	0.036500
N	-3.717400	-1.150400	0.286700
N	-3.286500	1.192600	0.051200
C	-2.441700	-1.448600	0.169500
C	-2.058100	-2.950900	0.174200
C	-5.544900	0.391000	-0.010100
C	-6.445800	-0.684300	-0.051100
H	-6.066300	-1.694900	0.020300
C	-7.808600	-0.455500	-0.179300
H	-8.508400	-1.280300	-0.211900
C	-8.271500	0.856400	-0.267800
C	-7.394400	1.940300	-0.227600
H	-7.777900	2.950000	-0.292900
C	-6.033800	1.703600	-0.099600
H	-5.340700	2.533500	-0.059800
C	-4.102700	0.139800	0.128300
Cl	-9.989600	1.150700	-0.429200
Cl	1.564000	-1.065100	-2.557400
Cl	1.086700	3.297300	1.307300
Cl	3.491000	4.017000	-0.193300
Cl	1.065400	3.243400	-1.641000
S	1.697500	-0.946300	-0.287800
N	1.398800	0.632500	-0.026500
N	3.717400	1.150500	-0.284600
N	3.287000	-1.192900	-0.052200
C	2.442200	1.448700	-0.161600
C	2.059100	2.951100	-0.162200
C	5.545800	-0.391900	0.001600
C	6.447000	0.683100	0.041500
H	6.067500	1.693900	-0.026200
C	7.810300	0.453700	0.163900
H	8.510300	1.278200	0.195600
C	8.273300	-0.858600	0.247700
C	7.395700	-1.942200	0.208400
H	7.779300	-2.952100	0.270000
C	6.034700	-1.704900	0.086300
H	5.341200	-2.534500	0.047200
C	4.103100	-0.140100	-0.130600

Cl	9.991900	-1.153500	0.401700

4e_B3LYP-D3/6-311++G(d,p)-CC_Dimer

Cl	-1.582700	0.984300	2.580700
Cl	-0.975100	-3.330400	-1.310600
Cl	-3.329600	-4.145800	0.219400
Cl	-0.917500	-3.281100	1.637700
S	-1.726800	0.881200	0.320500
N	-1.373800	-0.681900	0.034900
N	-3.666300	-1.290600	0.319300
N	-3.331400	1.069000	0.104800
C	-2.381500	-1.539900	0.181300
C	-1.940900	-3.026100	0.172500
C	-5.558300	0.180000	0.046200
C	-6.412100	-0.931400	0.007700
H	-5.990200	-1.925200	0.072800
C	-7.783800	-0.751700	-0.112400
H	-8.445500	-1.607500	-0.148500
C	-8.307100	0.538300	-0.197900
C	-7.465600	1.651300	-0.158400
H	-7.883100	2.647700	-0.226800
C	-6.094900	1.472900	-0.038500
H	-5.432900	2.327800	-0.003700
C	-4.100000	-0.015600	0.175100
C	-9.799400	0.736600	-0.272000
F	-10.129600	1.855200	-0.954000
F	-10.341400	0.857100	0.965300
F	-10.421500	-0.301000	-0.872600
Cl	1.572300	-0.978000	-2.571800
Cl	0.975100	3.327700	1.326000
Cl	3.331500	4.146000	-0.199200
Cl	0.920400	3.286100	-1.622400
S	1.726000	-0.880000	-0.311900
N	1.374600	0.682600	-0.021600
N	3.666200	1.290900	-0.314100
N	3.331200	-1.068900	-0.103100
C	2.382100	1.540400	-0.170100
C	1.942200	3.026800	-0.156700
C	5.558800	-0.180900	-0.052700
C	6.413200	0.930100	-0.015300
H	5.991500	1.924200	-0.076200
C	7.785400	0.749500	0.098200
H	8.447600	1.604900	0.133500
C	8.308500	-0.540900	0.178400
C	7.466400	-1.653500	0.140000
H	7.883800	-2.650100	0.204100
C	6.095300	-1.474300	0.026500
H	5.432800	-2.328700	-0.007400
C	4.100100	0.015600	-0.174700
C	9.801000	-0.739900	0.245400
F	10.426200	0.295800	0.846100
F	10.337600	-0.857300	-0.994500
F	10.133900	-1.860500	0.922900

5c_B3LYP-D3/6-311++G(d,p)-CC_Dimer

Cl	-1.639700	2.174500	1.383400
S	-1.780700	0.702000	-0.380300
N	-1.305400	-0.690700	0.345400
N	-3.591800	-1.232700	0.866600
N	-3.369800	0.607100	-0.649600
C	-2.273100	-1.426500	0.878300
C	-5.559000	-0.181000	-0.061300
C	-6.380500	-1.145000	0.543000
H	-5.922300	-1.950700	1.100800
C	-7.762200	-1.058200	0.421300
H	-8.391900	-1.806000	0.889300
C	-8.337400	-0.012500	-0.302000
H	-9.415700	0.053800	-0.394000
C	-7.525800	0.950200	-0.903700
H	-7.971800	1.765800	-1.460900
C	-6.143600	0.868700	-0.786800
H	-5.506700	1.615800	-1.241700
C	-4.092600	-0.265200	0.076000
H	-1.926800	-2.328800	1.378300
Cl	1.630300	-2.164100	-1.379900
S	1.781100	-0.696200	0.387000
N	1.307500	0.699600	-0.334100
N	3.593900	1.235700	-0.861600
N	3.371200	-0.606500	0.651500
C	2.275700	1.433500	-0.868500
C	5.560900	0.176000	0.057400
C	6.383400	1.138800	-0.547600
H	5.925800	1.947100	-1.102000
C	7.765200	1.047300	-0.430800
H	8.395700	1.794100	-0.899200
C	8.339600	-0.001800	0.288200
H	9.418000	-0.071700	0.376400
C	7.527000	-0.963400	0.890600
H	7.972300	-1.781600	1.444400
C	6.144600	-0.877200	0.778600
H	5.507000	-1.623300	1.233900
C	4.094300	0.265100	-0.074700
H	1.930600	2.338100	-1.365300

No. Points	32768
No. Scans	-1
Dummy Scans	0
Scan Count	20
SW +/-	2500.0
Filter	3000
Acq. Time	6.554s
Dwell	200u
Obs Freq	250.1346939
Obs base	250.1330000
O1 offset	1.6939 KHz
dcplfreq	250.1305000
O2 offset	0.5000 KHz
RCVR gain	100
DEC Mode	OFF
DEC Attn.	58
Sequence	1PULSE
Last Delay	2s

13 peaks found in p-OCH3 imidoylamidii

peak	ppm	freq	amp
1	7.965	1992.19	5451.29
2	7.953	1989.29	33923.04
3	7.944	1987.15	9595.97
4	7.925	1982.42	11538.70
5	7.917	1980.29	35244.58
6	7.260	1815.95	7526.31
7	6.990	1748.50	5183.39
8	6.979	1745.61	34401.95
9	6.970	1743.47	9581.47
10	6.951	1738.74	10512.28
11	6.943	1736.60	31739.22
12	3.861	965.88	153415.36
13	0.000	0.00	12684.90

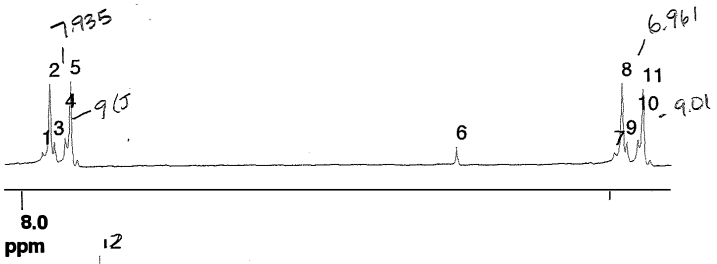

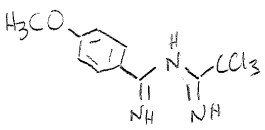

#	Start ppm	Stop ppm	Integral
2	8.09	7.80	1.91
3	7.12	6.83	1.96
1	3.92	3.82	3.00

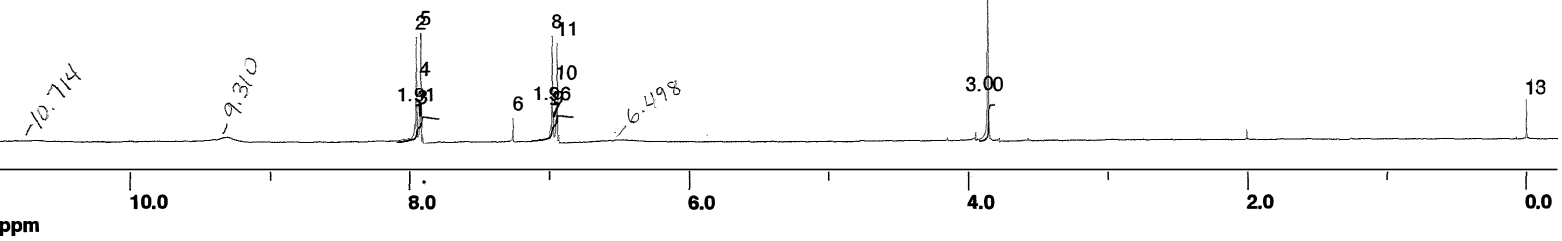

H1-NMR of **1a** in $CDCl_3$

Filename	p-OCH3 imidoylamidir
Nucleus	C13
No. Scans	-1
No. Points	32768
Scan Count	14528
SW +l-	8000.0
Filter	8000
Acq. Time	2.048s
Obs Freq	62.9034273
Obs base	62.8960000
O1 offset	7.4273 KHz
RCVR gain	800
DEC Mode	BB
DEC Attn.	108
Sequence	1PULSE with Decoupl
Last Delay	8s
Line Brdng	1.00
temp K	293.0

11 peaks found in p-OCH3 imidoylamidine 2

peak	ppm	freq	amp
1	168.146	10575.71	950478.88
2	164.226	10329.13	614516.19
3	163.022	10253.45	954916.94
4	129.361	8136.26	6786810.00
5	127.754	8035.19	825045.69
6	114.331	7190.95	7011011.00
7	98.175	6174.84	290966.03
8	77.758	4890.66	8328573.50
9	77.246	4858.43	8617529.00
10	76.741	4826.69	8470004.00
11	55.710	3503.94	3192918.00

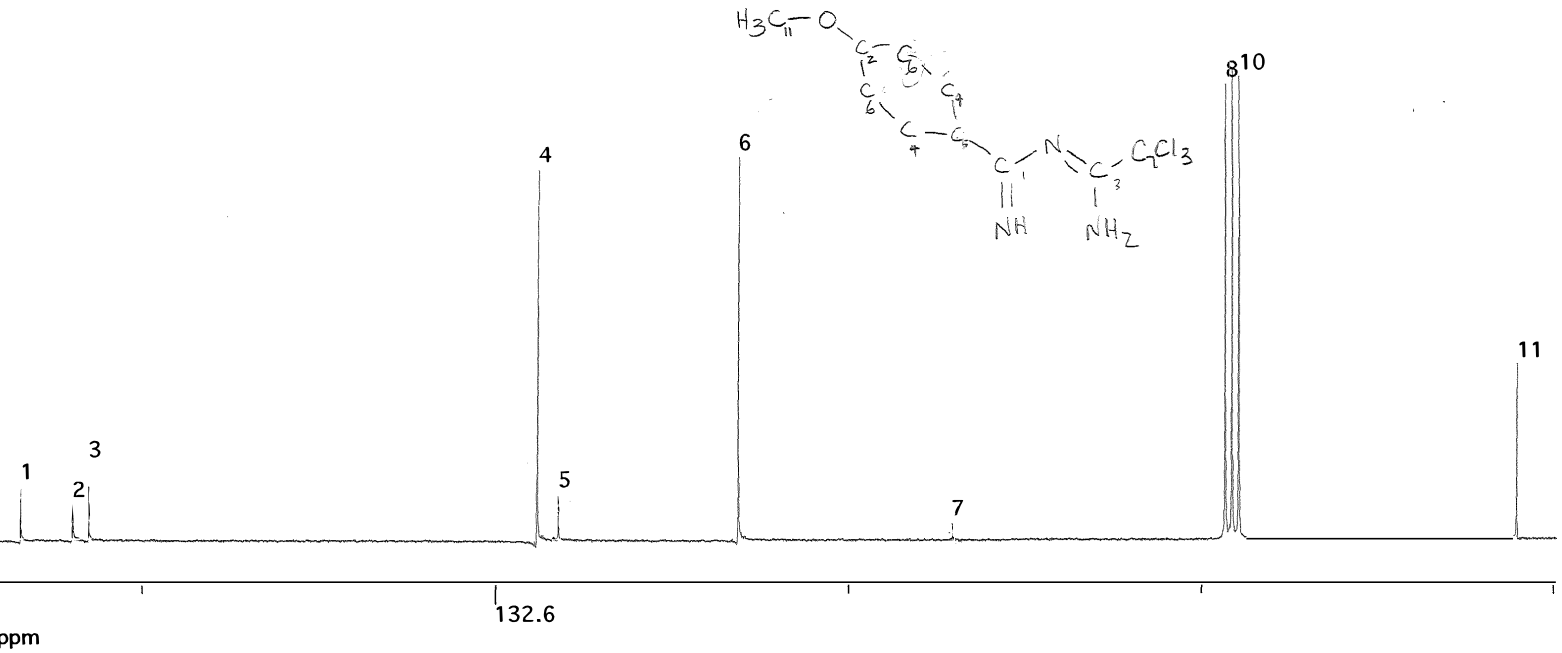

C13-NMR of **1a** in $CDCl_3$

Mode= 2 (Mid-IR)

Res=4 cm-1 Apod= Cosine Zero Filling= 1 x

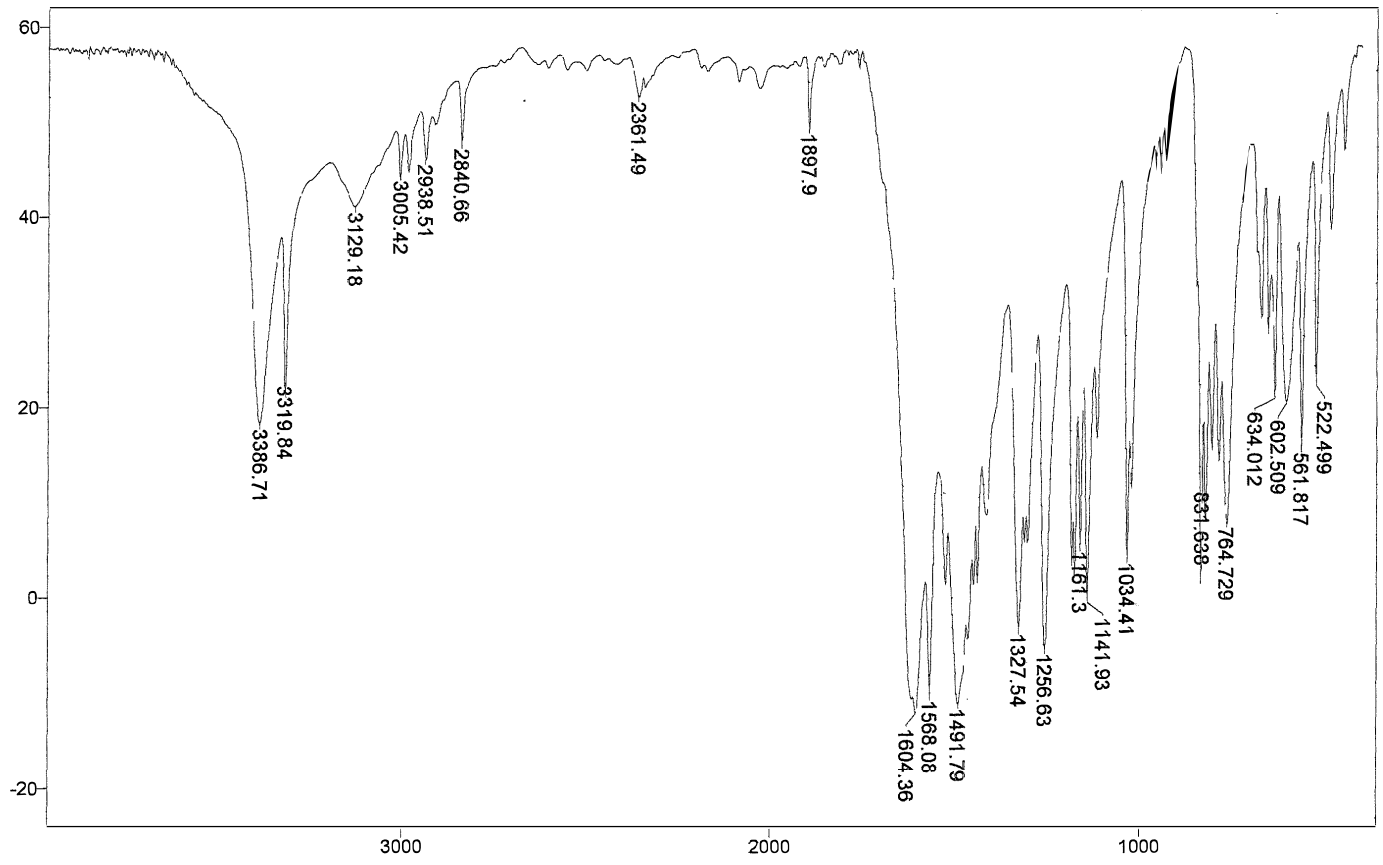

Transmittance / Wavenumber (cm-1)

FTIR of **1a** as a solid film.

Filename	CH3-imidoylamidine2
Nucleus	H1
No. Scans	-1
No. Points	32768
Scan Count	364
SW +l-	2500.0
Filter	3000
Acq. Time	6.554s
Obs Freq	250.1346939
Obs base	250.1330000
O1 offset	1.6939 KHz
RCVR gain	800
DEC Mode	OFF
DEC Attn.	58
Sequence	1PULSE
Last Delay	2s
Line Brdng	0.10
temp K	293.0

20 peaks found in CH3-imidoylamidine2

peak	ppm	freq	amp
1	7.938	1985.47	5312.75
2	7.859	1965.79	40594.69
3	7.852	1963.96	15934.59
4	7.846	1962.43	5934.85
5	7.843	1961.67	5512.63
6	7.825	1957.40	46044.18
7	7.809	1953.28	3102.22
8	7.698	1925.51	2820.97
9	7.666	1917.42	3407.25
10	7.389	1848.14	2341.75
11	7.355	1839.75	2529.44
12	7.266	1817.47	38281.65
13	7.264	1816.86	38159.19
14	7.252	1813.96	13317.15
15	7.250	1813.35	14686.02
16	7.232	1808.93	36233.53
17	7.222	1806.34	8479.07
18	7.214	1804.50	3590.03
19	7.212	1803.89	2995.92
20	7.209	1803.28	2439.98

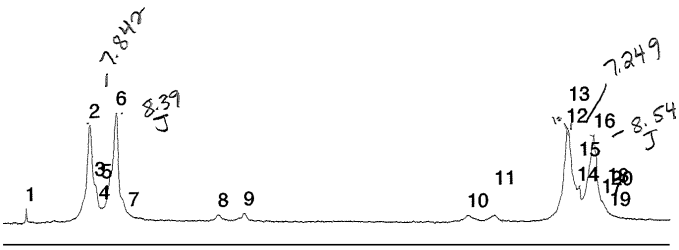

#	Start ppm	Stop ppm	Integral
4	10.84	10.52	0.47
5	9.43	9.23	0.68
2	7.92	7.65	1.74
3	7.41	7.15	1.94
6	6.72	6.42	0.58
1	2.55	2.33	3.00

2 peaks found in CH3-imidoylamidine2

peak	ppm	freq	amp
1	2.480	620.27	11132.38
2	2.402	600.74	147488.00

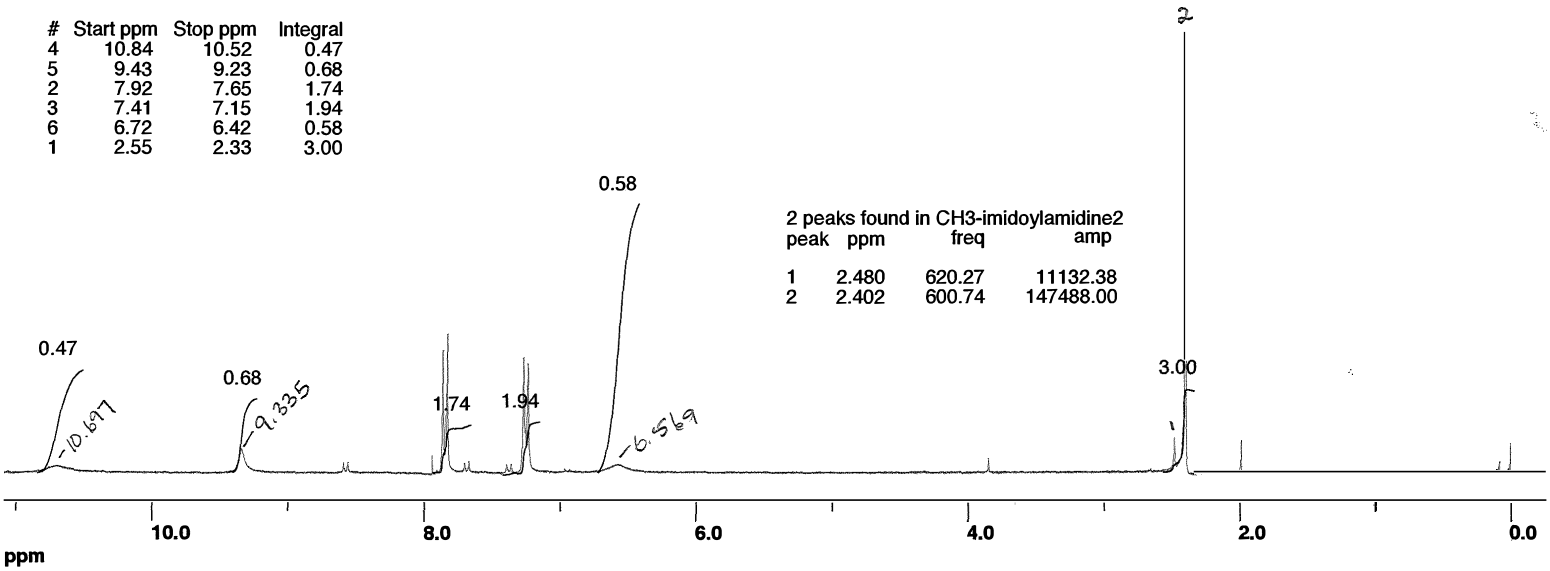

H1-NMR of **1b** in $CDCl_3$

1H_**1b**
CH3C6H4C2CCl3N3H3
1H spectrum
spin=22Hz, T=17.8Degree C

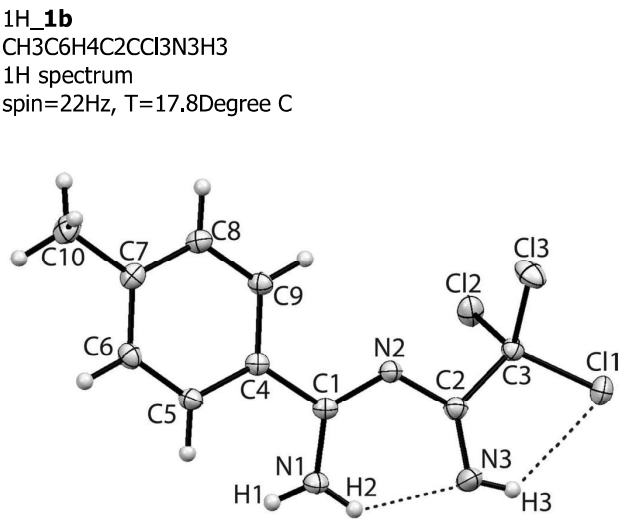

H1-NMR of 1b in CDCl3

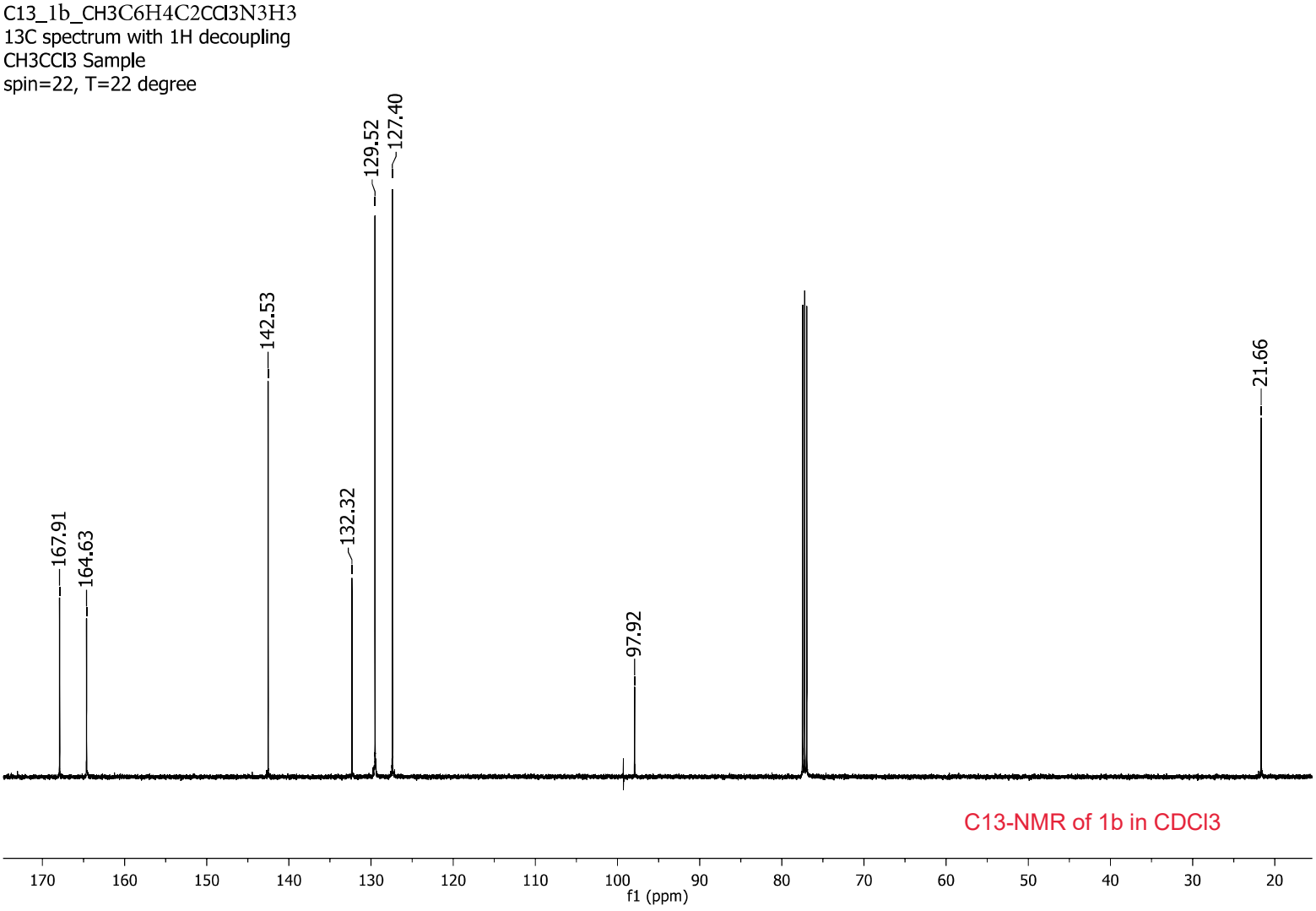
C13_1b_CH3C6H4C2CCl3N3H3
13C spectrum with 1H decoupling
CH3CCl3 Sample
spin=22, T=22 degree
167.91
164.63
142.53
132.32
129.52
127.40
97.92
21.66
C13-NMR of 1b in CDCl3
170
160
150
140
130
120
110
100
90
80
70
60
50
40
30
20
f1 (ppm)

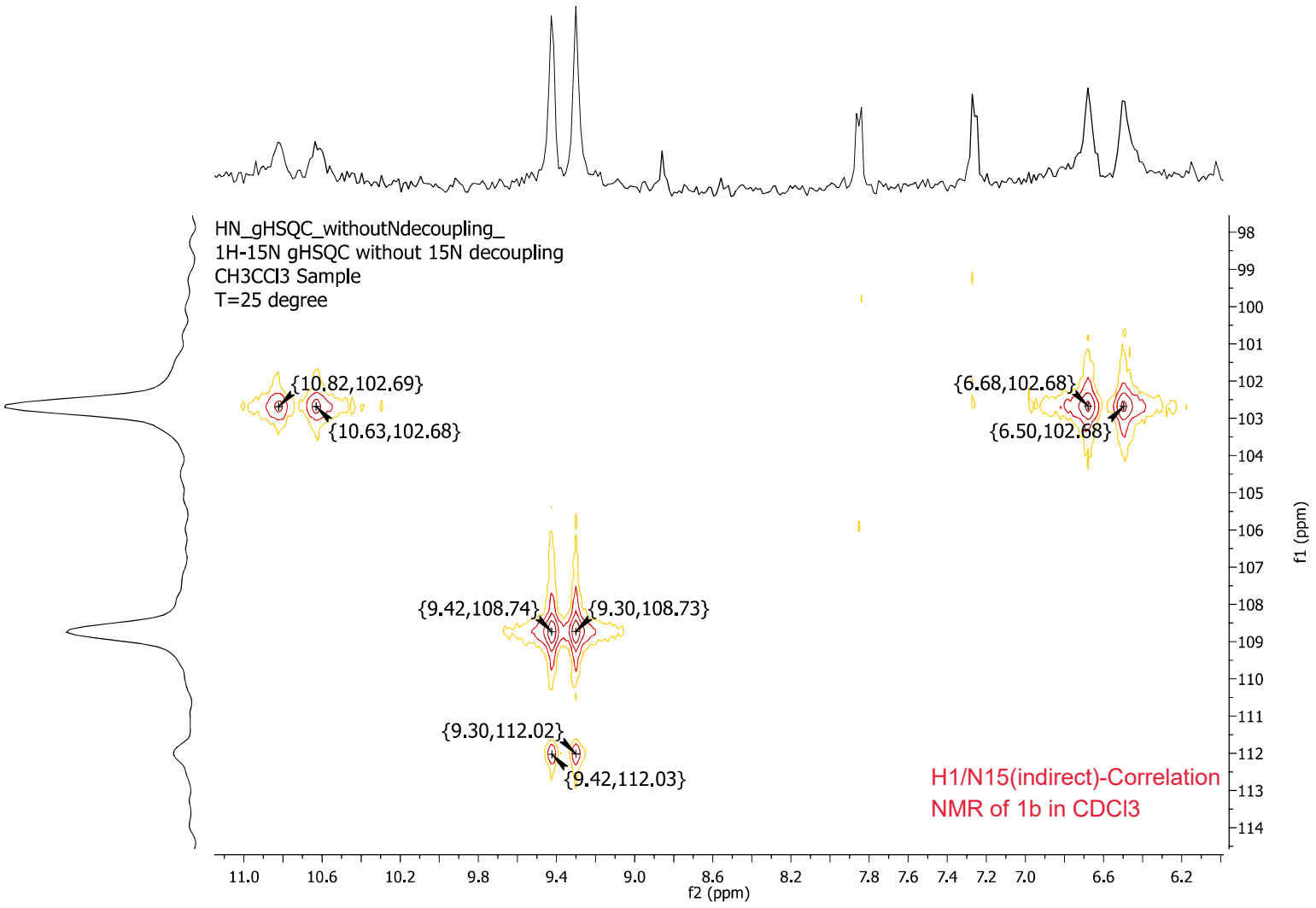
HN_gHSQC_withoutNdecoupling_
1H-15N gHSQC without 15N decoupling
CH3CCl3 Sample
T=25 degree
{10.82,102.69}
{10.63,102.68}
{6.68,102.68}
{6.50,102.68}
{9.42,108.74}
{9.30,108.73}
{9.30,112.02}
{9.42,112.03}
H1/N15(indirect)-Correlation
NMR of 1b in CDCl3
f2 (ppm)
f1 (ppm)

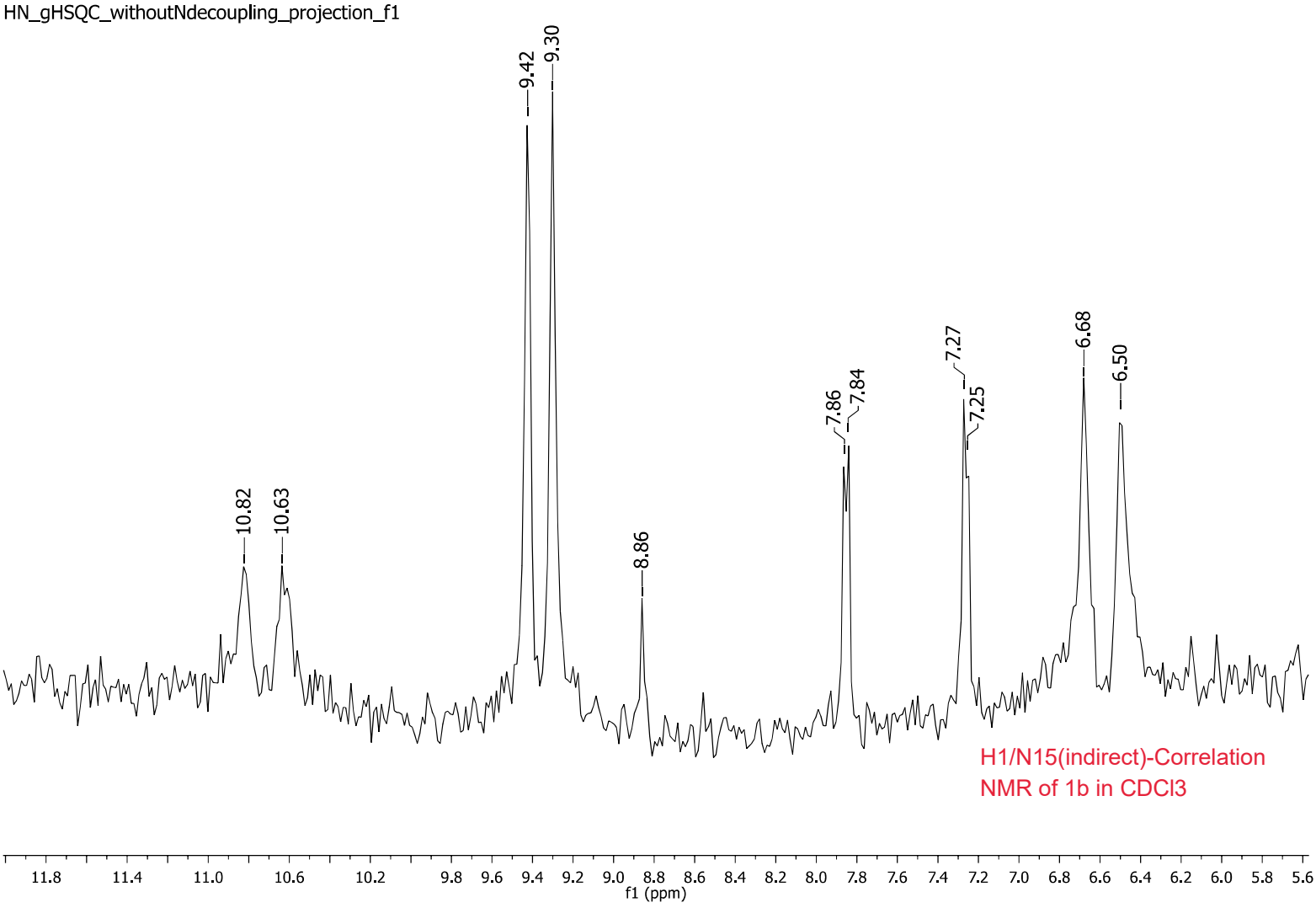
HN_gHSQC_withoutNdecoupling_projection_f1
9.42
9.30
10.82
10.63
8.86
7.86
7.84
7.27
7.25
6.68
6.50
H1/N15(indirect)-Correlation
NMR of 1b in CDCl3
11.8
11.4
11.0
10.6
10.2
9.8
9.6
9.4
9.2
9.0
8.8
8.6
8.4
8.2
8.0
7.8
7.6
7.4
7.2
7.0
6.8
6.6
6.4
6.2
6.0
5.8
5.6
f1 (ppm)

HN_gHSQC_withoutNdecoupling_08DEC02_projection_f2

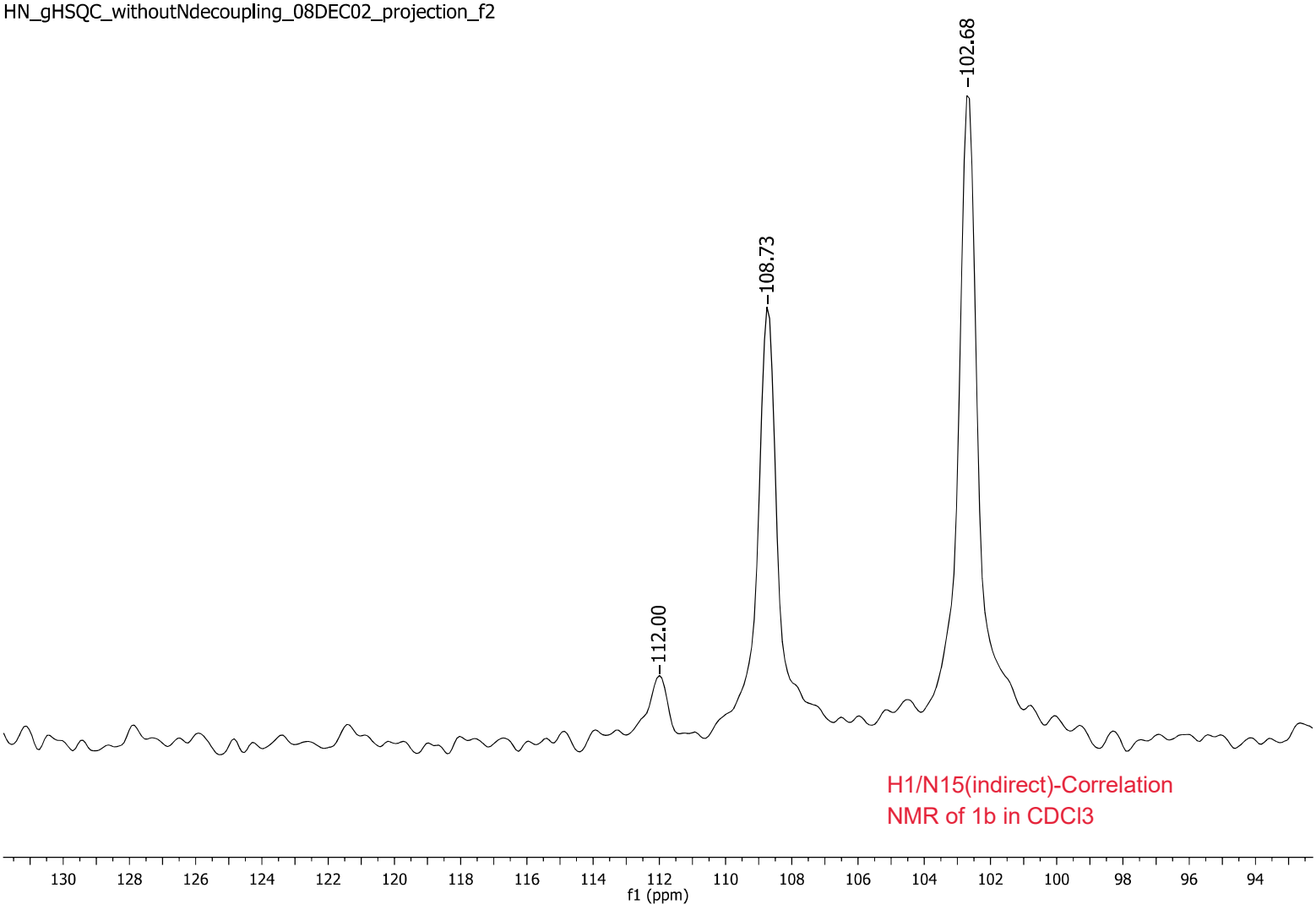

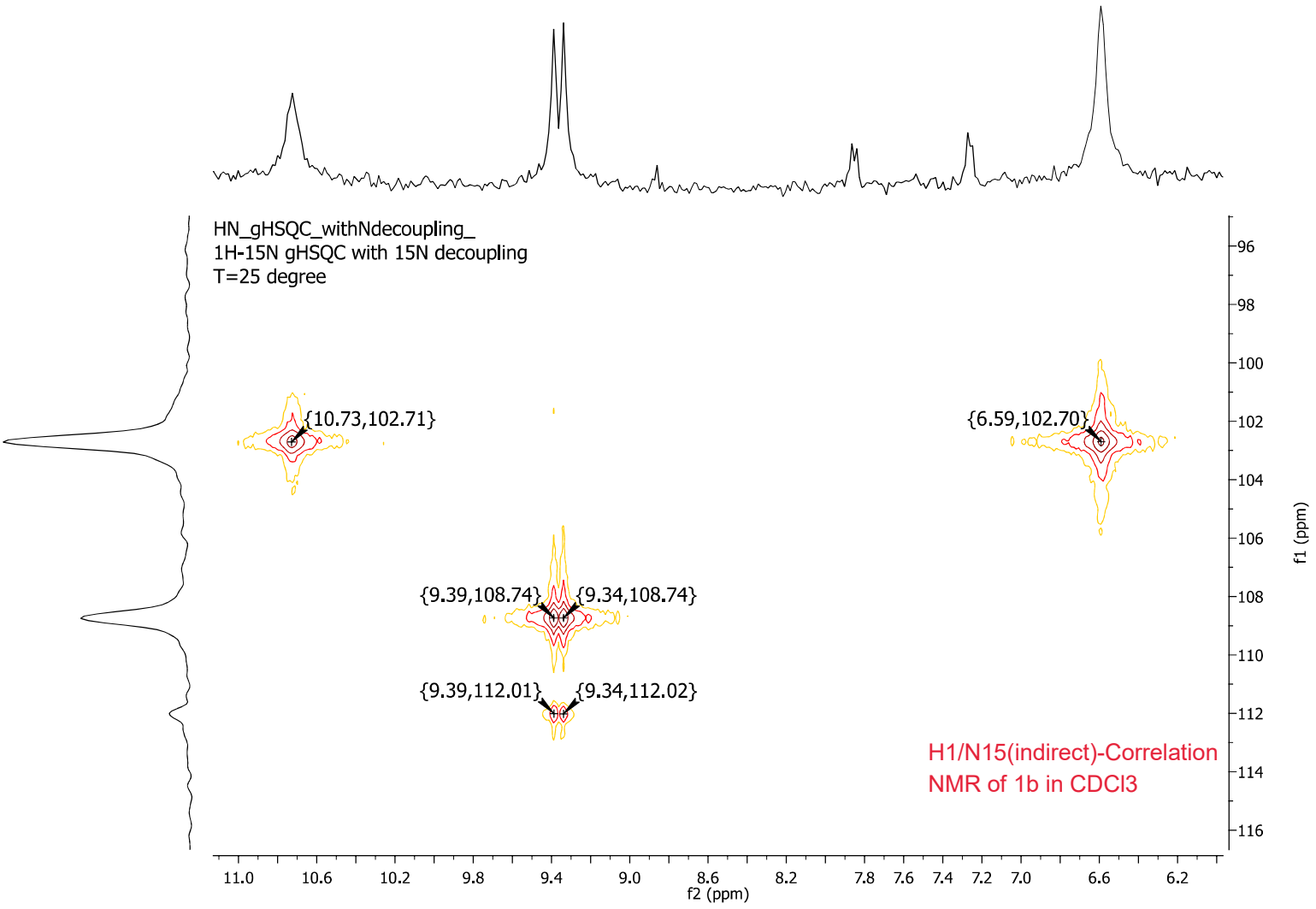
HN_gHSQC_withNdecoupling_
1H-15N gHSQC with 15N decoupling
T=25 degree
{10.73,102.71}
{6.59,102.70}
{9.39,108.74}
{9.34,108.74}
{9.39,112.01}
{9.34,112.02}
H1/N15(indirect)-Correlation
NMR of 1b in CDCl3
f2 (ppm)
f1 (ppm)

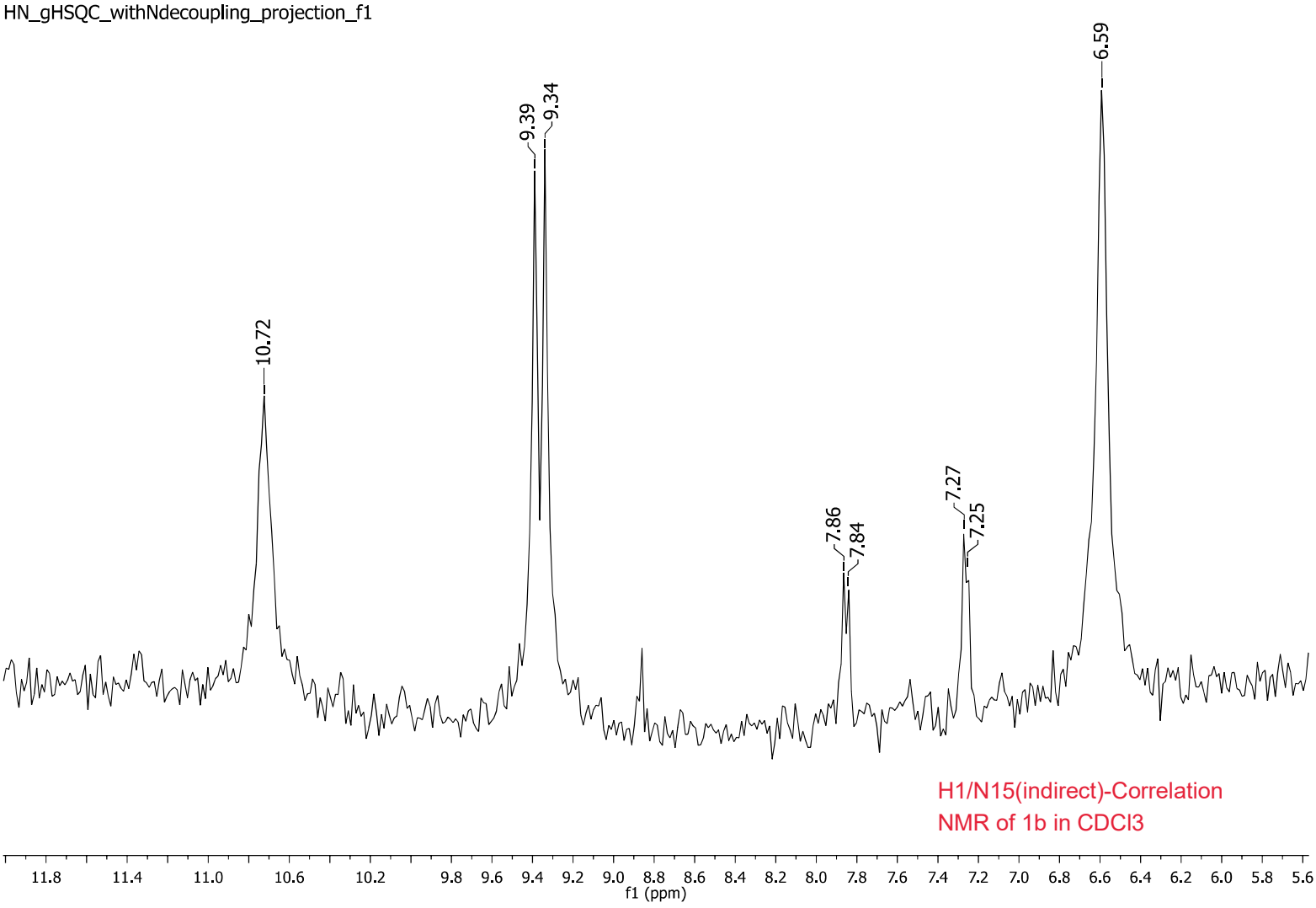
HN_gHSQC_withNdecoupling_projection_f1
10.72
9.39
9.34
7.86
7.84
7.27
7.25
6.59
H1/N15(indirect)-Correlation
NMR of 1b in CDCl3
11.8 11.4 11.0 10.6 10.2 9.8 9.6 9.4 9.2 9.0 8.8 8.6 8.4 8.2 8.0 7.8 7.6 7.4 7.2 7.0 6.8 6.6 6.4 6.2 6.0 5.8 5.6
f1 (ppm)

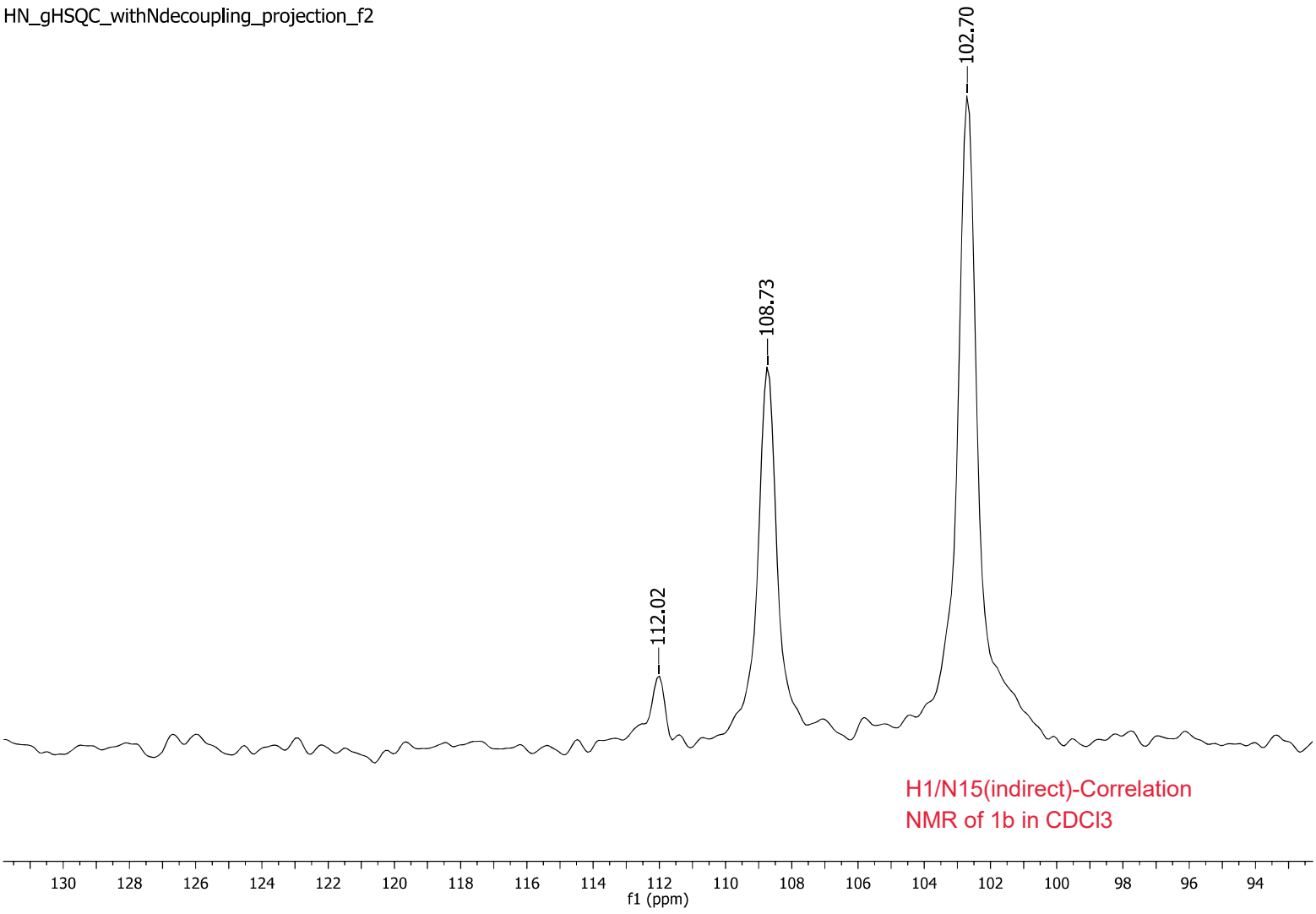
HN_gHSQC_withNdecoupling_projection_f2
102.70
108.73
112.02
H1/N15(indirect)-Correlation
NMR of 1b in CDCl3
130
128
126
124
122
120
118
116
114
112
110
108
106
104
102
100
98
96
94
f1 (ppm)

File # 1 : IMIAMI Mode= 2 (Mid-IR)

Sample Description: CH3/CCl3 imidoylamidine left in fridge

Scans= 10 Slow Res=4 cm-1 Apod= Cosine Zero Filling= 1 x

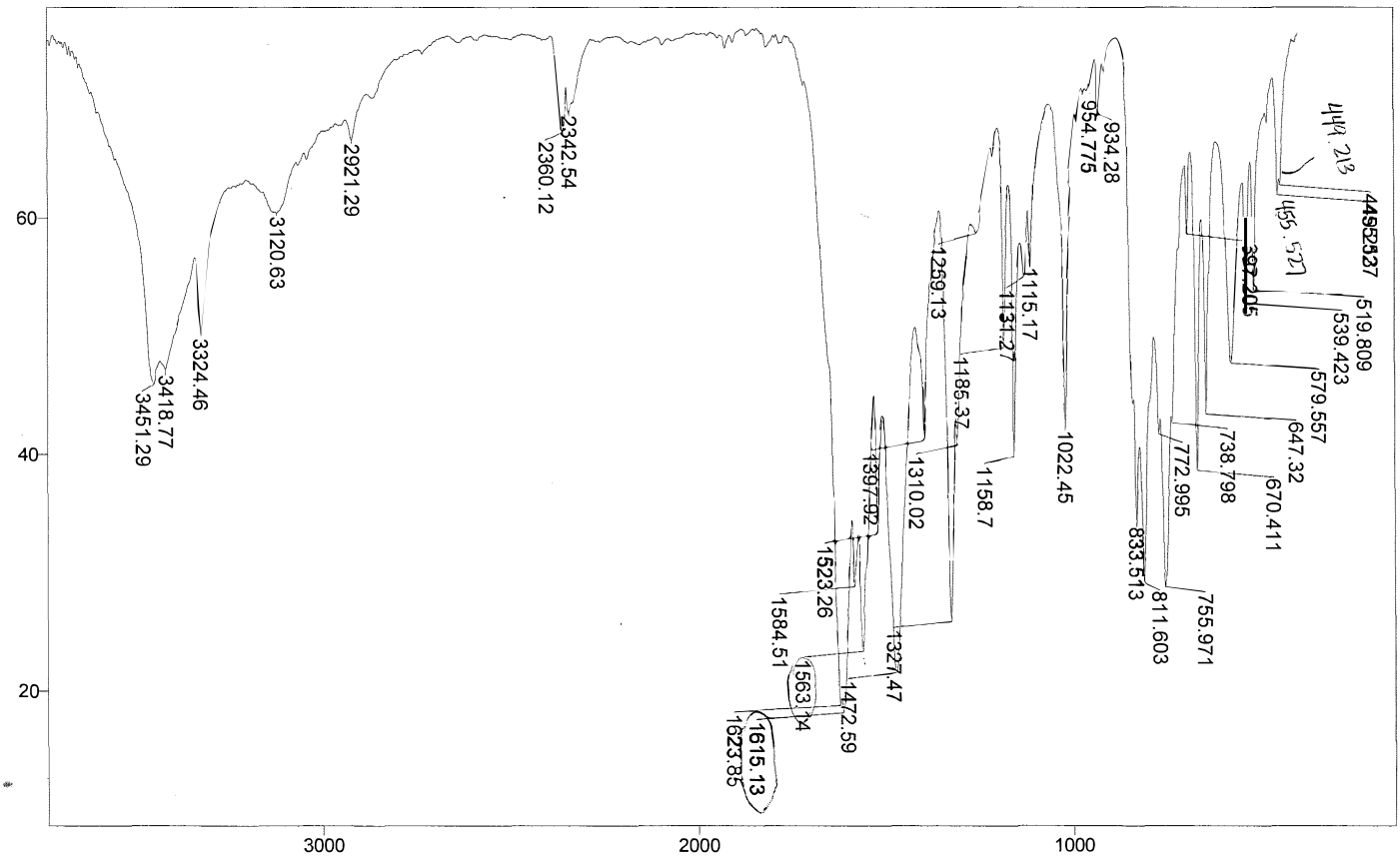

FTIR of **1b** as a solid film.

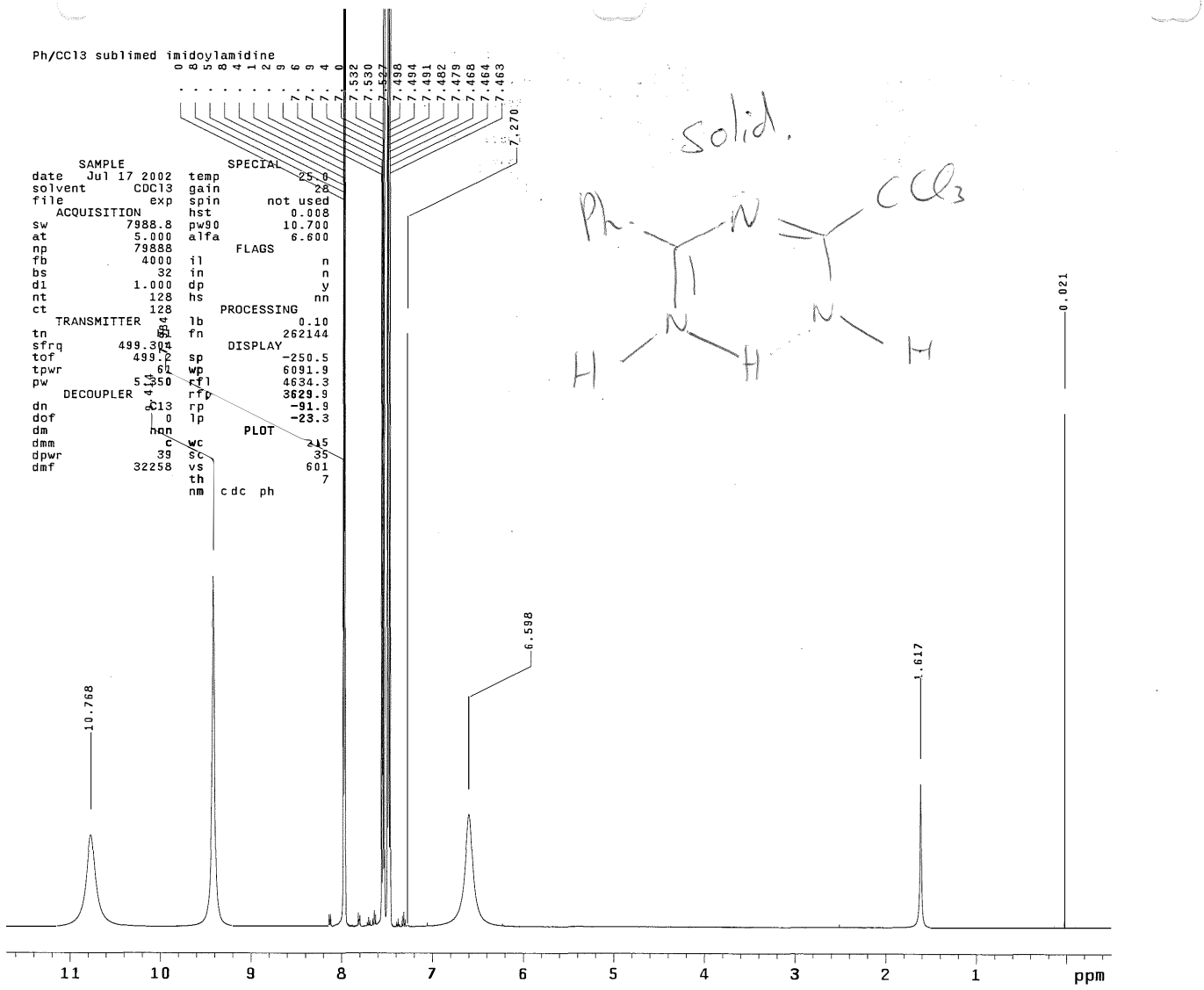

solid.

H1-NMR of **1c** in $CDCl_3$

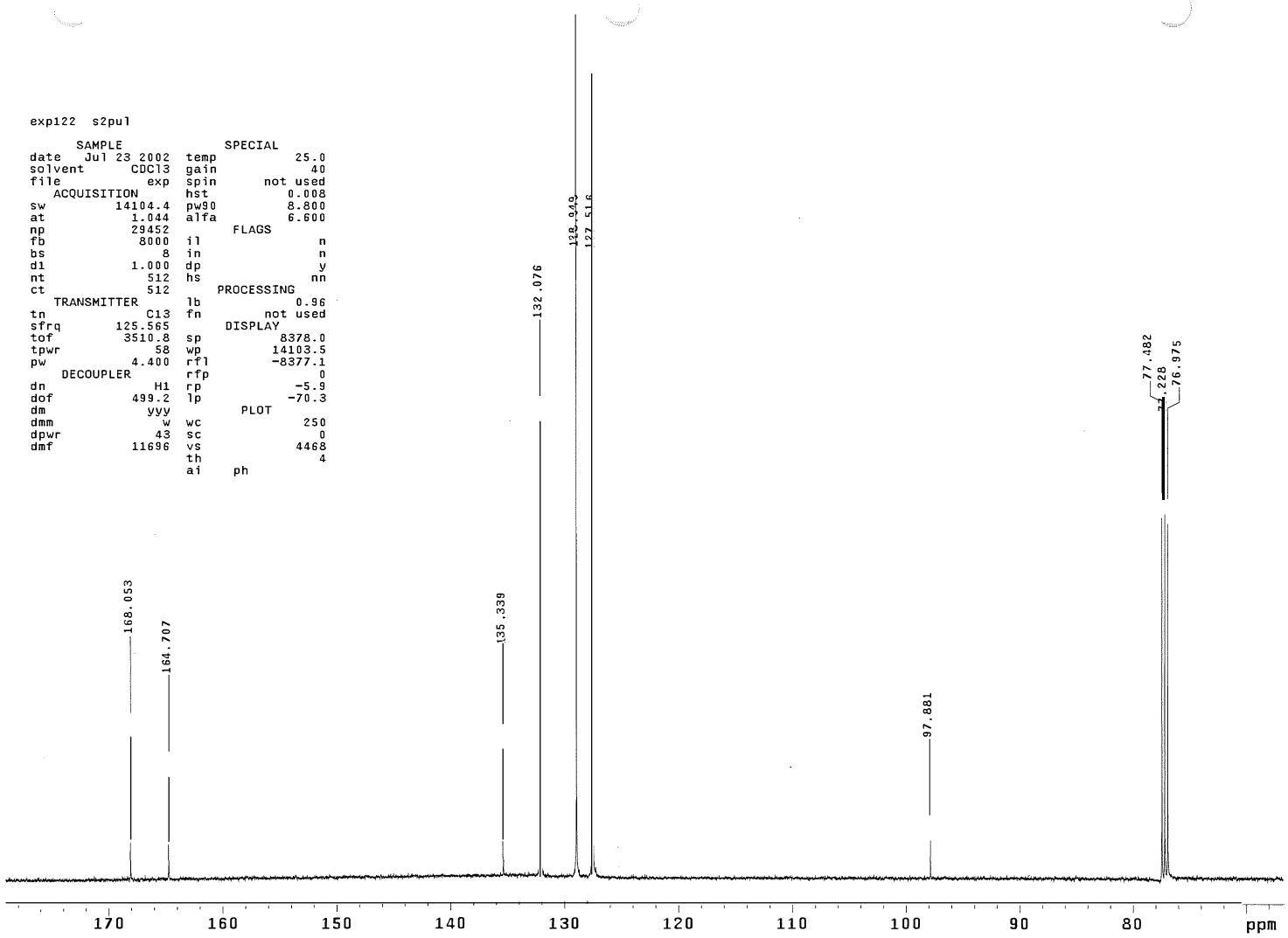

C13-NMR of **1c** in $CDCl_3$

Mode= 2 (Mid-IR)

Scans= 10 Slow | Res=4 cm-1 | Apod= Cosine | Zero Filling= 1 x

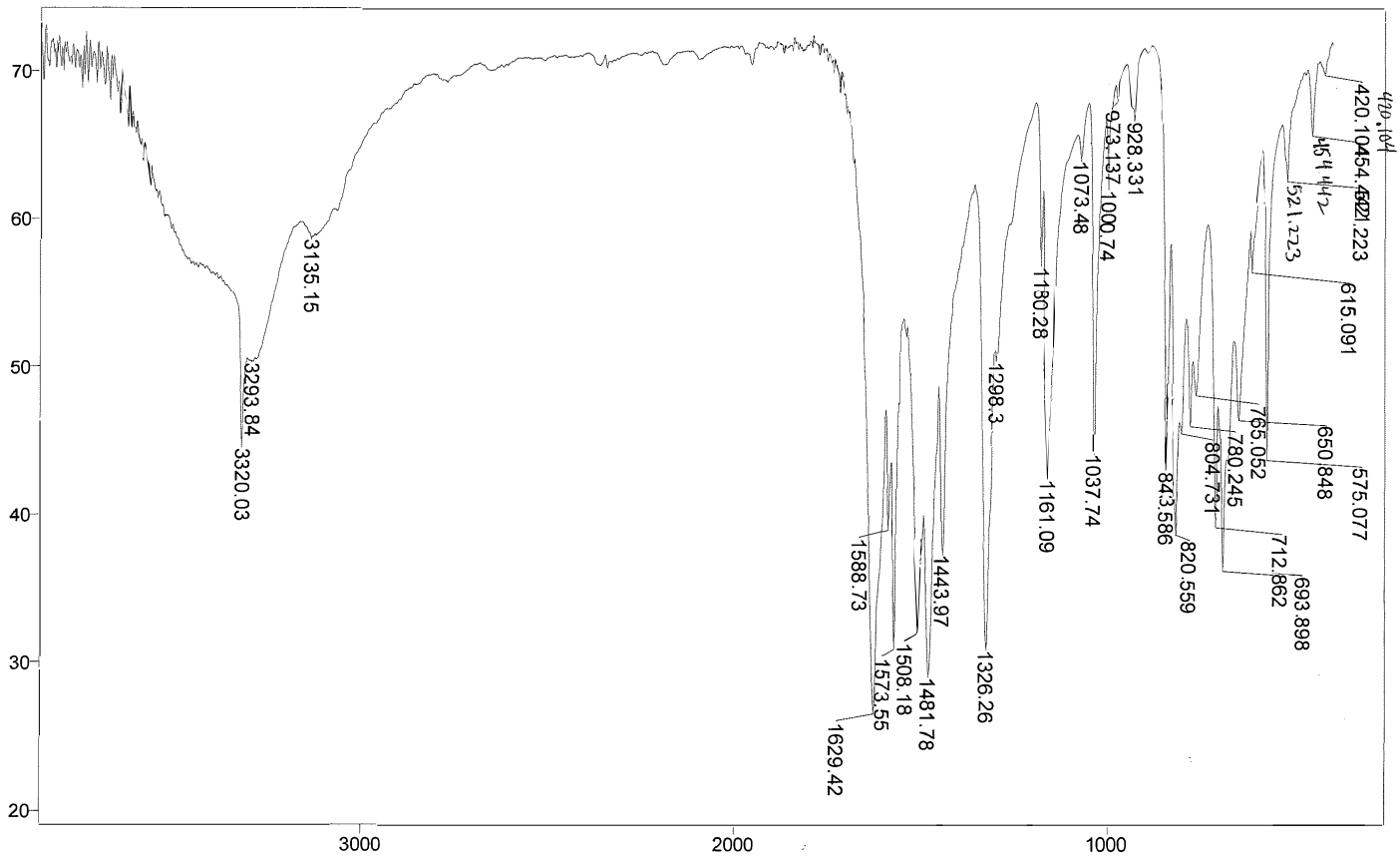

Transmittance / Wavenumber (cm-1)

FTIR of **1c** as a solid film.

Filename	proton 3
Nucleus	H1
No. Scans	-1
No. Points	32768
Scan Count	12
SW +l-	2500.0
Filter	3000
Acq. Time	6.554s
Obs Freq	250.1346939
Obs base	250.1330000
O1 offset	1.6939 KHz
RCVR gain	64
DEC Mode	OFF
DEC Attn.	58
Sequence	1PULSE
Last Delay	2s
Line Brdng	0.10
temp K	293.0
spin rate	0
Solvent	

12 peaks found in proton 3

peak	ppm	freq	amp
1	7.896	1975.10	5781.54
2	7.886	1972.66	39772.95
3	7.878	1970.52	13273.34
4	7.860	1965.94	14914.76
5	7.851	1963.81	45516.76
6	7.841	1961.36	6004.25
7	7.442	1861.42	6981.43
8	7.432	1858.98	46891.41
9	7.423	1856.84	14122.20
10	7.405	1852.26	13927.21
11	7.397	1850.13	38949.95
12	7.387	1847.69	4791.88

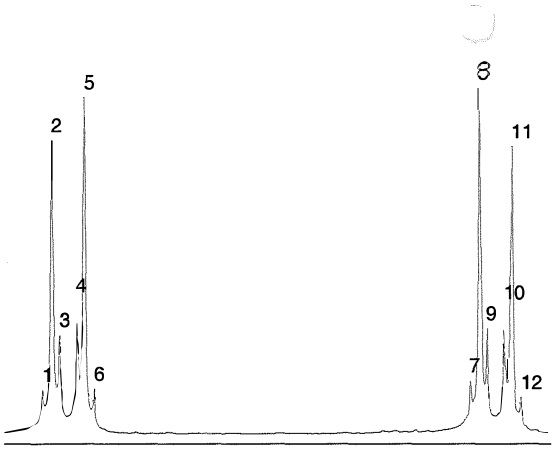

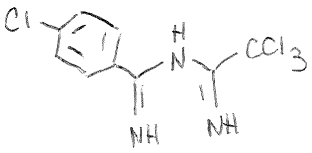

#	Start ppm	Stop ppm	Integral
3	11.03	10.52	0.69
4	9.67	9.26	0.84
1	7.96	7.78	2.00
2	7.53	7.34	2.01
5	6.83	6.36	0.67
6	2.01	1.99	0.01

H1-NMR of **1d** in $CDCl_3$

No. Points	32768
No. Scans	-1
Dummy Scans	0
Scan Count	8232
SW +l-	8000.0
Filter	8000
Acq. Time	2.048s
Dwell	62.5u
Obs Freq	62.9034273
Obs base	62.8960000
01 offset	7.4273 KHz
dcplfreq	250.1322620
02 offset	2.2620 KHz
RCVR gain	800
DEC Mode	BB
DEC Attn.	107
Sequence	1PULSE with Decoupling
Last Delay	8s
PW01	
PW02	
PW03	

10 peaks found in carbon 3

peak	ppm	freq	amp
1	168.006	10566.93	1391423.50
2	163.612	10290.56	932317.12
3	138.436	8707.06	1511951.88
4	133.894	8421.42	1261976.75
5	129.213	8126.98	10853139.00
6	128.926	8108.92	10320766.00
7	97.803	6151.40	428366.78
8	77.750	4890.17	3534272.00
9	77.238	4857.94	3566967.50
10	76.733	4826.20	3586625.50

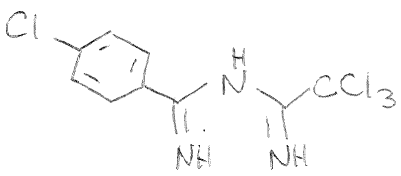

C13-NMR of **1d** in $CDCl_3$

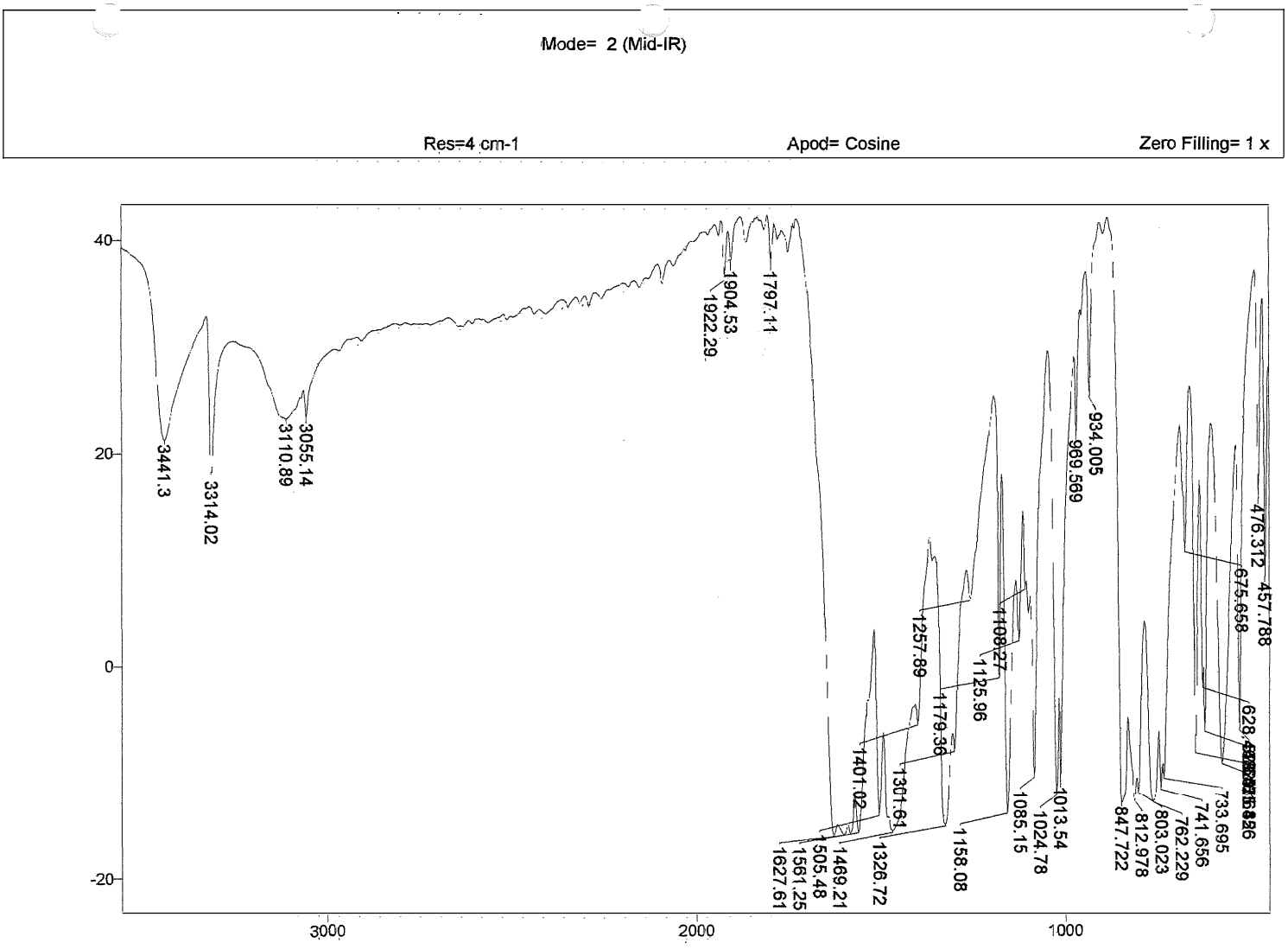

Transmittance / Wavenumber (cm-1)

FTIR of **1d** as a solid film.

Nucleus	H1
Dwell 1D	200u
SW +l-	2500.0
FILTER	3000
Scans 1D	-1
Scan Count	28
Points 1D	32768
Last Delay	2s
Obs Freq	250.1346939
F1 base	250.1330000
F1 offset	1.6939 KHz
RCVR gain	64
F2 freq	250.1305000
F2 base	250.1300000
F2 offset	0.5000 KHz
DEC Power	58
DEC Scheme	OFF
Dummy scan	0

10 peaks found in p-CF3 imidoylamidine 3

peak	ppm	freq	amp
1	9.511	2379.00	5850.49
2	8.078	2020.57	22530.82
3	8.046	2012.48	26620.45
4	7.958	1990.66	1432.23
5	7.742	1936.49	29049.31
6	7.709	1928.25	23962.94
7	7.259	1815.80	4998.45
8	2.006	501.71	12058.90
9	0.074	18.62	3174.22
10	0.000	0.00	7230.27

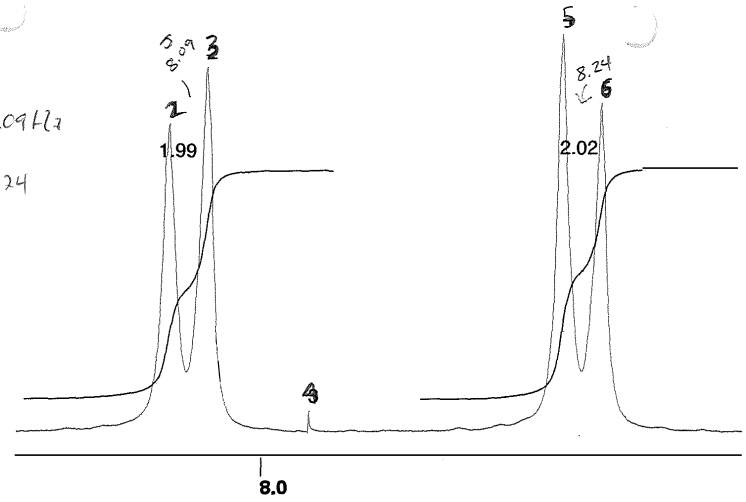

#	Start ppm	Stop ppm	Integral
3	11.35	10.52	0.77
4	9.78	9.31	0.91
1	8.20	7.94	1.99
2	7.86	7.59	2.02
5	6.92	6.34	0.79
6	2.10	1.90	0.15

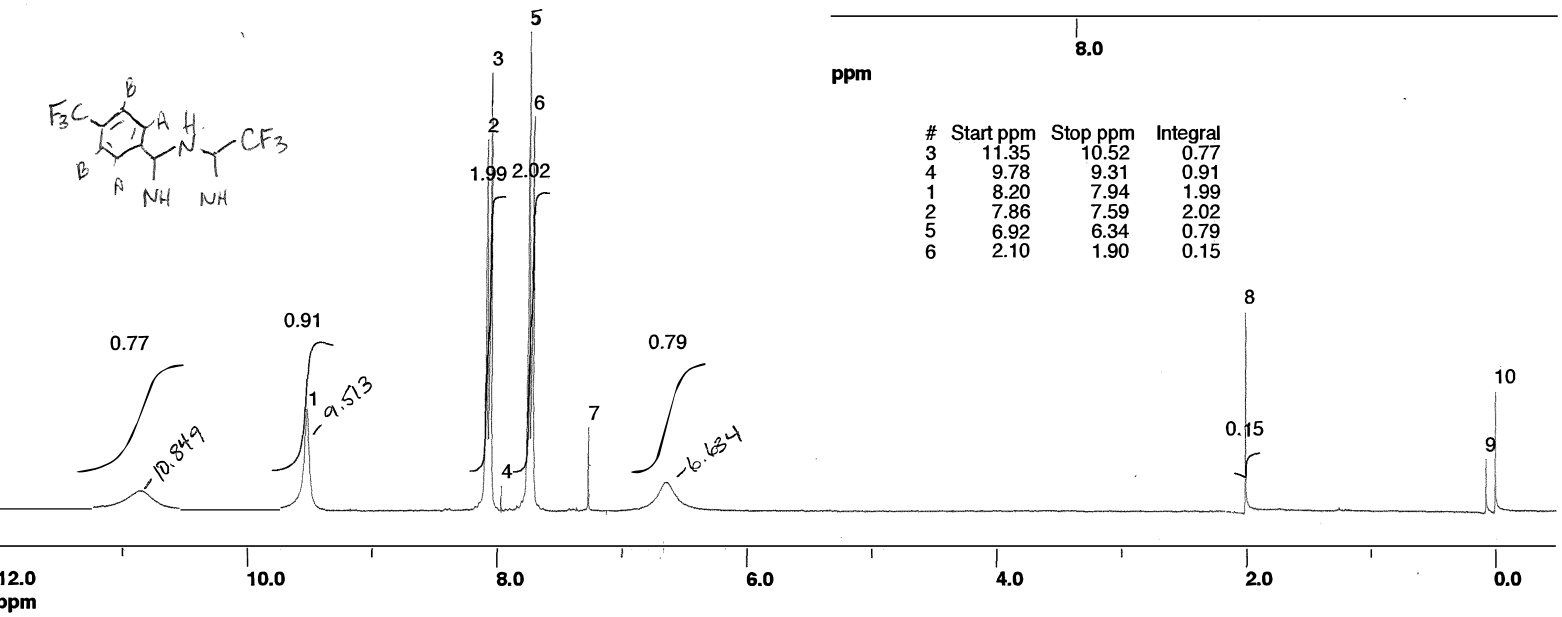

H1-NMR of **1e** in $CDCl_3$

Nucleus	C13
Dwell 1D	62.5u
SW +l-	8000.0
FILTER	8000
Scans 1D	-1
Scan Count	17780
Points 1D	32768
Last Delay	8s
Obs Freq	62.9034273
F1 base	62.8960000
F1 offset	7.4273 KHz
RCVR gain	800
F2 freq	250.1322620
F2 base	250.1300000
F2 offset	2.2620 KHz
DEC Power	108
DEC Scheme	BB
Dummy scan	0

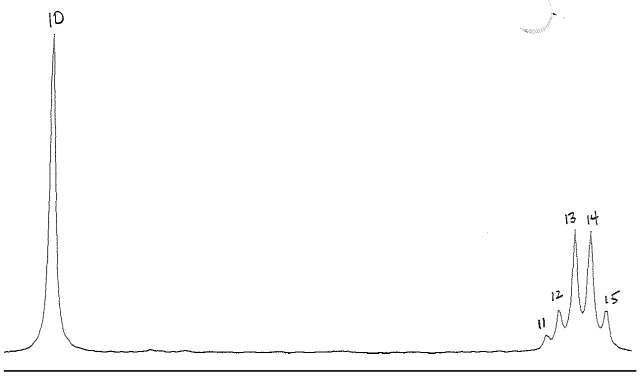

25 peaks found in p-CF3 imidoylamidine 5

peak	ppm	freq	amp
1	168.030	10568.39	1327116.12
2	163.387	10276.40	918641.56
3	138.902	8736.36	675983.81
4	138.886	8735.38	652070.69
5	134.609	8466.34	164719.50
6	134.089	8433.63	497825.72
7	133.568	8400.91	493574.62
8	133.048	8368.20	157941.41
9	130.471	8206.09	184219.75
10	128.025	8052.28	12078680.00
11	126.139	7933.63	673649.75
12	126.092	7930.70	1631660.50
13	126.030	7926.79	4668197.50
14	125.968	7922.88	4620320.50
15	125.906	7918.98	1587847.88
16	121.807	7661.16	477702.84
17	117.467	7388.21	162861.94
18	97.624	6140.17	438226.34
19	77.742	4889.68	7517279.50
20	77.432	4870.15	164736.64
21	77.238	4857.94	7546056.00
22	76.725	4825.71	7668668.00
23	76.430	4807.16	187324.44
24	76.368	4803.25	171855.38
25	76.329	4800.81	160739.09

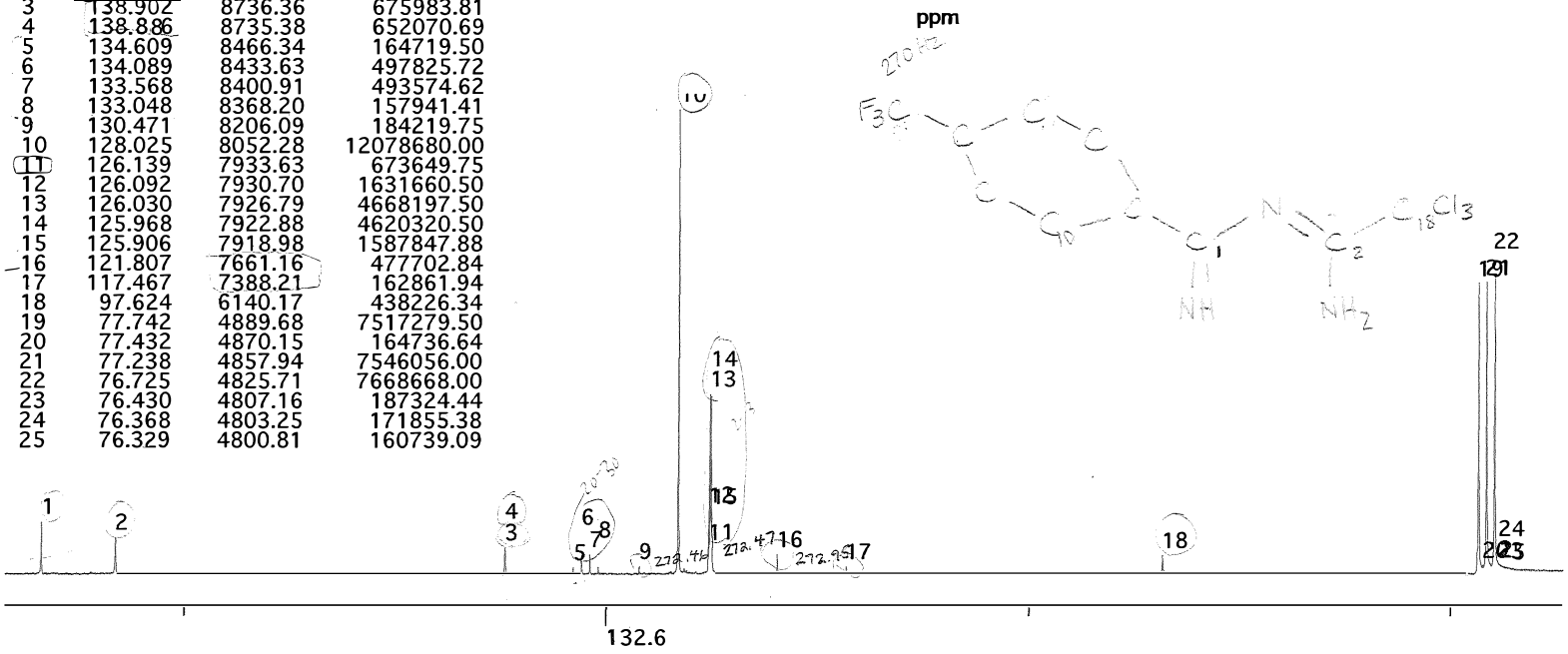

C13-NMR of **1e** in $CDCl_3$

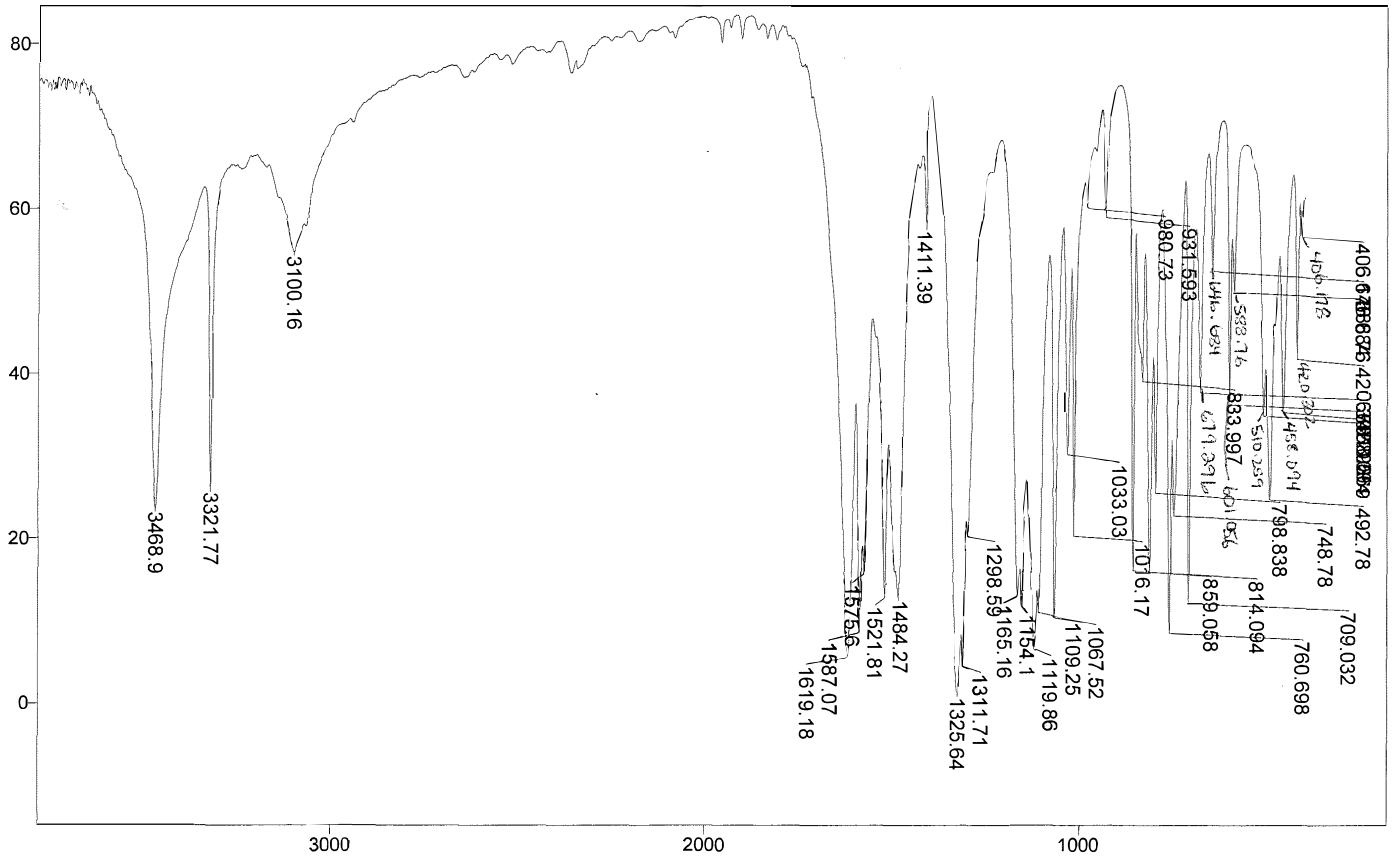

FTIR of **1e** as a solid film.

Transmittance / Wavenumber (cm-1)

Filename	thiatriazine OCH3, S-Cl
Nucleus	H1
No. Scans	-1
No. Points	32768
Scan Count	20
SW +/-	2500.0
Filter	3000
Acq. Time	6.554s
Obs Freq	250.1346939
Obs base	250.1330000
O1 offset	1.6939 KHz
RCVR gain	200
DEC Mode	OFF
DEC Attn.	58
Sequence	1PULSE
Last Delay	2s
Line Brdng	0.10
temp K	293.0

18 peaks found in thiatriazine OCH3, S-Cl 3

peak	ppm	freq	amp
1	8.508	2128.14	12101.55
2	8.500	2126.01	3992.81
3	8.479	2120.97	3526.08
4	8.471	2118.99	13795.26
5	8.460	2116.09	1968.89
6	8.118	2030.49	1188.51
7	7.262	1816.56	22034.58
8	7.062	1766.36	1163.74
9	7.050	1763.46	13418.94
10	7.042	1761.32	7044.54
11	7.022	1756.44	3852.35
12	7.013	1754.30	13898.57
13	7.003	1751.56	4527.17
14	3.947	987.40	6355.44
15	3.939	985.26	57951.34
16	3.924	981.60	1072.84
17	3.896	974.58	14511.55
18	3.838	960.08	3655.78

0.15 Hz per pt.

9.15

9.16

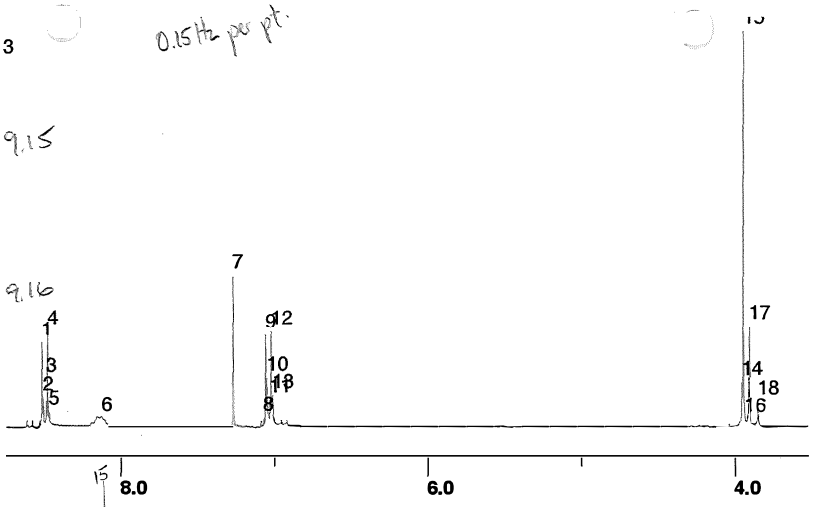

#	Start ppm	Stop ppm	Integral
2	8.54	8.42	1.10
3	7.11	6.90	1.97
1	3.99	3.82	3.00

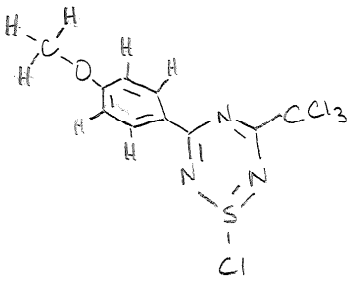

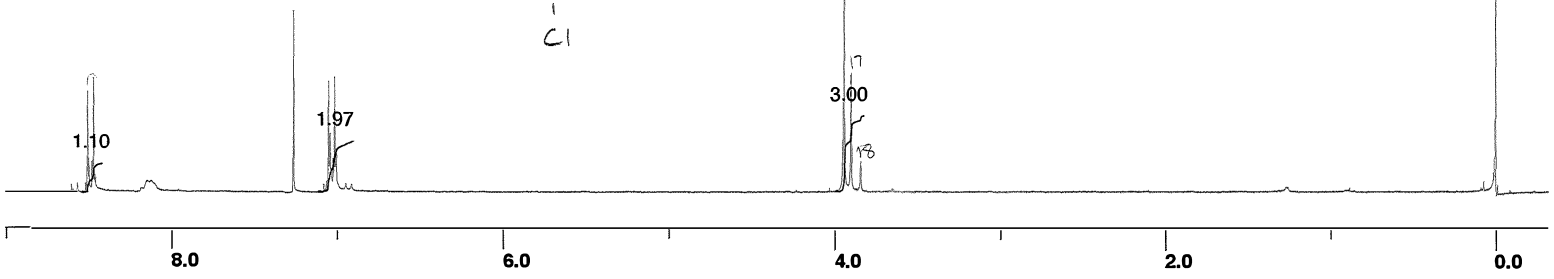

H1-NMR of **4a** in $CDCl_3$

Filename	thiatriazine CH3, S-Cl
Nucleus	H1
No. Scans	-1
No. Points	32768
Scan Count	116
SW +l-	2500.0
Filter	3000
Acq. Time	6.554s
Obs Freq	250.1346939
Obs base	250.1330000
O1 offset	1.6939 KHz
RCVR gain	200
DEC Mode	OFF
DEC Attn.	58
Sequence	1PULSE
Last Delay	2s
Line Brdng	0.10
temp K	293.0

5 peaks found in thiatriazine CH3, S-Cl

peak	ppm	freq	amp	
1	8.413	2104.34	94567.47	8.24
2	8.380	2096.10	124605.20	
3	7.370	1843.41	99507.20	8.54
4	7.336	1834.87	116636.86	
5	7.259	1815.80	34204.45	

#	Start ppm	Stop ppm	Integral
1	8.46	8.26	1.65
2	7.45	7.20	2.03
3	2.61	2.29	3.00

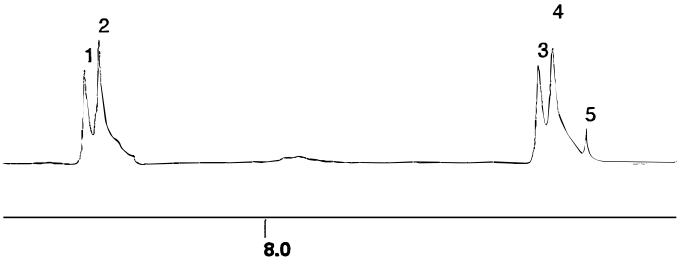

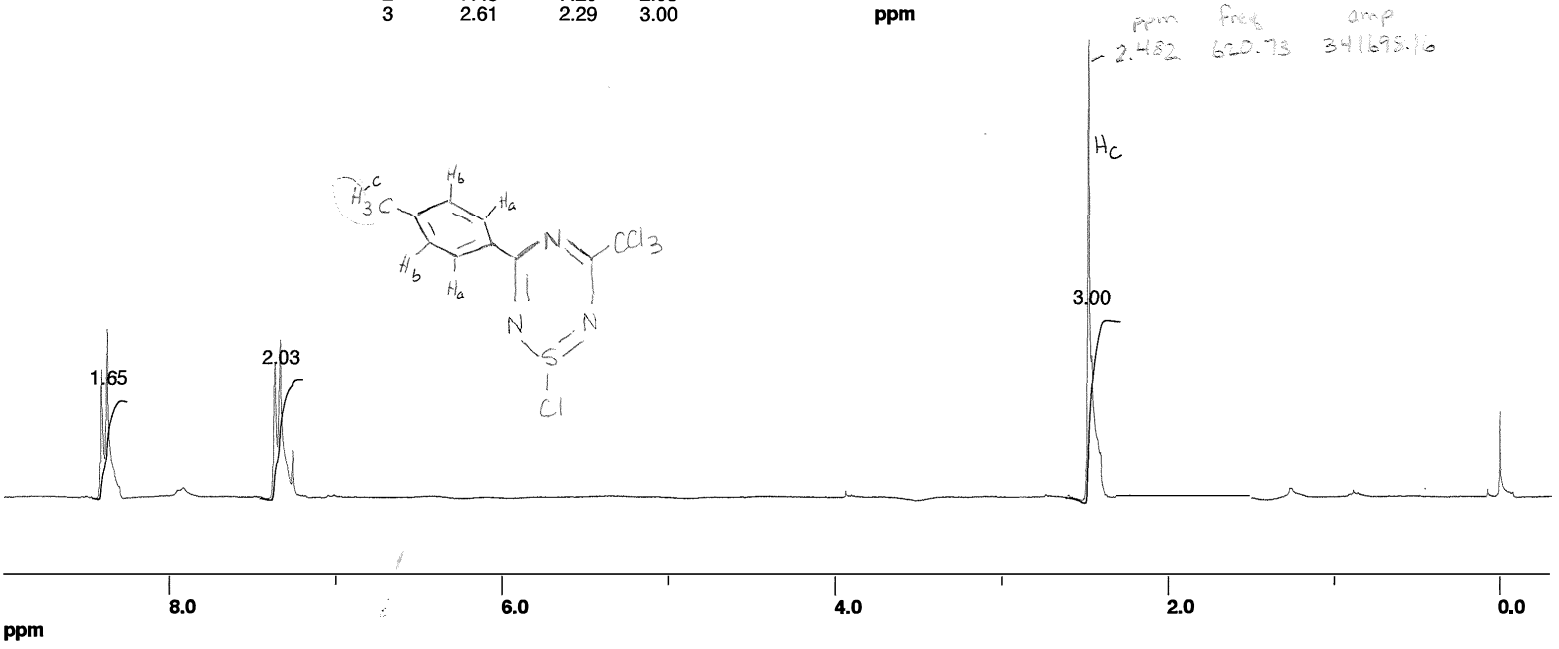

H1-NMR of **4b** in $CDCl_3$

Filename	thiatriazine S-Cl 6
Nucleus	H1
No. Scans	-1
No. Points	32768
Scan Count	120
SW +l-	2500.0
Filter	3000
Acq. Time	6.554s
Obs Freq	250.1346939
Obs base	250.1330000
O1 offset	1.6939 KHz
RCVR gain	100
DEC Mode	OFF
DEC Attn.	58
Sequence	1PULSE
Last Delay	2s
Line Brdng	0.10
temp K	293.0
spin rate	0
Solvent	

25 peaks found in thiatriazine S-Cl 5

peak	ppm	freq	amp
1	8.529	2133.48	161790.05
2	8.527	2132.87	133135.39
3	8.524	2132.11	177890.88
4	8.521	2131.50	82810.78
5	8.519	2130.89	75170.98
6	8.518	2130.58	65785.48
7	8.504	2127.08	67538.52
8	8.496	2125.09	221355.50
9	8.490	2123.57	181051.44
10	7.739	1935.73	48598.68
11	7.710	1928.41	103955.61
12	7.686	1922.45	65267.31
13	7.680	1921.08	113145.15
14	7.675	1919.71	53504.56
15	7.594	1899.41	134713.83
16	7.591	1898.80	174177.20
17	7.585	1897.28	85448.24
18	7.568	1893.01	56877.24
19	7.565	1892.24	142248.31
20	7.559	1890.87	218287.84
21	7.558	1890.41	133436.81
22	7.555	1889.65	64496.13
23	7.537	1885.38	50170.52
24	7.531	1883.70	105317.16
25	7.527	1882.78	73182.46

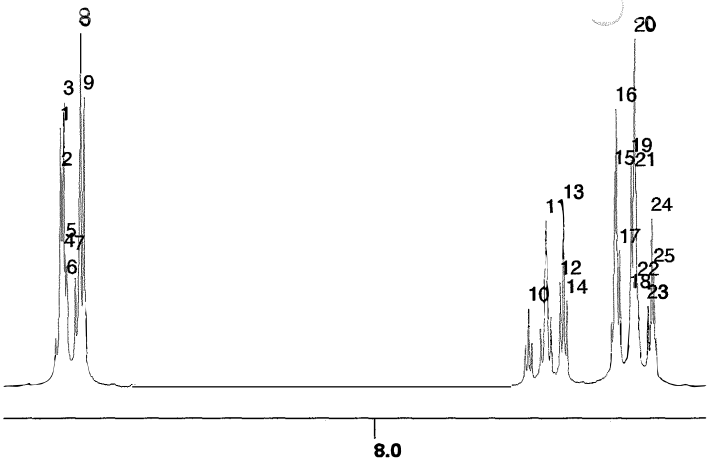

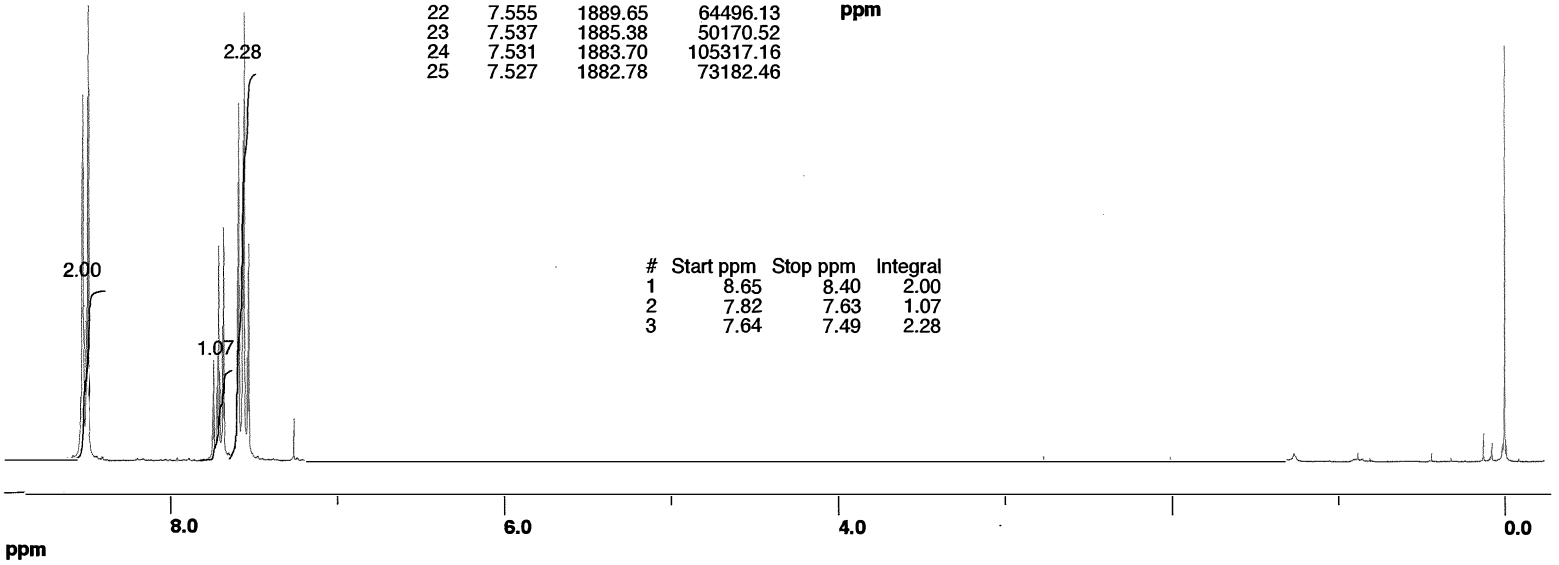

#	Start ppm	Stop ppm	Integral
1	8.65	8.40	2.00
2	7.82	7.63	1.07
3	7.64	7.49	2.28

Mar. 15, **NMR tube sealed under vacuum**

Pg 39

H1-NMR of **4c** in $CDCl_3$

Nucleus	C13
Dwell 1D	62.5u
SW +l-	8000.0
FILTER	8000
Scans 1D	-1
Scan Count	4924
Points 1D	32768
Last Delay	10s
Obs Freq	62.9034273
F1 base	62.8960000
F1 offset	7.4273 KHz
RCVR gain	800
F2 freq	250.1322620
F2 base	250.1300000
F2 offset	2.2620 KHz
DEC Power	108
DEC Scheme	BB
Dummy scan	0

11 peaks found in Thiatriazine with S-Cl, 13C

peak	ppm	freq	amp
1	172.765	10866.24	517312.66
2	171.337	10776.40	518676.84
3	135.758	8538.61	1555210.00
4	134.228	8442.41	413683.50
5	130.510	8208.53	3287813.50
6	129.306	8132.84	3522393.25
7	95.753	6022.49	97502.41
8	77.742	4889.68	2313833.50
9	77.230	4857.45	2341286.00
10	77.090	4848.66	92686.85
11	76.725	4825.72	2369809.25

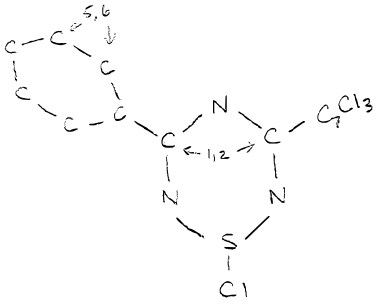

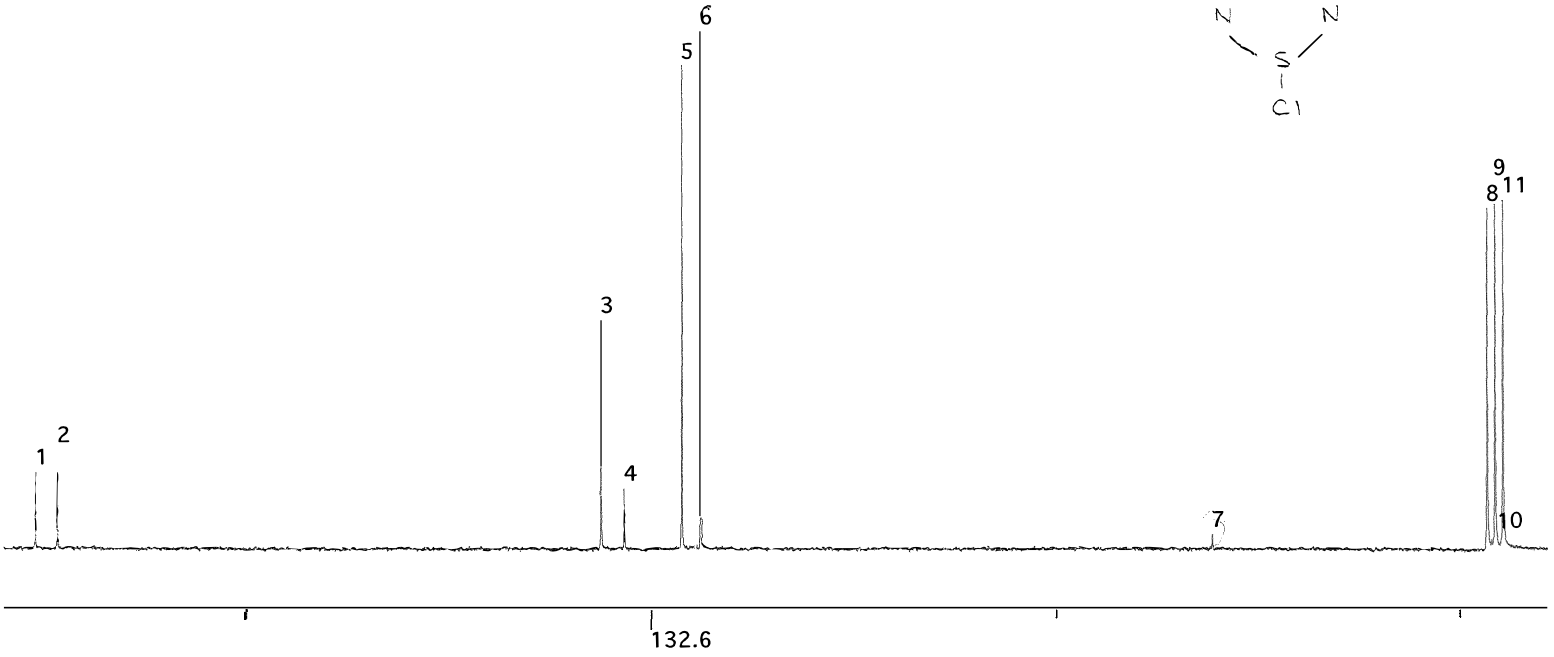

C13-NMR of **4c** in $CDCl_3$

: Mode= 2 (Mid-IR) :53 AM

Sample :

Scans= Res=4 cm-1 Apod= Cosine Zero Filling= 1 x

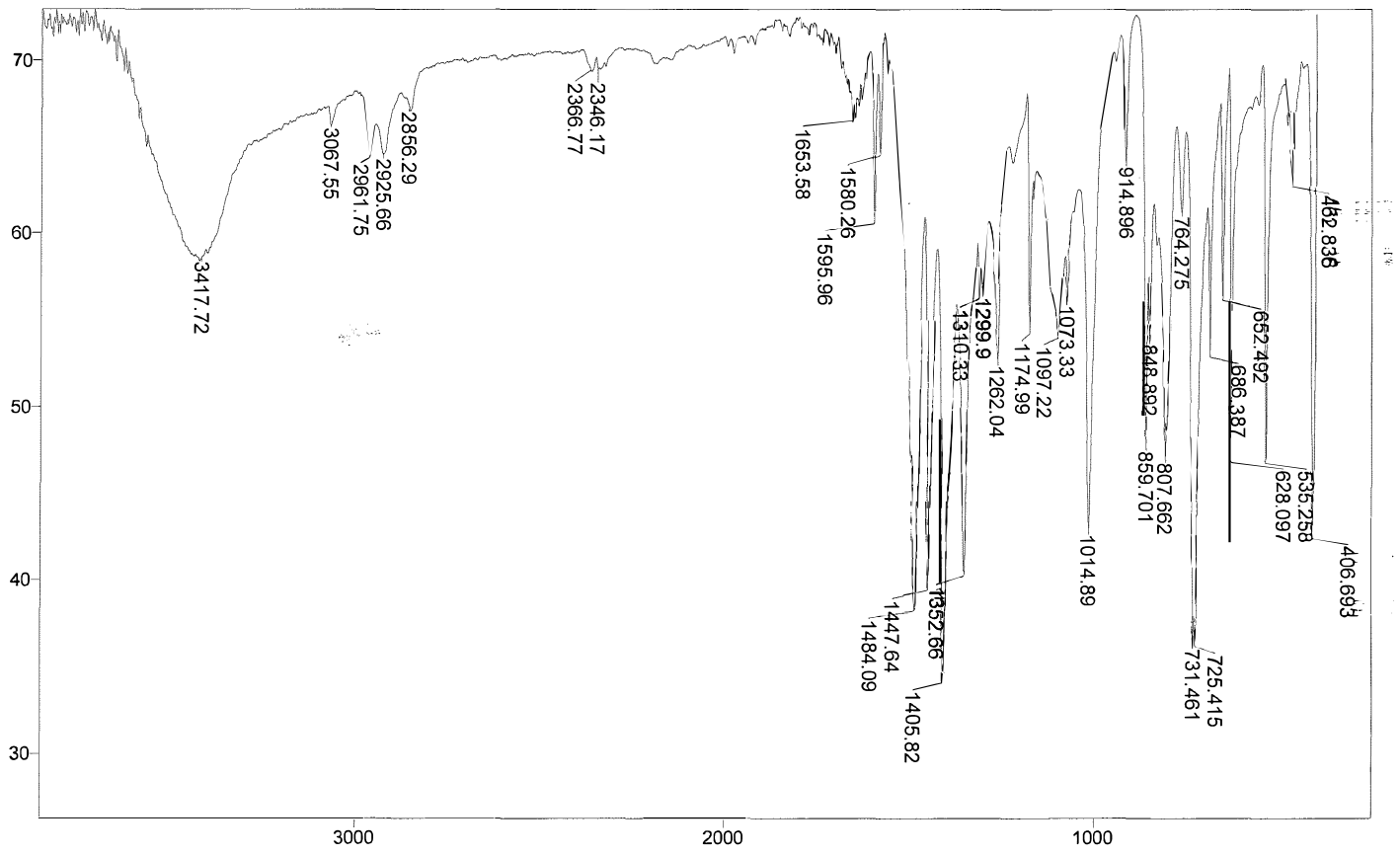

FTIR of **4c** as a solid film.

Transmittance / Wavenumber (cm-1)

Filename	thiatriazine Cl, S-Cl 2
Nucleus	H1
No. Scans	-1
No. Points	32768
Scan Count	20
SW +l-	2500.0
Filter	3000
Acq. Time	6.554s
Obs Freq	250.1346939
Obs base	250.1330000
O1 offset	1.6939 KHz
RCVR gain	200
DEC Mode	OFF
DEC Attn.	58
Sequence	1PULSE
Last Delay	2s
Line Brdng	0.10
temp K	293.0

18 peaks found in thiatriazine Cl, S-Cl

peak	ppm	freq	amp	
1	8.473	2119.29	7408.64	
2	8.464	2117.00	48032.45	9.00
3	8.455	2114.87	15768.84	
4	8.436	2110.14	17211.35	
5	8.428	2108.00	52382.20	
6	8.418	2105.71	6507.75	
7	7.561	1891.33	8789.47	
8	7.552	1888.89	51213.82	
9	7.544	1886.90	16876.88	8.85
10	7.536	1885.07	3036.35	
11	7.524	1882.02	16130.07	
12	7.516	1880.04	49985.31	
13	7.506	1877.59	5799.98	
14	7.262	1816.41	16901.39	
15	1.263	315.86	1427.90	
16	0.881	220.34	1348.47	
17	0.072	18.01	3099.37	
18	0.000	0.00	15385.83	

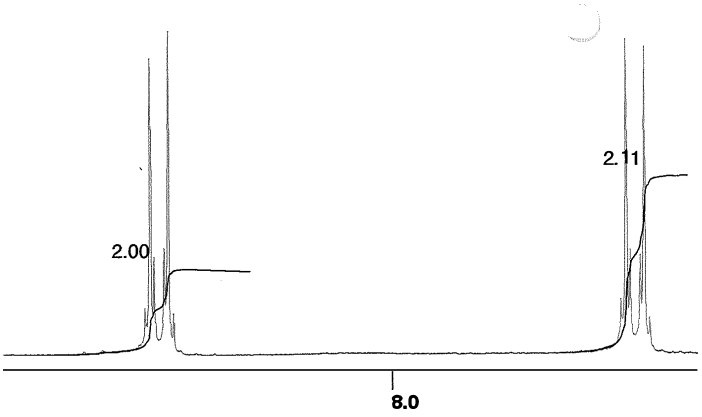

#	Start ppm	Stop ppm	Integral
1	8.72	8.27	2.00
2	7.67	7.43	2.11

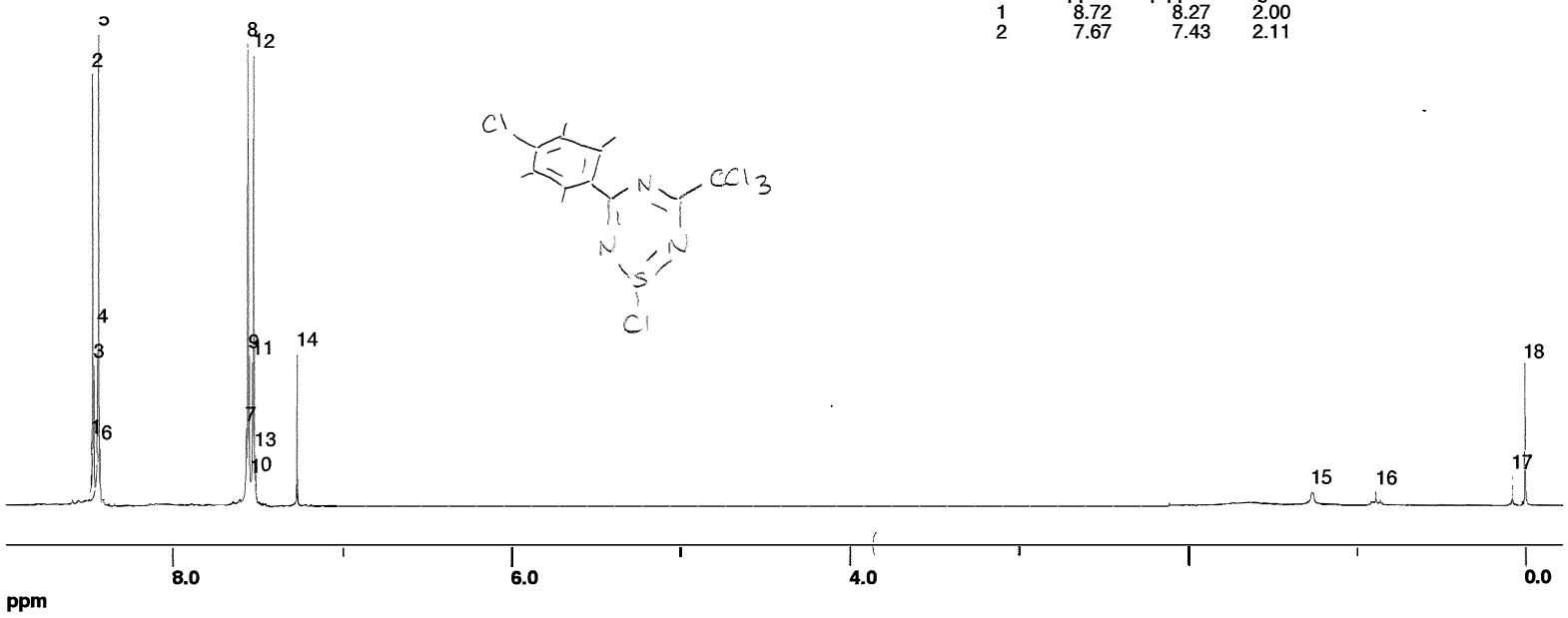

H1-NMR of **4d** in $CDCl_3$

Filename	proton 18
Nucleus	H1
No. Scans	-1
No. Points	32768
Scan Count	12
SW +l-	2500.0
Filter	3000
Acq. Time	6.554s
Obs Freq	250.1346939
Obs base	250.1330000
O1 offset	1.6939 KHz
RCVR gain	200
DEC Mode	OFF
DEC Attn.	58
Sequence	1PULSE
Last Delay	2s
Line Brdng	0.10
temp K	293.0
spin rate	0
Solvent	

7 peaks found in proton 18

peak	ppm	freq	amp
1	8.746	2187.62	15210.07
2	8.743	2186.85	18186.88
3	8.710	2178.77	19279.63
4	8.707	2178.00	17248.65
5	7.944	1986.96	22175.42
6	7.911	1978.72	20128.85
7	7.908	1978.11	18137.29

1. 8.566 2142.64
2. 8.563 2141.98
3. 8.531 2133.79
4. 8.528 2133.03
5. 7.764 1941.99
6. 7.731 1933.75
7. 7.728 1933.14
8. 7.189 1798.10

#	Start ppm	Stop ppm	Integral
1	8.83	8.66	2.00
2	8.04	7.85	2.10
3	1.81	1.59	0.20

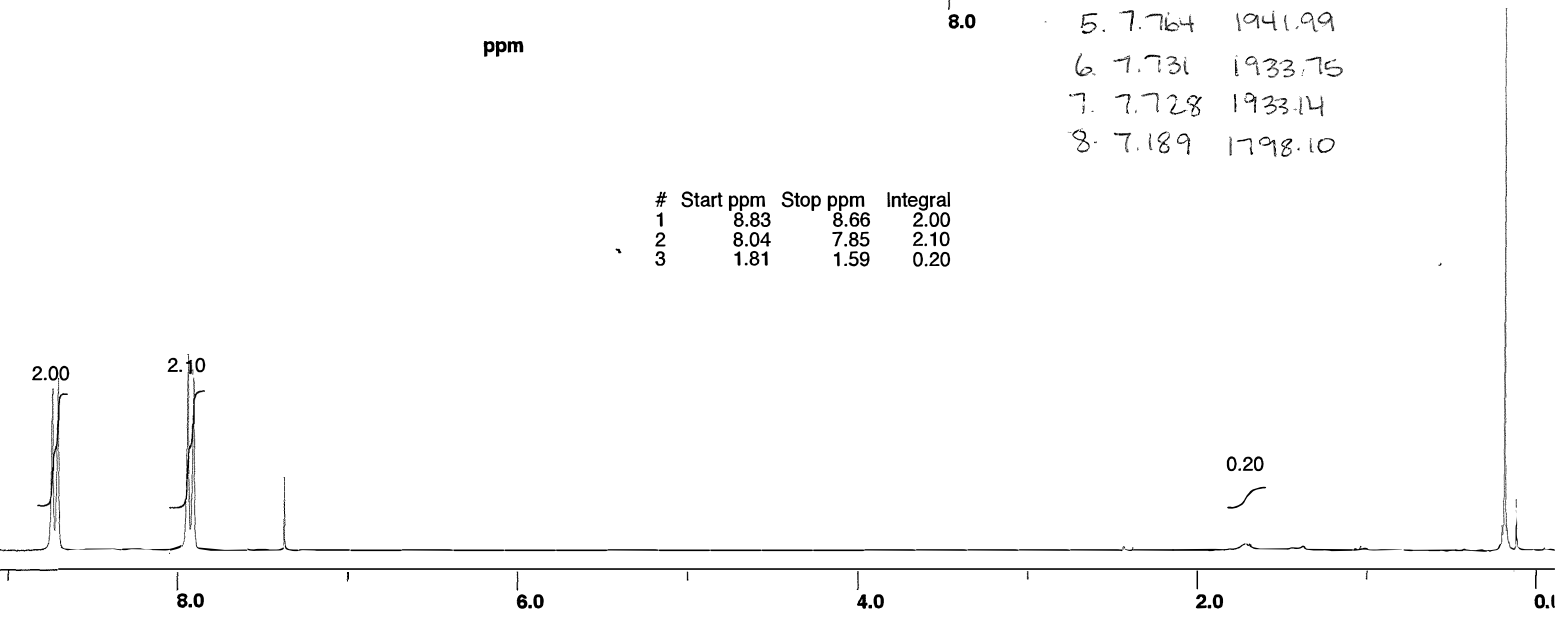

H1-NMR of **4e** in $CDCl_3$